



UNIVERSIDADE FEDERAL DO PARÁ
INSTITUTO DE TECNOLOGIA
PROGRAMA DE PÓS-GRADUAÇÃO EM CIÊNCIA E TECNOLOGIA DE
ALIMENTOS

VÂNIA MARIA BORGES CUNHA

TECNOLOGIA SUPERCRÍTICA APLICADA À EXTRAÇÃO DO ÓLEO DE
BACABA-DE-LEQUE (*Oenocarpus distichus*), DETERMINAÇÃO DE COMPOSTOS
BIOATIVOS E AVALIAÇÃO DOS PARÂMETROS DE PROCESSO.

BELÉM/PA

2021

VÂNIA MARIA BORGES CUNHA

**TECNOLOGIA SUPERCRÍTICA APLICADA À EXTRAÇÃO DO ÓLEO DE
BACABA-DE-LEQUE (*Oenocarpus distichus*), DETERMINAÇÃO DE COMPOSTOS
BIOATIVOS E AVALIAÇÃO DOS PARÂMETROS DE PROCESSO.**

Tese de doutorado submetida ao Programa de Pós -
Graduação em Ciência e Tecnologia de Alimentos,
da Universidade Federal do Pará, como parte dos
requisitos exigidos para a obtenção do título de
Doutora em Ciência e Tecnologia de Alimentos

ÁREA DE CONCENTRAÇÃO: Produtos vegetais.

ORIENTADOR: Prof. Dr. Raul Nunes de Carvalho Júnior

CO-ORIENTADORA: Prof^a. Dra. Marilena Emmi Araújo.

BELÉM/PA

2021

**Dados Internacionais de Catalogação na Publicação (CIP) de acordo com ISBD
Sistema de Bibliotecas da Universidade Federal do Pará
Gerada automaticamente pelo módulo Ficat, mediante os dados fornecidos pelo(a) autor(a)**

C972t Cunha, Vânia Maria Borges.
Tecnologia supercrítica aplicada à extração do óleo de bacaba-de-leque (*Oenocarpus distichus*), determinação de compostos bioativos e avaliação dos parâmetros de processo / Vânia Maria Borges Cunha. — 2021.
139 f. : il.

Orientador(a): Prof. Dr. Raul Nunes de Carvalho Júnior
Coorientação: Prof^a. Dra. Marilena Emmi Araújo
Tese (Doutorado) - Universidade Federal do Pará, Instituto de Tecnologia, Programa de Pós-Graduação em Ciência e Tecnologia de Alimentos, Belém, 2021.

1. Óleo de bacaba-de-leque. 2. Compostos bioativos. 3. Propriedades funcionais. 4. Extração por fluido supercrítico. 5. Aumento de escala. I. Título.

CDD 660.284248

VÂNIA MARIA BORGES CUNHA

**TECNOLOGIA SUPERCRÍTICA APLICADA À EXTRAÇÃO DO ÓLEO DE
BACABA-DE-LEQUE (*Oenocarpus distichus*), DETERMINAÇÃO DE COMPOSTOS
BIOATIVOS E AVALIAÇÃO DOS PARÂMETROS DE PROCESSO.**

DATA DA AVALIAÇÃO: ____/____/____

NOTA: _____

BANCA EXAMINADORA

Prof. Dr. Raul Nunes de Carvalho Júnior (PPGCTA/FEA/UFPA - Orientador)

Prof^a. Dra. Marilena Emmi Araújo (PPGEQ/FEQ/UFPA – Co-orientadora)

Prof. Dr. Antônio Manoel da Cruz Rodrigues (PPGCTA/FEA/UFPA – Membro Interno)

Prof^a. Dra. Luiza Helena Meller da Silva (PPGCTA/FEA/UFPA – Membro Interno)

Prof. Dr. Emanuel Negrão Macêdo (PRODERNA/FEQ/UFPA - Membro Externo)

Dra. Flavia Cristina Seabra Pires (LABTECS/PCT/UFPA - Membro Externo)

BELÉM/PA

2021

Dedico este trabalho, primeiramente, a Deus.
Aos meus pais, que sempre me apoiaram em tudo, e, especialmente, ao meu irmão Paulo (*in memoriam*), com toda saudade, amor e gratidão.
Ao meu esposo, João Carlos, que esteve ao meu lado em todos os momentos.

AGRADECIMENTOS

Antes de tudo, quero agradecer a Deus, que me deu o dom da vida e forças para superar todas as dificuldades durante a realização deste trabalho.

Aos meus pais, Maria e Alfredo, por todo o esforço que fizeram para que eu pudesse estudar, por sempre me incentivarem e acreditarem em mim.

Aos meus irmãos, por sempre estenderem as mãos nos momentos mais difíceis.

Ao meu esposo, João Carlos, por todo o apoio e amor que me dedicou no decorrer desses anos de estudo. Em particular, pela paciência e compreensão durante os momentos de estresse e ansiedade.

Ao meu orientador, Prof. Dr. Raul Nunes de Carvalho Júnior, por ter me aceitado em seu grupo de pesquisa, o LABEX, e por todas as orientações dadas durante a realização deste projeto de pesquisa.

À Prof^ª. Dra. Marilena Emmi Araújo por toda orientação, apoio e amizade ao longo de todos esses anos. Obrigada por compartilhar seus conhecimentos e por todos os seus ensinamentos. Sempre admirei sua dedicação à pesquisa.

Às amigas Marcilene Paiva, Marielba Rodriguez Salazar, Fernanda Wariss, Wanessa Almeida e Priscila Bezerra por todo apoio, amizade, pelos bons momentos. Agradeço, principalmente, por terem me ajudado nos experimentos, quando eu não sabia nem por onde começar, e pelo auxílio na escrita dos artigos. Também agradeço aos colegas do LABEX pelos momentos de descontração e pela troca de conhecimento.

RESUMO

A espécie *Oenocarpus distichus* é uma palmeira nativa dos biomas da Amazônia brasileira, conhecida popularmente como bacaba-de-leque. Seu valor econômico baseia-se, principalmente, na exploração do palmito e na extração do óleo da polpa dos frutos, que é empregado para fins comestíveis. Apesar disso, essa espécie ainda é pouco conhecida quanto ao seu potencial de exploração, principalmente com relação às características funcionais e sua contribuição nutricional às populações locais e à sociedade de um modo geral. Por isso, foram produzidos, nesta tese, três artigos de pesquisa a fim de promover a valorização da espécie no cenário industrial. Os estudos foram realizados aplicando o dióxido de carbono supercrítico (Sc-CO₂) para a extração do óleo da polpa liofilizada de bacaba-de-leque em diferentes condições de processo. No primeiro artigo, foram aplicadas as temperaturas de operação de 50 °C, combinada com as pressões de 150, 220 e 350 bar, e 60 °C, combinada com as pressões de 190, 270 e 420 bar, para obter o melhor rendimento em óleo. Sua composição química foi avaliada, bem como os teores de compostos bioativos presentes na polpa antes e depois da extração. Os rendimentos máximos de óleo foram alcançados a 50 °C/350 bar (45,23%) e 60 °C/270 bar (45,90%). Os ácidos oleico, palmítico e linoleico, assim como os triglicerídeos preditos OLiO, PLiO, OOO, POP e POO foram predominantes na composição do óleo, independente das condições de extração, conferindo ótimos índices de qualidade funcional. Houve um aumento nos teores de compostos fenólicos totais, antocianinas totais e na capacidade antioxidante dos extratos da polpa de bacaba-de-leque após a extração. No segundo artigo, foram investigadas as propriedades nutricionais e físico-químicas do óleo extraído por Sc-CO₂ a 50 °C/350 bar, bem como a sua estabilidade térmica, a presença de compostos funcionais e o efeito citotóxico. O óleo apresentou 21,36 µg / g de óleo de carotenoides totais. Os parâmetros de qualidade, que definem as propriedades físico-químicas, apresentaram valores dentro dos padrões recomendados pela legislação para óleos vegetais brutos e foram semelhantes aos óleos comestíveis comercializados no Brasil e em outros países. Os perfis termogravimétricos indicaram relativa estabilidade térmica até 210 °C. As bandas espectrais, determinadas por FTIR, mostraram que o método de extração e as condições operacionais aplicadas não alteraram o perfil de grupos funcionais característicos. Os testes de citotoxicidade revelaram que o óleo extraído não apresentou efeito citotóxico. O terceiro artigo consiste em um estudo das cinéticas de extração supercrítica do óleo de bacaba-de-leque em dois vasos de extração (V₁ e V₂) em diferentes vazões de solvente (Q_{CO₂}) a 50 °C/350 bar e 60 °C/270 bar. Os dados experimentais foram ajustados adequadamente pela modificação do modelo de células quebradas e intactas (BIC), proposta na literatura. Por fim, foram avaliados procedimentos de aumento de escala experimental e predito, correlacionando variáveis de operação em diferentes geometrias do leito. Os parâmetros de operação aplicados não influenciaram nos rendimentos finais de óleo, no entanto, os estágios iniciais da extração foram visivelmente afetados. O uso da correlação entre altura e diâmetro do leito (H_b/D_b) e Q_{CO₂}, para uma mesma massa de alimentação (F), não foi suficiente para reproduzir as curvas cinéticas experimentais de V₁ (5×10⁻⁵ m³) para V₂ (10⁻⁴ m³). Porém, quando expressas em função do consumo de solvente, as curvas convergiram para uma mesma linha, mostrando que a quantidade total de CO₂ consumida foi responsável pela eficiência do processo. Na predição do aumento de escala, o aumento de F e Q_{CO₂} para um mesmo H_b/D_b se mostrou adequado para reproduzir o comportamento cinético da escala experimental em escalas maiores. Os resultados desses estudos mostraram que o óleo de bacaba-de-leque se apresenta como um produto de alta qualidade, atribuída a sua composição química e propriedades funcionais, e fornecem informações que permitem o aperfeiçoamento e a viabilidade técnica da extração do óleo para possível aplicação em escala comercial.

Palavras chaves: Óleo de bacaba-de-leque. Compostos bioativos. Propriedades funcionais. Extração por fluido supercrítico. Aumento de escala

ABSTRACT

The *Oenocarpus distichus* species is a native palm from Brazilian Amazon biomes, popularly known as bacaba-de-leque. Its economic value is mainly based on the palm heart exploitation and the fruits pulp oil extraction, used for edible purposes. Despite this, there is little knowledge about this species, especially regarding its functional characteristics and its nutritional contribution to local populations and society in general. Therefore, in this thesis, three research manuscripts were produced in order to promote the valorization of the species in the industrial scenario. The studies were carried out by applying supercritical carbon dioxide (Sc-CO₂) for the extraction of oil from the lyophilized bacaba-de-leque pulp under different process conditions. In the first article, the operating temperatures of 50 °C was applied, combined with pressures of 150, 220 and 350 bar, and 60 °C, combined with pressures of 190, 270 and 420 bar, to obtain the best oil yield. Its chemical composition was evaluated, as well as the bioactive compounds contents present in the pulp before and after extraction. The maximum oil yields were reached at 50 °C/350 bar (45.23%) and 60 °C/270 bar (45.90%). The oleic, palmitic, and linoleic acids, as well as the predicted triglycerides OLiO, PLiO, OOO, POP, and POO were predominant in the oil composition, independent of the extraction conditions, and presented excellent functional quality. There was an increase in phenolic compounds, total anthocyanins contents, and antioxidant capacity of the bacaba-de-leque pulp extracts after the Sc-CO₂ extraction. In the second article, the nutritional and physicochemical properties of the oil extracted by Sc-CO₂ at 50 °C/350 bar were investigated, as well as its thermal stability, the presence of functional compounds and the cytotoxic effect. The extracted oil showed 21.36 µg/g oil of total carotenoids. The quality parameters evaluated, which define the physicochemical properties, presented values within the standards recommended by the legislation for crude vegetable oils, and were similar to those of edible oils marketed in Brazil and in other countries. The thermogravimetric profiles indicated relative thermal stability at 210 °C. The spectral bands, determined by FTIR, showed that the extraction method and the operating conditions applied did not alter the characteristic functional group profile. The cytotoxicity tests revealed that the extracted oil had no cytotoxic effect. The third article consists of a study of the supercritical extraction kinetics of bacaba-de-leque oil in two extraction vessels (V_1 and V_2) at different solvent flows (Q_{CO_2}) at 50 °C/350 bar and 60 °C/270 bar. The experimental data were properly adjusted by modifying the Broken-and-Intact Cell (BIC) model, proposed in the literature. Lastly, experimental and predicted scale-up procedures were evaluated, correlating operational variables in different bed geometries. The operational parameters applied did not influence the final oil yields. However, the initial stages of extraction were visibly affected. The use of the correlation between bed height and diameter (H_b/D_b) and Q_{CO_2} , for the same feed mass (F), was not enough to reproduce the experimental kinetic curves from V_1 ($5 \times 10^{-5} \text{ m}^3$) to V_2 (10^{-4} m^3). However, when expressed as a function of solvent consumption, the curves converged to the same line, showing that the total amount of CO₂ consumed was responsible for the process efficiency. In predicting scale-up, the increase of F and Q_{CO_2} for the same H_b/D_b proved to be adequate to reproduce the kinetic behavior of the experimental scale in larger scales. The results of these studies showed that bacaba-de-leque oil is presented as a high-quality product, which is attributed to its chemical composition and functional properties, and provide information that allows the improvement and technical feasibility of oil extraction for possible application on a commercial scale.

Keywords: Bacaba-de-leque oil. Bioactive compounds. Functional properties. Supercritical fluid extraction. Scale-up

SUMÁRIO

1. INTRODUÇÃO GERAL E OBJETIVOS.....	11
1.1. INTRODUÇÃO GERAL.....	11
1.2. OBJETIVOS	13
1.2.1. Objetivo geral	13
1.2.2. Objetivos específicos	13
CAPÍTULO 1	15
1.1. Carbon Dioxide Use in High Pressure Extraction Processes.....	15
CAPÍTULO 2	46
2.1. Bacaba-de-leque (<i>Oenocarpus distichus</i> Mart.) Oil Extraction Using Supercritical CO ₂ and Bioactive Compounds Determination in the Residual Pulp.....	46
CAPÍTULO 3	57
3.1. Physicochemical Properties, Thermal Behavior, and Cytotoxic Effect of bacaba-de-leque (<i>Oenocarpus distichus</i>) Oil Extracted by Supercritical CO ₂	57
CAPÍTULO 4	94
4.1. Supercritical Extraction Kinetics of the Bacaba-de-leque (<i>Oenocarpus distichus</i>) Oil: Experimental Data, Mathematical Modeling and Scaling Up Study.....	94
CONCLUSÃO GERAL	133
TRABALHOS DESENVOLVIDOS DURANTE O PERÍODO DO DOUTORADO. ...	134

1. INTRODUÇÃO GERAL E OBJETIVOS

1.1. INTRODUÇÃO GERAL

As palmeiras do gênero *Oenocarpus*, pertencentes à família *Arecaceae*, são plantas nativas encontradas nos biomas da Amazônia brasileira. A espécie *Oenocarpus distichus* é uma das variedades desse gênero, conhecida popularmente como bacaba-de-leque, e produz frutos comestíveis de cor roxo escuro e polpa esverdeada. Sua importância econômica baseia-se, principalmente, na exploração do palmito e na extração do óleo dos frutos, que é empregado para fins comestíveis. Apesar disso, há pouco conhecimento sobre essa espécie, especialmente, sobre sua composição química. Mas sabe-se que os frutos de espécies do gênero *Oenocarpus* são potenciais fontes de compostos bioativos com capacidade antioxidante, tais como fenólicos, flavonoides e antocianinas. Também são uma das principais fontes de óleos vegetais de alta qualidade, ricos em ácidos graxos insaturados, que podem ser consideradas gorduras saudáveis e com potencial cardioprotetor. Essas informações são muito importantes porque podem indicar possíveis propriedades funcionais dos frutos, incentivar o seu consumo e gerar novas alternativas de uso com capacidade para serem explorados como alimentos funcionais.

O óleo e outros compostos presentes na polpa dos frutos dessas palmeiras podem ser extraídos por vários métodos. Porém, para garantir suas propriedades e a qualidade do produto, é importante levar em consideração o método de extração a ser aplicado, uma vez que, atualmente, há uma atenção maior sobre os riscos à saúde humana e ao meio ambiente relacionados ao uso de solventes orgânicos no processamento de alimentos e outros produtos. A extração por fluido supercrítico (SFE) é uma tecnologia de separação que se destaca nesse contexto, com grande potencial para ser aplicada no processamento de óleos e gorduras e para a recuperação/separação de vários tipos de substâncias bioativas. Suas vantagens sobre os métodos convencionais estão largamente descritas na literatura.

Considerando esse contexto e com o objetivo de promover a valorização da espécie *Oenocarpus distichus* no cenário industrial, este trabalho aplicou a tecnologia de extração supercrítica para a obtenção do óleo da polpa liofilizada de bacaba-de-leque, onde foram determinadas as condições operacionais (T, P, ρ) de extração mais adequadas para obter os melhores rendimentos em óleo. A composição química e as propriedades funcionais do óleo foram avaliadas. O teor de compostos bioativos presentes na polpa dos frutos antes e depois da extração também foi analisado. O processo de extração foi estudado fazendo uma

avaliação da influência das variáveis de operação sobre o rendimento global e das cinéticas de extração do óleo, obtidas em leitos de extração de diferentes geometrias. Por fim, foi feita uma avaliação de procedimentos de aumento de escala. Com isso, as etapas de desenvolvimento desta tese estão divididas em quatro capítulos.

O capítulo 1 é constituído por um capítulo de livro intitulado “*Carbon Dioxide Use in High Pressure Extraction Processes*”. Nesse capítulo, foi feita uma revisão da literatura sobre o processo de extração por fluido supercrítico, retratando, principalmente, as propriedades termodinâmicas, térmicas e de transporte, bem como as aplicações do dióxido de carbono (CO₂) em processos de extração a altas pressões. Essa etapa inicial do desenvolvimento da tese serviu de suporte para compreender como essas propriedades poderiam influenciar o rendimento e o comportamento da extração do óleo de bacaba-de-leque com o uso do CO₂ em estado supercrítico.

Os capítulos 2, 3 e 4, apresentados na forma de artigos científicos, referem-se aos resultados da pesquisa realizada durante o período do doutorado.

No capítulo 2, consta o artigo “*Bacaba-de-leque (Oenocarpus distichus Mart.) oil extraction using supercritical CO₂ and bioactive compounds determination in the residual pulp*”. Nesse capítulo, foi feito um estudo das condições operacionais (T, P, ρ) da extração com CO₂ supercrítico para a obtenção do óleo da polpa liofilizada de bacaba-de-leque. O óleo extraído foi avaliado quanto ao seu perfil de ácidos graxos, que foi utilizado para estimar sua provável composição de triglicerídeos. A polpa liofilizada (antes da extração) e a polpa desengordurada (torta residual obtida após a extração) também foram avaliadas, onde foram determinados o teor de compostos fenólicos e antocianinas totais e sua atividade antioxidante. As extrações foram realizadas nas temperaturas de operação de 50 °C, combinada com as pressões de 150, 220 e 350 bar, e 60 °C, combinada com as pressões de 190, 270 e 420 bar.

No capítulo 3, consta o artigo “*Physicochemical properties, thermal behavior, and cytotoxic effect of bacaba-de-leque (Oenocarpus distichus) oil extracted by supercritical CO₂*”. Nessa etapa, foi dada continuidade ao estudo das características do óleo de bacaba-de-leque relacionadas à sua composição química. Foram avaliadas as propriedades nutricionais e físico-químicas, a estabilidade térmica e o efeito citotóxico do óleo extraído por CO₂ supercrítico na condição de 50 °C e 350 bar.

No capítulo 4, consta o artigo “*Supercritical extraction kinetics of the bacaba-de-leque (Oenocarpus distichus) oil: Experimental Data, mathematical modeling and scaling up study*”. Nessa última etapa, foi realizado um estudo das cinéticas de extração do óleo de bacaba-de-leque obtidas em diferentes vasos de extração e vazão de solvente, verificando a

adequação de um modelo matemático de transferência de massa, proposto na literatura. Isso permitiu determinar e avaliar os parâmetros cinéticos pelo ajuste dos dados experimentais e estudar a ampliação de escala do processo a partir da correlação das variáveis de operação (vazão de solvente e massa de alimentação) em diferentes geometrias do leito (altura e diâmetro do leito).

1.2. OBJETIVOS

1.2.1. Objetivo geral

Determinar as condições operacionais da extração via CO₂ supercrítico para obter o melhor rendimento em óleo da polpa de bacaba-de-leque, investigando a sua composição química e propriedades funcionais, bem como o teor de compostos bioativos da polpa, antes e depois da extração. Além disso, avaliar parâmetros cinéticos pelo ajuste de dados experimentais das cinéticas de extração do óleo para aplicação no estudo de aumento de escala.

1.2.2. Objetivos específicos

- Extrair o óleo da polpa liofilizada de bacaba-de-leque utilizando dióxido de carbono supercrítico em diferentes condições operacionais (T, P, ρ);
- Definir as variáveis operacionais mais adequadas para a extração e prever a solubilidade do óleo em Sc-CO₂, usando a equação de estado cúbica de Peng-Robinson;
- Investigar o perfil de ácidos graxos presentes no óleo;
- Estimar a provável composição em triglicerídeos do óleo extraído;
- Avaliar os índices de qualidade funcional do óleo;
- Investigar os compostos bioativos e a atividade antioxidante do extrato da polpa liofilizada de bacaba-de-leque, antes e depois da extração;
- Avaliar as características nutricionais e físico-químicas, a estabilidade térmica e o efeito citotóxico do óleo;
- Estudar as cinéticas de extração do óleo de bacaba-de-leque em diferentes vasos de extração e vazão de solvente;
- Verificar a adequação do modelo BIC modificado para calcular e avaliar os parâmetros cinéticos pelo ajuste dos dados experimentais;

- Estudar a ampliação de escala do processo a partir da correlação das variáveis de operação (vazão de solvente e massa de alimentação) em diferentes geometrias do leito (altura e diâmetro do leito).

CAPÍTULO 1

1.1. Carbon Dioxide Use in High Pressure Extraction Processes

Carbon Dioxide Use in High-Pressure Extraction Processes

Vânia Maria Borges Cunha, Marcilene Paiva da Silva,
Wanessa Almeida da Costa,
Mozaniel Santana de Oliveira,
Fernanda Wariss Figueiredo Bezerra,
Anselmo Castro de Melo,
Rafael Henrique Holanda Pinto,
Nelio Teixeira Machado, Marilena Emmi Araujo and
Raul Nunes de Carvalho Junior

Additional information is available at the end of the chapter

<http://dx.doi.org/10.5772/intechopen.71151>

Abstract

This chapter describes the use of carbon dioxide at high pressures as an alternative for the extraction of bioactive compounds in a more sustainable way, addressing some of its physicochemical properties, such as pressure, temperature, density, solvation, selectivity, and its interaction with the solute when modified by other solvents such as ethanol and water. This extraction process is considered chemically “green,” when compared to conventional extraction processes using toxic organic solvents.

Keywords: supercritical CO₂, high pressure, density, vegetable matrix, bioactive compounds

1. Introduction

Separation technologies with fluids at high pressures are essentially vital to get new natural products of vegetable or marine origin that have biological activity, so-called bioactive extracts. Among the developed technologies, the supercritical fluid technology offers products free of residual solvent and that typically present high quality, when compared to products obtained by conventional techniques. The extracts of bioactive compounds can be obtained by extraction

of solid matrices (leaves, seeds, pulps, etc.) or by extraction/fractionation of liquid mixtures (aqueous solutions, fish oils, microalgae oils, vegetable oil, deodorize distillates, etc.) [1–5]. In processes at high pressures, which are near or above the critical point (pressure and temperature), the solvent density increases drastically and this is the most important parameter associated to the solvent power. As illustrated in **Figure 1**, carbon dioxide, a non-toxic substance, acting as solvent, co-solvent, or anti-solvent, is the most important fluid used in the supercritical fluid technology in extraction, separation, fractionation, micronization, and encapsulation processes applied to obtain extracts concentrated with bioactive compounds for food, pharmaceutical, and cosmetic applications [6–9].

Carbon dioxide has a critical temperature near to room temperature, contributing to the operating conditions (pressure and temperature) to extract thermolabile substances, such as bioactive compounds. In addition, this substance is non-polar and to enlarge the application spectrum to extract bioactive compounds, ethanol, water, or both are usually used as co-solvents. Moreover, carbon dioxide acts as co-solvent when in the mixture it is used more than 60% of ethanol or water, and as anti-solvent, when the solute extract is not soluble in carbon dioxide during the depressurizing step.

The information accuracy related to the physical (pressure, temperature, and density) and transport properties (diffusivity, viscosity) and the accuracy of thermodynamic and mass transfer relations used for the solvent, co-solvent, and solute reach directly the costs of investment in extraction/separation units in supercritical conditions. The thermodynamic phase equilibrium determines the limits for the mass transfer among different phases, which are

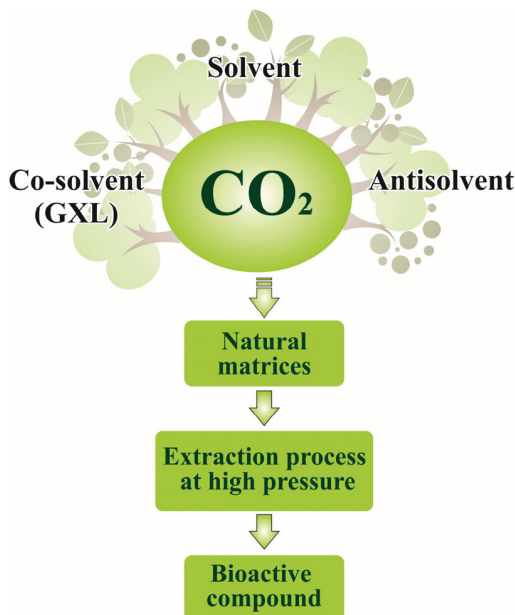


Figure 1. Carbon dioxide applications.

involved in various processes. The cubic equations of state are the most commonly applied models for the correlation and prediction of phase equilibrium at high pressures and are available in major commercial process simulators. In addition, they are used to calculate other thermodynamic properties, for both pure substances and mixtures, among which, the liquid and vapor phases density, enthalpy, and entropy.

This chapter intends to show the recent application scenarios of the carbon dioxide use at high pressures as solvent, to obtain natural extracts enriched with bioactive compounds, including the use of water as co-solvent to enhance the mixture solvating power. In this chapter, the description of the experimental strategy used for the supercritical carbon dioxide extraction of bioactive compounds from açai berry pulp was emphasized. The primary properties of pure carbon dioxide were also described and calculated using equations of state.

2. Diagrams of pure substances

2.1. P-T diagram

The pressure versus temperature (P-T) diagram describes the different aggregation states of pure substances called solid, liquid, and vapor/gas.

Figure 2 is a schematic representation of the P-T diagrams for carbon dioxide and the substances most commonly employed as co-solvent, ethanol, and water, in high-pressure extraction processes

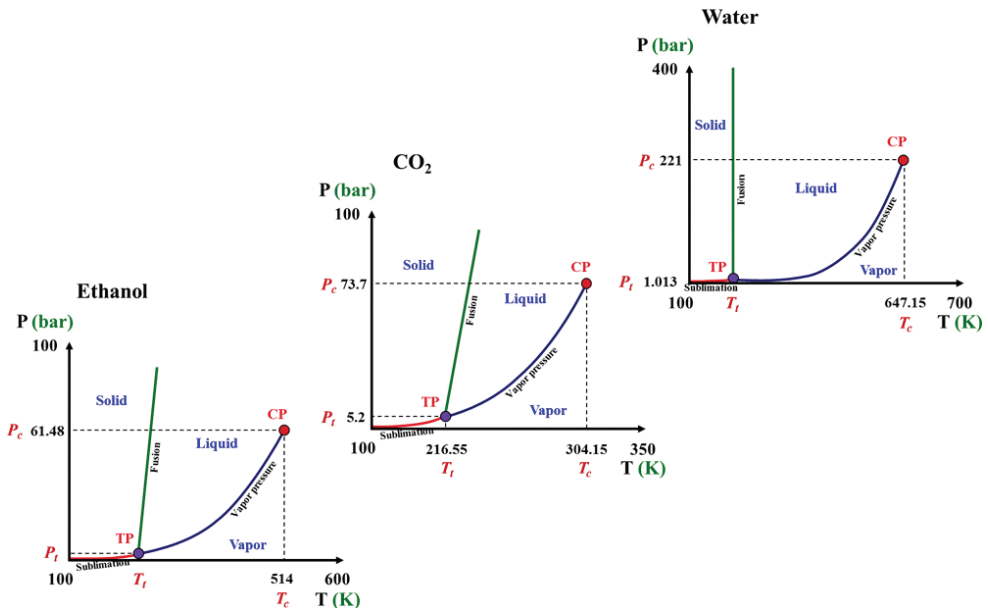


Figure 2. Solid-liquid-gas-supercritical fluid phase diagram. TP = triple point. CP = critical point. P_c = critical pressure. T_c = critical temperature. T_t = triple point temperature. P_t = triple point pressure.

of bioactive compounds. The curves represent the boundaries (phase transition or phase equilibrium) between the different states, known as saturation curves. The curve between the solid and liquid phases is called fusion; the curve between solid and vapor phases is called sublimation and that one between liquid and vapor phases is called vapor pressure (also known as boiling curve).

The behavior of the thermodynamic diagrams of pure substances culminates in the determination of the reference equilibrium points that has great importance in the development of thermodynamic models for different processes applications. In the P-T diagram, there are two points: the triple point, where the three phases are in equilibrium and the critical point, which is particularly of fundamental interest for applications in processes that use solvents at high pressures.

The critical point of a pure substance is the maximum thermodynamic state reached by the saturation curve between liquid and vapor phases. When the substance is in the state above the critical temperature (T_c) and the critical pressure (P_c), it is called supercritical fluid, and when the pressure is above P_c and the temperature below T_c , the thermodynamic state is called subcritical liquid. The technology with fluids at high pressures consists in the use of substances that act like solvent when they are in the thermodynamic state near or above the critical point. The triple point of carbon dioxide is at pressure of 5.18 bar and at temperature of 216.58 K (-56.57°C), and the critical point is at pressure of 73.7 bar and at temperature of 304.15 K (31°C) [10].

2.2. P- ρ -T diagram

Density (ρ) is the most important thermodynamic property to define the solvating power of a solvent at high pressures, increasing the density of the solvent increases its solvating power. To better understand the influence of density on the solvating power to increase or decrease the solubility of an extract within a solvent at high pressures, one needs information concerning the density as a function of system pressure and temperature.

Figure 3 shows the schematic representation of the density behavior ($\rho = 1/V$) of a pure substance with temperature and pressure variations, where V is the specific volume (volume per mass unit). In **Figure 3**, the density versus pressure isotherms are presented in descending order from T1 to T9. The red line represents the saturation curve between the liquid and vapor phases. The highest point of the saturation curve is the critical point. The dotted line within the saturation curve is the two-phase region. In the saturation curve, there is a sudden difference in the density between the liquid and vapor phases.

The behavior of the P- ρ -T diagram shows that the density at constant temperature increases with the increasing pressure and at constant pressure increases with the decreasing temperature. In the region near the critical point, small variations of pressure and/or temperature cause great variations in density. For carbon dioxide, the critical point is at the pressure of 73.7 bar and at the temperature of 304.15 K (31°C); it makes carbon dioxide the most applied solvent to extract thermo-sensible substances.

Below the critical temperature, in the subcritical region, the isotherms present two types of behavior: for the vapor region, at constant pressure, the density increases with the decreasing temperature and for the liquid region, the density varies very little with the temperature.

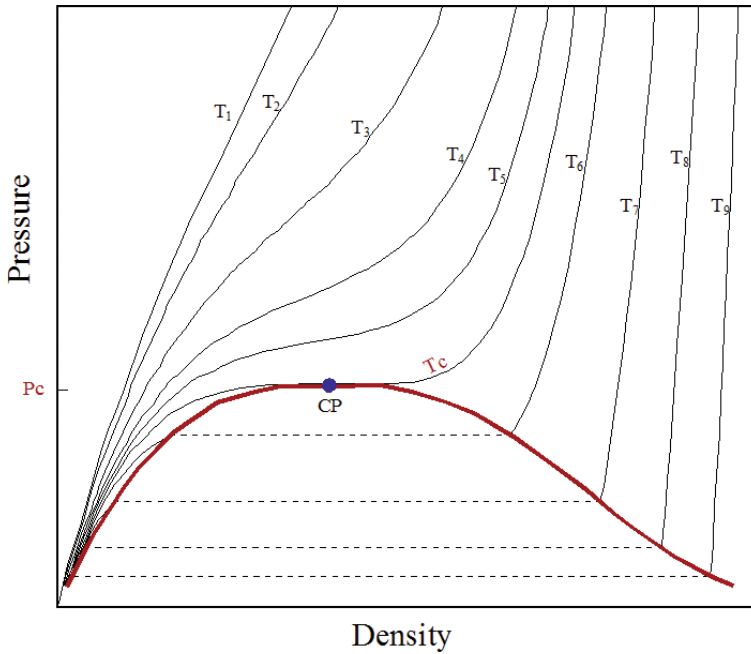


Figure 3. Pressure-density (P-ρ) phase diagram for carbon dioxide. CP = critical point (P_c , T_c , and ρ_c). CP = critical point (P_c , T_c , and ρ_c).

3. Supercritical fluid extraction

The extraction/separation processes applied to solid matrix using carbon dioxide as solvent are the most studied supercritical processes in the search for new natural products that have biological activity, according to numerous applications described in the literature [1, 4–6, 11–18].

3.1. General process steps

Generally, the supercritical fluid extraction applied to a natural solid matrix consists of three steps: the system supply of solvent/co-solvent, the extraction unit, and the extract separation system from solvent/co-solvent. **Figure 4** presents a general scheme of the supercritical fluid extraction unit without solvent recycle. The system supply of solvent/co-solvent consists by a booster air-driven fluid pump, a cooling bath, a co-solvent recipient, a co-solvent pump, and a mixer. The extract separation system from solvent/co-solvent consists by a control valve for extraction pressure reduction and a separation vessel to collect the extract.

Regarding the extraction, the supercritical solvent continuously flows through a fixed bed of solid particles and dissolves the extractable components of the solid. The solvent is fed into the extractor and evenly distributed at the inlet of the fixed bed. The system solvent and soluble components leave the extractor and feed the precipitator/separator, where the solvent products

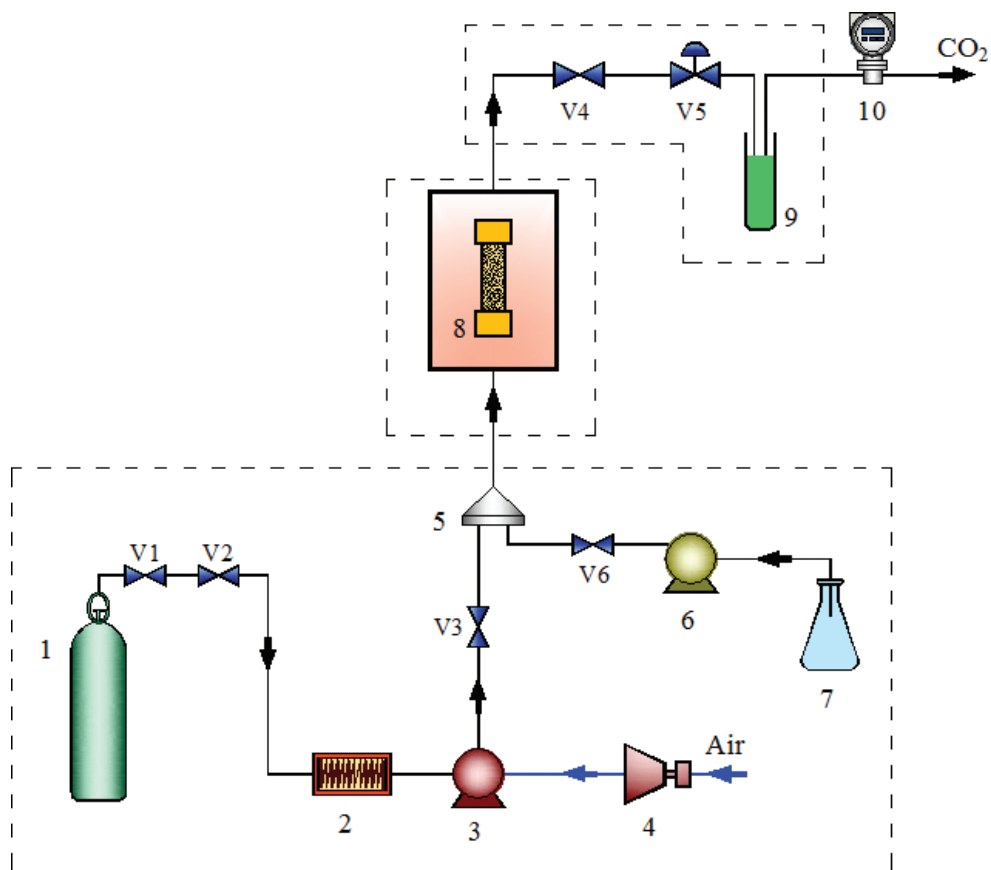


Figure 4. Scheme of a supercritical fluid extraction plant applying solvent/co-solvent. CO₂ cylinder (1); cooling bath (2); booster (CO₂ pump-3 and Compressor-4); mixer (5); CO-solvent pump (6); co-solvent recipient (7); extraction unit (8); control valve (V-5); separation vessel (9); flow meter (10).

are separated by expansion (depressurizing), since at low pressures the density of the solvent sharply decreases, therefore it decreases the solubilizing power of the solvent as well and the products precipitate.

The choice of the operating condition (P and T) is a determining factor that contributes to the maximization of the extracts solubility in the supercritical solvent, and consequently the extraction yields. Thus, increasing the density of the supercritical fluid, the solubility of the solvent maximizes. The solubility increasing can also occur when a co-solvent is added, which changes the solvent power and, in this way, the new solvent is a mixture [19, 20].

To design a high-pressure fluid extraction process of valuable compounds from new natural solid matrices, it is necessary to define the size of the extraction unit and some important parameters have to be determined to obtain the optimum process conditions for each application. Brunner

[19] and Kiran et al. [21] described the most important parameters, and among the variables that determine the process, operating conditions (pressure and temperature), amount of solvent, conditions of solvent removal from extract (precipitation), pretreatment of solid matrix, and other mass transfer parameters can be highlighted.

In general, the parameters that define the behavior of the mass transfer at processes at high pressures are related to the configuration of the bed: particle size, height, and diameter, preparation of the raw material, solvent flow, among others, which contribute to define the shape of the kinetic extraction curves. The phenomenological discussions about supercritical fluid extraction mass transfer applied to solid matrices have been discussed in the literature [19, 22–24].

3.2. Supercritical carbon dioxide extraction of bioactive compounds: a case study

The experimental strategy used for the supercritical carbon dioxide extraction process of bioactive compounds is based on the previous results collected by our research group in obtaining açai extracts [25].

Açai is a dark purple, berry-like fruit from typical Amazon palm tree *Euterpe oleracea* Mart., integrated in the daily dietary habit of the native people.

Recently, many studies have suggested its use as a functional food or food ingredient due to its antioxidant activity, explained by the high content of phenolic compounds, such as anthocyanins, specially cyanidin-3-glucoside and cyanidin-3-rutinoside, flavones, and phenolic acids [26–28]. Phenolic constituents are generally associated with health-promoting properties and prevention of diseases [29–33]. Anthocyanins constitute a group of pigments, also important in the food industry, for the replacement of artificial colors [34–36].

The supercritical extraction experiments of the lyophilized açai pulp under development were carried out in a Spe-ed™ SFE commercial unit (Allentown, PA, USA: model 7071 from Applied Separations) which is coupled to the solvent + co-solvent delivery system of Laboratory of Supercritical Extraction (LABEX), Faculty of Food Engineering-UFPA. The schematic representation of the supercritical extraction system is shown in **Figure 5**.

The first step consisted of the extraction with supercritical CO₂ (pure) to obtain extracts rich in fatty acids and byproducts of the residual solid matrix (defatted pulp). Analyses of the content of bioactive compounds (anthocyanins and total phenolic compounds) were performed. The second stage that is under development consists of the extraction with supercritical CO₂ combined with water as co-solvent applied to the residual solid matrix to obtain extracts concentrated in anthocyanins.

In the first stage, Batista et al. [25] subjected samples of lyophilized açai pulp to the supercritical carbon dioxide extraction process. Among the results, the study of the process variables (temperature, pressure, and solvent density) that maximize the extraction yield of açai oil, the quantification of the total anthocyanins content and total phenolic compounds content, and the evaluation of the allelopathic potential of the extracts obtained can be highlighted.

Figure 6 shows the experimental results of the 50, 60, and 70°C isotherms on dry basis and their standard deviations. In this study, the highest global yield was equal to $45.4 \pm 0.58\%$,

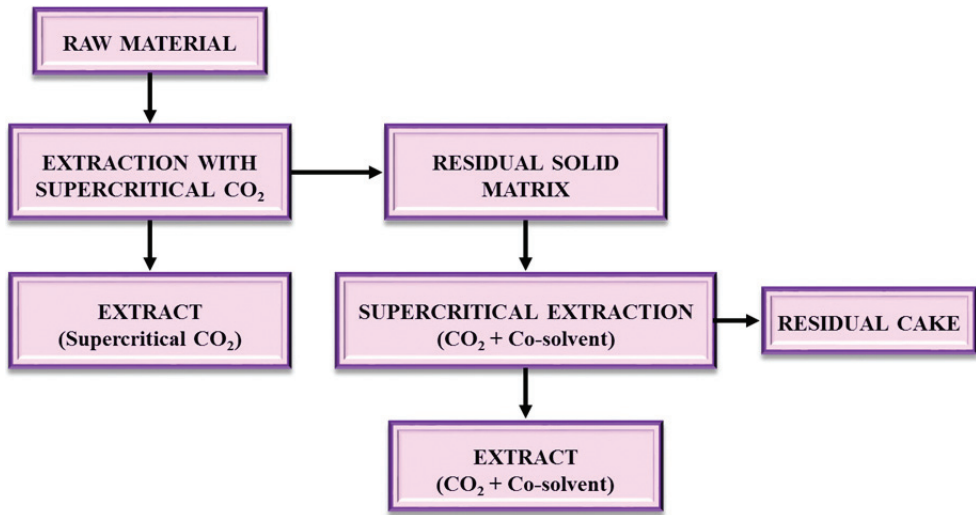


Figure 5. Experimental protocol for the bioactive compounds extraction.

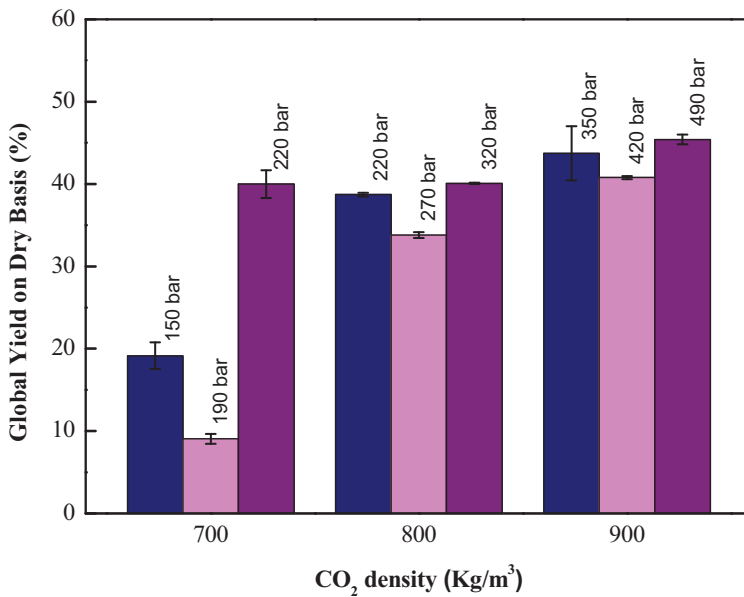


Figure 6. Global yield on dry basis versus density of supercritical CO₂ extraction of lyophilized açai berry oil. (■) 50°C, (■) 60°C, and (■) 70°C isotherms [17].

obtained at 70°C and 490 bar, while the lowest global yield was equal to $9.07 \pm 0.6\%$, obtained at 60°C and 190 bar. The density is related to the CO₂ solubility and is directly influenced by temperature and pressure. Here, the most important parameter was the density, since when it increased (in all isotherms), the oil global yield also increased.

The analysis of the phenolic compounds in the lyophilized açai berry pulp showed an increase in its content comparing the samples before and after the extraction with supercritical CO₂, in different conditions. Its highest content was equal to 7565 mg/100 g and was obtained in the condition of 70°C and 350 bar. The standard deviation for each condition was lower than 0.18% (**Figure 7**). Regarding anthocyanins, there was also an increase in its content. Before the extraction with supercritical CO₂, the total concentration was equal to 96.58 ± 0.11 mg/100 g, and after the extraction, it reached up to 137.5 mg/100 g of sample in the condition of 50°C and 220 bar. The standard deviation was lower than 0.15%. **Figure 8** shows the values obtained and their specific deviation. It can be inferred that since the extracts of the lyophilized açai berry pulp obtained by supercritical CO₂ are rich in phenolic compounds and anthocyanins, it presents great potential in nutraceutical applications.

The results of the fatty acid profile analysis of açai extracts indicate a low saturated/unsaturated ratio except for the condition of 70°C and 320 bar. The SFA content reached 99.67% at the condition of 70°C and 320 bar.

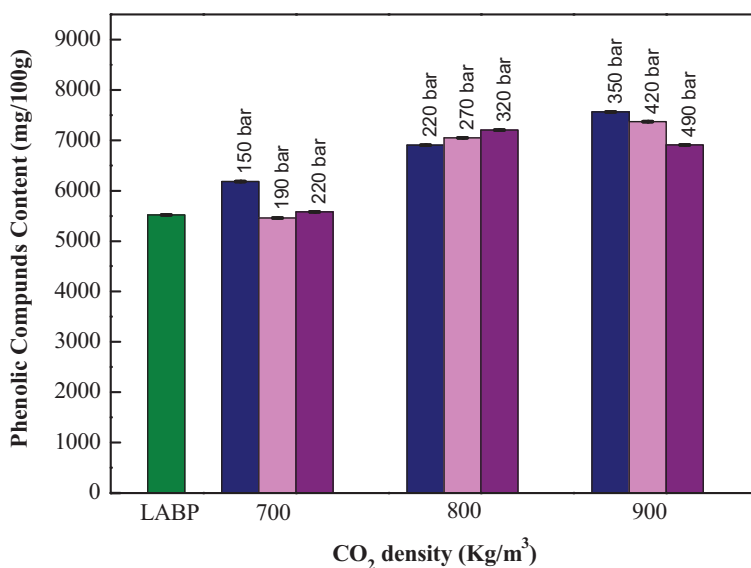


Figure 7. Total phenolic compounds content in lyophilized açai berry pulp before and after extraction with supercritical CO₂. (■) 50°C, (■) 60°C, and (■) 70°C isotherms [17].

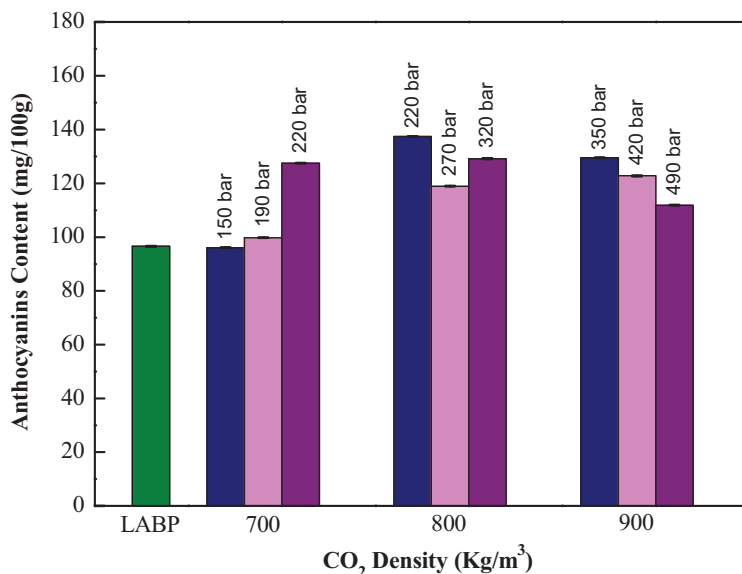


Figure 8. Total anthocyanins compounds content in lyophilized açai berry pulp before and after extraction with supercritical CO₂. (■) 50°C, (■) 60°C, and (■) 70°C isotherms [17].

4. High-pressure carbon dioxide properties

4.1. Thermodynamic properties

The influence of the density in the solvation power by the tunable operating conditions (P , T) is the most important thermodynamic effect in the high-pressure fluid processes.

Above the critical point, the supercritical extraction process can operate over a wide range of operating conditions (P , T) and the simplest density behavior can be obtained through an isotherm, being possible to select a wide range of operating pressures, as shown in **Figure 3** of the item 2.2 for the isotherms $T_1 > T_2 > T_3 > T_4 > T_5$.

The density is defined by the inverse of specific volume, and for practical purpose, could be calculated by volumetric properties (P - V - T) using equation of state.

4.1.1. P - V - T diagram calculation with equations of state

To describe the P - V - T diagram behavior, it is necessary to use precise equations of state (EOS) with specific parameters for pure substances. In the case of carbon dioxide, the equations of Bender [19] and Span and Wagner [37] are the most used. The Bender equation is presented below, where the parameters were determined from experimental PVT data of carbon dioxide. **Table 1** shows the parameters of the Bender equation.

i	a _i	i	a _i
1	0.22488558	11	0.12115286
2	0.13717965 × 10 ³	12	0.10783386 × 10 ⁻³
3	0.14430214 × 10 ⁵	13	0.43962336 × 10 ⁻²
4	0.29630491 × 10 ⁷	14	-0.36505545 × 10 ⁸
5	0.20606039 × 10 ⁹	15	0.19490511 × 10 ¹¹
6	0.45554393 × 10 ⁻¹	16	-0.29186718 × 10 ¹³
7	0.77042840 × 10 ⁻²	17	0.24358627 × 10 ⁸
8	0.40602371 × 10 ⁵	18	-0.37546530 × 10 ¹¹
9	0.40029509	19	0.11898141 × 10 ¹⁴
10	-0.39436077 × 10 ⁻³	20	0.50000000 × 10 ¹

Table 1. Bender equation constants for CO₂ [19].

$$P = \frac{T}{V} \left[R + \frac{B}{V} + \frac{C}{V^2} + \frac{D}{V^3} + \frac{E}{V^4} + \frac{F}{V^5} + \left(G + \frac{H}{V^2} \right) \frac{1}{V^2} \exp(-a_{20}/V^2) \right] \quad (1)$$

where

$$B = a_1 - \frac{a_2}{T} - \frac{a_3}{T^2} - \frac{a_4}{T^3} - \frac{a_5}{T^4} \quad (2)$$

$$C = a_6 + \frac{a_7}{T} + \frac{a_8}{T^2} \quad (3)$$

$$D = a_9 + \frac{a_{10}}{T} \quad (4)$$

$$E = a_{11} + \frac{a_{12}}{T} \quad (5)$$

$$F = \frac{a_{13}}{T} \quad (6)$$

$$G = \frac{a_{14}}{T^3} + \frac{a_{15}}{T^4} + \frac{a_{16}}{T^5} \quad (7)$$

$$H = \frac{a_{17}}{T^3} + \frac{a_{18}}{T^4} + \frac{a_{19}}{T^5} \quad (8)$$

$$a_{20} \approx V_C^2 \quad (9)$$

Figure 9 shows the calculation with Bender equation [19] of state for the P-V-T diagram isotherms and saturation curve, including an isotherm close to the critical temperature of the carbon dioxide. The calculations were performed using a Microsoft Excel spreadsheet. The equation presents accuracy in calculations when compared to data taken from IUPAC International Thermodynamic Table.

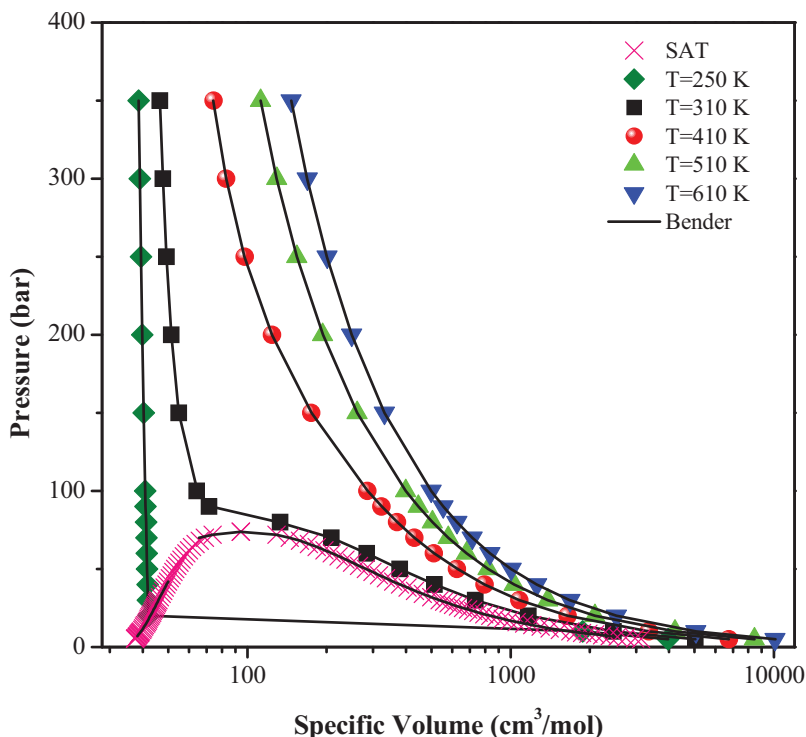


Figure 9. P-V-T diagram of carbon dioxide calculated with Bender EOS and compared to IUPAC data (symbols).

However, for applications of supercritical technology, it is necessary to calculate other thermodynamic properties. The thermodynamic properties of the pure solvent (density, enthalpy, and entropy) and the thermodynamic properties of the solute/solvent mixture, among which the equilibrium compositions, enthalpies, and mixing entropies, must be calculated in the operating conditions throughout the process. The cubic equation of state, also called Van der Waals type equation, represents an alternative, since the Bender-type equation described above is complex. In these cases, the cubic equations of state of Peng-Robinson (PR) [38] and Soave Redlich-Kwong (SRK) [39] are presented as the most commonly applied options in process simulations (Table 2). These equations of state use various thermodynamic properties and the following physical properties of the pure substance: critical pressure, critical temperature, and the acentric factor, which are tabulated, in the case of carbon dioxide.

Table 3 shows the calculated values of the carbon dioxide densities for some isotherms above the critical point using the equations of Peng-Robinson [38] and Soave-Redlich-Kwong [39]. The computational package PE 2000 developed by Pfohl et al. [40] was used for calculations. The results are compared to data taken from IUPAC International Thermodynamic Table and from NIST Chemistry Webbook (NIST Standard Reference Database). The Peng-Robinson equation of state presented the best results for the carbon dioxide density calculation in the conditions of pressure and temperature of Table 3 when compared with different databases.

Cubic equations	
PR	$P = \frac{RT}{V-b} - \frac{a(T)}{V(V+b) + b(V-b)}$ $a = 0.45724 \frac{R^2 T_c^2}{P_c} \times \alpha(T_r, \omega)$ $b = 0.07780 \frac{RT_c}{P_c}$ $\alpha(T_r, \omega) = \{1 + km[1 - (T_r)^{1/2}]\}^2$ $km = 0.37464 + 1.54226\omega - 0.26992\omega^2$
SRK	$P = \frac{RT}{V-b} - \frac{a(T)}{V(V+b)}$ $a = 0.42748 \frac{R^2 T_c^2}{P_c} \times \alpha(T_r, \omega)$ $b = 0.08664 \frac{RT_c}{P_c}$ $\alpha(T_r, \omega) = \{1 + km[1 - (T_r)^{1/2}]\}^2$ $km = 0.480 + 1.574\omega - 0.176\omega^2$

Table 2. Cubic equations of state.

Pressure (bar)	Temperature (°C/K)	CO ₂ density (kg/m ³)			
		PR	SRK	NIST	IUPAC
100	36.85/310	617.3	563.0	683.4	686.5
200		847.8	763.8	855.5	857.0
300		941.1	846.6	921.5	922.7
100	46.85/320	418.1	390.6	444.6	449.4
200		781.5	707.9	801.5	803.1
250		845.3	763.8	848.0	849.5
300		893.0	805.9	882.4	883.7
400		963.2	868.2	933.2	934.4
100	66.85/340	260.5	246.2	258.1	258.6
200		643.2	589.3	678.7	680.5
250		731.7	666.7	751.9	753.3
300		794.4	721.8	800.6	801.8
400		882.9	799.6	866.7	867.9

Table 3. Carbon dioxide density calculated with different equations of state.

Figure 10 shows the calculation with Peng-Robinson [38] equation of state for P-V-T diagram isotherms and saturation curve, including an isotherm close to the critical temperature of the carbon dioxide. The Peng-Robinson equation of state was able to describe all the phases of the carbon dioxide P-V-T diagram for the isotherms studied when compared to data taken from IUPAC International Thermodynamic Table.

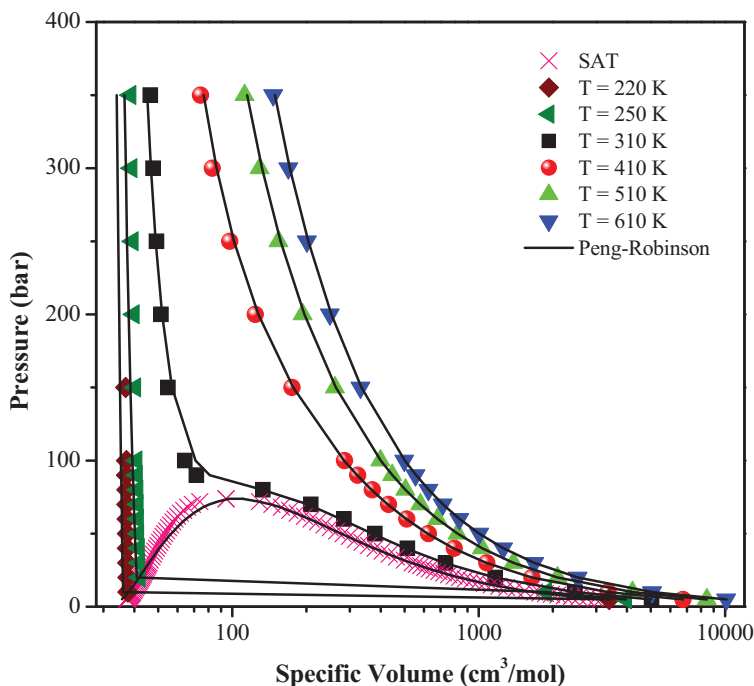


Figure 10. PVT diagram of carbon dioxide calculated with Peng-Robinson EOS and compared to IUPAC data (symbols).

From a process point of view, the accuracy of the cubic equations of state was good, considering that the operating conditions commonly applied in CO_2 extraction at high pressures are close to the values of temperature and pressure used in Table 3.

4.2. Other high-pressure carbon dioxide properties

The application of the high-pressure fluid extraction technologies in both laboratory and industrial scales requires not only the knowledge of the physical and thermodynamic properties of the solvent, but also requires the understanding of thermal and transport properties behavior. Among them, the most commonly cited are viscosity, diffusivity, thermal conductivity, and dielectric constant.

The dielectric constant describes the ability of a solvent to be polarized. The dielectric constant value is associated with the ability to dissolve electrolytes or polar compounds. The dielectric constant increases with temperature for most substances [41]. The dielectric constant of supercritical carbon dioxide with approximate value of a hydrocarbon alone does not characterize it as an important solvent; it only identifies it as a non-polar substance. Its solvation power is mainly related to the considerable increase of its density in the supercritical region with the properties as viscosity and diffusivity complementing the characteristics that makes supercritical carbon dioxide a differentiated solvent.

Under supercritical conditions, the thermal conductivity is influenced by both temperature and pressure and at constant pressure this property increases with increasing temperature, and on the other hand, at constant temperature, the thermal conductivity increases with pressure [42].

Carbon dioxide and other supercritical solvents have low viscosity and high diffusivity values. The viscosity and thermal conductivity of gases and liquids differ by one to two orders of magnitude, and the diffusivity values of gases and liquids differ by four orders of magnitude [41].

In the supercritical state, the substances have intermediate characteristics between the properties of a gas and a liquid, which contributes to more favorable hydrodynamic properties than the liquids, with diffusion coefficients close to those of a gas, which provides a fast and efficient mass transfer. Another feature of the supercritical fluid includes its low viscosity, which facilitates the penetration of the fluids into a solid matrix. Therefore, high diffusivity and low viscosity lead to a faster extraction time providing a dissolving power so that the supercritical fluid is considered a solvent.

Table 4 shows that supercritical fluids are characterized by transport properties (viscosity and diffusivity) between gases and liquids. The viscosity of a supercritical fluid is smaller than the viscosity of a gas and the diffusivity of the liquid is greater than the diffusivity of a supercritical fluid. In summary, the scheme of **Figure 11** shows the basic properties of supercritical carbon dioxide, which become fundamental in high pressures extraction processes.

	Unit	Gas	SCF	Liquid
Viscosity	Pa s	10^{-5}	10^{-4} to 10^{-5}	10^{-3}
Diffusivity	cm^2/s	10^{-1}	10^{-3} to 10^{-4}	10^{-6}

Table 4. Order of magnitude of transport properties.

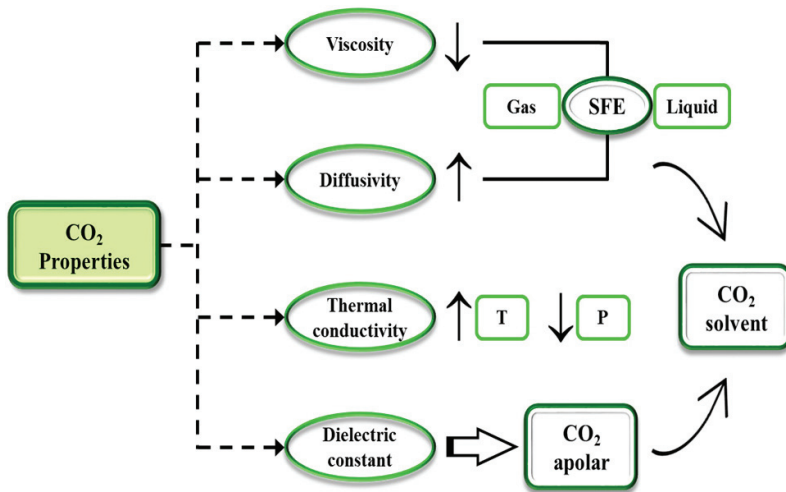


Figure 11. Carbon dioxide properties.

5. High-pressure carbon dioxide applications

The most cited drawback of using supercritical carbon dioxide as solvent is the high investment cost for equipment acquisition and operation. However, the extraction with supercritical carbon dioxide presents a lower extraction time because of its diffusivity and low surface tension, greater selectivity in the compounds of interest and little or no consumption of organic solvents [43–46].

5.1. Essential oil extraction

Essential oils have been used to prevent or treat human diseases for several centuries. The extraction of the volatile compounds present in edible or medicinal aromatic plants is generally carried out by hydrodistillation; however, the authors report that some compounds may undergo hydrolysis during the extraction period [47]. Although there are other techniques for isolating essential oils, the use of CO₂ as supercritical fluid has been considered a “chemically green” unconventional extraction technique that does not alter or degrade the substances present in oils because it uses relatively low temperatures in the extraction process.

Guan et al. [48] performed a comparison between conventional extraction methods and extraction with supercritical CO₂ and observed that the extraction using supercritical CO₂ as solvent was less effective with recovery rate of 57.36% for eugenol compared to steam distillation with 58.2%, but it was more effective when compared to hydrodistillation with recovery rate of 48.82% and Soxhlet extraction with 57.24%. However, when compared with the extraction of eugenol acetate, the extraction with supercritical CO₂ presented higher yields in relation to the other extraction methods.

Extraction of chemically active volatile molecules with supercritical CO₂ is very widespread [49–51]. This is due to the possible applications as agents that promote biological activities [52], such as antioxidant activity [53], anti-inflammatory activity [54], insecticidal activity [55], and phytotoxic activity [56]. In **Table 5**, some studies in the literature on the extraction of essential oils with supercritical CO₂ can be observed.

Aromatic plant	Bioactive compounds	References
<i>Juniperus communis</i> L.	Germacrene D and 1-octadecene.	[57]
<i>Satureja hortensis</i>	γ-Terpinene, thymol, and carvacrol	[58]
<i>Myrtus communis</i> L.	Methyl eugenol, 1,8 cineole, and beta- caryophyllene	[59]
<i>Leptocarpha rivularis</i>	α-thujone, β-caryophyllene, and caryophyllene oxide	[60]
<i>Piper nigrum</i> L.	β-caryophyllene, limonene, sabinene, 3-carene, β-pinene, and α-pinene	[53]
<i>Camellia sinensis</i> L.	9-Thiabicyclo[3.3.1]non-7-en-2-ol, tricosane, heneicosane, tetracosane, and dibutyl phthalate	[61]

Table 5. Published studies on extraction of essential oils using CO₂ as supercritical fluid.

As given above, it is observed that the process of extraction of essential oils using supercritical CO₂ is ecologically a cleaner method than the conventional ones, and it has been seen as one of the most viable alternatives.

5.2. Phytosterols extraction

Phytosterols (plant sterols) are non-volatile triterpenes. The great majority of these compounds are formed by carbon with one or two carbon-carbon double bonds [62]. And the most common phytosterols found in plants are β -sitosterol, campesterol, and stigmasterol [63]. These compounds have various biological activities such as lowering the total serum or plasma cholesterol levels and the low-density lipoprotein cholesterol levels. In addition, they have antitumor activities inhibiting the development of colon cancer [64, 65].

For the extraction of these phytosterols, the supercritical CO₂ has been shown to be an efficient technique for extraction of fixed oils from vegetable matrices. Studies report that this solvent may be superior to obtain oils in relation to the conventional extraction, exhibiting a recovery rate of phytosterols of 836.5 mg/100 g versus 30.5/100 g using a Soxhlet-type extraction apparatus [66]. A very important parameter for the extraction of phytosterols with supercritical CO₂ is the increase of the pressure, because it favors the solvation power and consequently the solubilization of these compounds, with a recovery rate of up to 7262.80 mg.kg⁻¹ [67]. **Table 6** presents some articles published in the literature on the extraction of phytosterols using supercritical CO₂.

5.3. Carotenoid extraction

Carotenoids are tetraterpenes present in plants that have several applications in food [72], cosmetic [73], and pharmaceutical [74] areas. Some of the benefits provided by these pigments are: antioxidant activity and strengthening of the immune system against degenerative diseases such as cancer, cardiovascular diseases, muscle degeneration, inflammation, hypertension, insulin resistance and obesity [75, 76].

Because of their hydrophobic characteristics, carotenoids are usually extracted using organic solvents such as hexane and petroleum ether. Carotenoids with hydrophilic characteristics can be obtained with more polar solvents such as acetone, ethanol, and ethyl acetate [77]. The

Plants	Phytosterols	References
<i>Cucurbita pepo</i> convar	Desmosterol, campesterol, stigmasterol, β -sitosterol, spinasterol, Δ 7,22,25-stigmastatrienol, Δ 7-stigmastenol, Δ 7,25-stigmastadienol, and Δ 7-avenasterol	[68]
<i>Brassica napus</i>	β -sitosterol, campesterol and brassicasterol	[69]
<i>Hippophae rhamnoides</i> L.	β -sitosterol	[70]
<i>Sesamum indicum</i> L.	β -sitosterol + sitostanol, cholesterol, campesterol + campestanol +24-methylene cholesterol, Δ -5 avenasterol and stigmasterol, while lower levels of Δ -5,24 stigmastadienol, brassicasterol, clerosterol + Δ -5-23 stigmastadienol, Δ -7 avenasterol, eritrodiol and Δ -7 stigmasterol	[71]

Table 6. Phytosterols extracted using supercritical CO₂

techniques used to extract this compound may be maceration, Soxhlet, microwave-assisted extraction [78, 79], ultrasound-assisted extraction [80], pressurized liquid extraction [81, 82], and supercritical fluid technology using low temperature. The process is performed in a short time in relation to conventional processes and does not use toxic solvents to collect the compound of interest [83]. In **Table 7**, some published works that used supercritical CO₂ to obtain carotenoids are shown.

5.4. Fatty acids extraction

Fatty acids (FA) belong to the lipid class and differ according to the size of the C chain (2–80), the presence or absence of double bonds (saturated or unsaturated) or their radical function as the groups hydroxyl, epoxy, and halogen atoms [89]. Ingestion of FA is essential to have an adequate energy balance in the human organism in addition to reducing the risk of some diseases such as diabetes [90], hypertension [91], coronary diseases [92], and inflammation [93].

Some of its applications are in food, nutraceutical, and cosmetic industries, and in the production of lubricants, biodiesel, and glycerol [94–96]. Some of the extraction methods that can be used to obtain FA are mechanical extraction [97], extraction by supercritical fluids and organic solvent [98], microwave-assisted extraction [99], and supercritical CO₂ extraction [98]. **Table 8** shows some studies that used supercritical CO₂ to obtain the main classes of the FA group.

5.5. Extraction with supercritical CO₂ modified with ethanol/water

The extraction with supercritical CO₂ modified with water in different proportions is carried out to obtain bioactive compounds of high polarity, because as mentioned above, CO₂ is an

Raw material	Carotenoid	References
Tomato juice	Lycopene and β -carotene	[84]
<i>Hemerocallis disticha</i>	Lutein and zeaxanthin	[85]
<i>Dunaliella salina</i>	9-cis and trans- β -carotenes	[86]
<i>Undaria pinnatifida</i> , <i>Haematococcus pluvialis</i> , and <i>Chlorella vulgaris</i>	Fucoxanthin, astaxanthin, lutein, and β -carotene	[87]
<i>Fucus serratus</i> and <i>Laminaria digitata</i>	Xanthophyll and fucoxanthin	[88]

Table 7. Published studies about carotenoid extraction using CO₂

Raw material	Fatty acid	Reference
<i>Cucurbita ficifolia</i> , Bouché	ω 6-linoleic acid, palmitic acid, oleic acid	[100]
<i>Farfantepenaeus paulensis</i>	Palmitic acid, oleic acid, stearic acid, palmitoleic acid, and linoleic acid	[101]
<i>Cannabis sativa</i> L.	Linoleic acid and linolenic acid	[102]
<i>Chaetoceros muelleri</i>	Myristic acid, palmitic acid, and palmitoleic acid	[103]
Saw Palmetto	Lauric acid, myristic acid, and oleic acid	[104]

Table 8. Published studies about fatty acids extraction using CO₂

Raw material	Compounds	References
<i>Myrciaria cauliflora</i>	Anthocyanin	[8]
Elderberry (<i>Sambucus nigra</i>)	Anthocyanins	[110]
<i>Vitis vinifera</i> var. <i>Malvasia nera</i>	Anthocyanins	[111]
<i>Arrabidaea chica</i>	Anthocyanins and luteolin	[112]
<i>Scutellaria lateriflora</i> L.	Baicalin, dihydrobaicalin, lateriflorin, ikonnikoside I, scutellarin, oroxylin A 7-O-glucuronide, oroxylin A, baicalein, wogonin	[113]
<i>Vaccinium myrtillus</i> L.	Delphinidin 3-O-galactoside, delphinidin 3-O-glucoside, cyanidin 3-O-galactoside, delphinidin 3-O-arabinoside, cyanidin 3-O-glucoside, petunidin 3-O-galactoside, cyanidin 3-O-arabinoside, petunidin 3-O-glucoside, peonidin 3-O-galactoside, petunidin 3-O-arabinoside, peonidin 3-O-glucoside, malvidin 3-O-galactoside, peonidin 3-O-arabinoside, malvidin 3-O-glucoside, malvidin 3-O-arabinoside and malvidin 3-O-xyloside	[114]

Table 9. Phenolic compounds extracted with supercritical CO₂ modified with ethanol/water.

non-polar molecule and does not have “power” to solubilize polar substances as is the case of the phenolic compounds (phenolic acids and flavonoids) [105, 106]. As previously mentioned, parameters of processes, such as temperature and pressure, can influence the extraction of bioactive compounds. Besides these two parameters, anthocyanins are also important for the extraction of phenolic compounds. Solvent flow rate, percentage of co-solvent, co-solvent type (ethanol or water), and extraction time are parameters that directly implicate the yield of these substances at the end of the extraction process [107].

Further examples of extraction of phenolic compounds using supercritical CO₂ modified with co-solvents can be analyzed in the studies [106, 108, 109]. They extracted various flavonoids like quercetin, catechin, epicatechin from cranberry, blueberry, and raspberry. **Table 9** presents some studies in which supercritical CO₂ modified with ethanol/water were used to extract chemically active phenolic compounds.

6. Conclusion

Carbon dioxide can be safely applied in high-pressure extraction processes due to its numerous advantageous characteristics. It is neither toxic nor inflammable, being able to act as solvent, co-solvent, or anti-solvent, which allows it to be used in natural products and foodstuff processing that require treatments intending to preserve their nutritional and sensory properties. Since it is a non-polar substance, it is suitable for extraction of non-polar bioactive compounds when used in pure form. When associated with a polar co-solvent, it can be used for extraction of polar compounds such as phenolic compounds and anthocyanins. Therefore, these characteristics make carbon dioxide the most important fluid used in high-pressure processes for extraction, separation, fractionation, micronization, and encapsulation, applied to obtain concentrated extracts with bioactive compounds for food, pharmaceutical, and cosmetic applications.

Acknowledgements

Costa W.A. (1427204/2014), Cunha V.M.B. (1566277/2015), Oliveira M.S. (1662230/2016), Silva M.P. (1636612/2016), Bezerra F.W.F. (1718822/2017), Pinto R.H.H. (1662902/2016) thank CAPES for the doctorate scholarship.

Author details

Vânia Maria Borges Cunha¹, Marcilene Paiva da Silva¹, Wanessa Almeida da Costa², Mozaniel Santana de Oliveira¹, Fernanda Wariss Figueiredo Bezerra¹, Anselmo Castro de Melo¹, Rafael Henrique Holanda Pinto¹, Nelio Teixeira Machado³, Marilena Emmi Araujo³ and Raul Nunes de Carvalho Junior^{1,2*}

*Address all correspondence to: raulncj@ufpa.br

1 LABEX/FEA (Faculty of Food Engineering), Program of Post-Graduation in Food Science and Technology, Federal University of Para, Belém, Pará, Brazil

2 Program of Post-Graduation in Natural Resources Engineering, Federal University of Para, Belém, Pará, Brazil

3 Laboratory of Separation Processes and Applied Thermodynamics (TERM@), Faculty of Chemical Engineering-UFPA, Belém, Pará, Brazil

References

- [1] Sahena F, Zaidul ISM, Jinap S, Karim AA, Abbas KA, Norulaini NAN, Omar AKM. Application of supercritical CO₂ in lipid extraction—A review. *Journal of Food Engineering*. 2009;**95**:240-253. DOI: 10.1016/j.jfoodeng.2009.06.026
- [2] Vardanega R, Prado JM, Meireles MAA. Adding value to agri-food residues by means of supercritical technology. *Journal of Supercritical Fluids*. 2015;**96**:217-227. DOI: 10.1016/j.supflu.2014.09.029
- [3] Fornari T, Vázquez L, Torres CF, Ibáñez E, Señoráns FJ, Reglero G. Countercurrent supercritical fluid extraction of different lipid-type materials: Experimental and thermodynamic modeling. *Journal of Supercritical Fluids*. 2008;**45**:206-212. DOI: 10.1016/j.supflu.2008.03.001
- [4] Rubio-Rodríguez N, Beltrán S, Jaime I, de Diego SM, Sanz MT, Carballido JR. Production of omega-3 polyunsaturated fatty acid concentrates: A review. *Innovative Food Science & Emerging Technologies*. 2010;**11**:1-12. DOI: 10.1016/j.ifset.2009.10.006
- [5] Herrero M, Ibáñez E. Green processes and sustainability: An overview on the extraction of high added-value products from seaweeds and microalgae. *Journal of Supercritical Fluids*. 2015;**96**:211-216. DOI: 10.1016/j.supflu.2014.09.006

- [6] Herrero M, Mendiola JA, Cifuentes A, Ibáñez E. Supercritical fluid extraction: Recent advances and applications. *Journal of Chromatography. A.* 2010;**1217**:2495-2511. DOI: 10.1016/j.chroma.2009.12.019
- [7] Beh CC, Mammucari R, Foster NR. Lipids-based drug carrier systems by dense gas technology: A review. *Chemical Engineering Journal.* 2012;**188**:1-14. DOI: 10.1016/j.cej.2012.01.129
- [8] Santos DT, Albarelli JQ, Beppu MM, Meireles MAA. Stabilization of anthocyanin extract from Jabuticaba skins by encapsulation using supercritical CO₂ as solvent. *Food Research International.* 2013;**50**:617-624. DOI: 10.1016/j.foodres.2011.04.019
- [9] Keven Silva E, Meireles MAA. Encapsulation of food compounds using supercritical technologies: Applications of supercritical carbon dioxide as an antisolvent. *Food and Public Health.* 2014;**4**:247-258. DOI: 10.5923/j.fph.20140405.06
- [10] Smith R, Inomata H, Peters C. Introduction to supercritical fluids: A spreadsheet-based approach. *Supercritical Fluid Science and Technology.* 2013;**4**:55-119. DOI: 10.1016/B978-0-444-52215-3.00002-7
- [11] Casas L, Mantell C, Rodríguez M, Torres A, Macías FA, Martínez de la Ossa E. Effect of the addition of cosolvent on the supercritical fluid extraction of bioactive compounds from *Helianthus annuus* L. *Journal of Supercritical Fluids.* 2007;**41**:43-49. DOI: 10.1016/j.supflu.2006.09.001
- [12] Passos CP, Silva RM, Da Silva FA, Coimbra MA, Silva CM. Supercritical fluid extraction of grape seed (*Vitis vinifera* L.) oil. Effect of the operating conditions upon oil composition and antioxidant capacity. *Chemical Engineering Journal.* 2010;**160**:634-640. DOI: 10.1016/j.cej.2010.03.087
- [13] Pereira CG, Meireles MAA. Supercritical fluid extraction of bioactive compounds: Fundamentals, applications and economic perspectives. *Food and Bioprocess Technology.* 2010;**3**:340-372. DOI: 10.1007/s11947-009-0263-2
- [14] Moraes MN, Zabot GL, Prado JM, Meireles MAA. Obtaining antioxidants from botanic matrices applying novel extraction techniques. *Food and Public Health.* 2013;**3**:195-214. DOI: 10.5923/j.fph.20130304.04
- [15] Danh LT, Han LN, Triet NDA, Zhao J, Mammucari R, Foster N. Comparison of chemical composition, antioxidant and antimicrobial activity of lavender (*Lavandula angustifolia* L.) essential oils extracted by supercritical CO₂, hexane and hydrodistillation. *Food and Bioprocess Technology.* 2013;**6**:3481-3489. DOI: 10.1007/s11947-012-1026-z
- [16] Rodrigues RB, Lichtenthaler R, Zimmermann BF, Papagiannopoulos M, Fabricius H, Marx F, Maia JGS, Almeida O. Total oxidant scavenging capacity of *Euterpe oleracea* Mart. (Açaí) seeds and identification of their polyphenolic compounds. *Journal of Agricultural and Food Chemistry.* 2006;**54**:4162-4167. DOI: 10.1021/jf058169p
- [17] Piras A, Rosa A, Marongiu B, Atzeri A, Dessì MA, Falconieri D, Porcedda S. Extraction and separation of volatile and fixed oils from seeds of *Myristica fragrans* by supercritical

- CO₂: Chemical composition and cytotoxic activity on Caco-2 cancer cells. *Journal of Food Science*. 2012;**77**:C448-C453. DOI: 10.1111/j.1750-3841.2012.02618.x
- [18] de Oliveira MS, da Costa WA, Pereira DS, Botelho JRS, de Alencar Menezes TO, de Aguiar Andrade EH, da Silva SHM, da Silva Sousa Filho AP, de Carvalho RN. Chemical composition and phytotoxic activity of clove (*Syzygium aromaticum*) essential oil obtained with supercritical CO₂. *Journal of Supercritical Fluids*. 2016;**118**:185-193. DOI: 10.1016/j.supflu.2016.08.010
- [19] Brunner G. *Gas Extraction*. Heidelberg: Steinkopff; 1994. DOI: 10.1007/978-3-662-07380-3
- [20] Kiran E, Brennecke JF. Current state of supercritical fluid science and technology. In: Comstock MJ, editor. *Supercritical Fluid Engineering Science, Fundamentals and Applications*. 514th ed. California: Los Angeles; 1992. pp. 1-8. DOI: 10.1021/bk-1992-0514.ch001
- [21] Kiran E, Debenedetti PG, Peters CJ. *Supercritical Fluids. Fundamentals and Applications*. Dordrecht: Springer Netherlands; 2000. DOI: 10.1007/978-94-011-3929-8
- [22] Meireles MAA. *Extracting Bioactive Compounds for Food Products: Theory and Applications*. 1st ed. London, New York: CRC Press Taylor & Francis Group Boca Raton; 2008
- [23] Jesus SP, Meireles MAA. Supercritical fluid extraction: A global perspective of the fundamental concepts of this eco-friendly extraction technique. In: Chemat F, Vian MA, editors. *Green Chemistry and Sustainable Technology*. Berlin, Heidelberg: Springer Berlin Heidelberg; 2014. pp. 39-72. DOI: 10.1007/978-3-662-43628-8_3
- [24] Sovová H, Stateva RP. Supercritical fluid extraction from vegetable materials. *Reviews in Chemical Engineering*. 2011;**27**:79-156. DOI: 10.1515/REVCE.2011.002
- [25] de Batista CCR, de Oliveira MS, Araújo ME, Rodrigues AMC, Botelho JRS, da Silva Souza Filho AP, Machado NT, Carvalho RN. Supercritical CO₂ extraction of açai (*Euterpe oleracea*) berry oil: Global yield, fatty acids, allelopathic activities, and determination of phenolic and anthocyanins total compounds in the residual pulp. *Journal of Supercritical Fluids*. 2016;**107**:364-369. DOI: 10.1016/j.supflu.2015.10.006
- [26] Dias ALS, Rozet E, Chataigné G, Oliveira AC, Rabelo CAS, Hubert P, Rogez H, Quetin-Leclercq J. A rapid validated UHPLC-PDA method for anthocyanins quantification from *Euterpe oleracea* fruits. *Journal of Chromatography B*. 2012;**907**:108-116. DOI: 10.1016/j.jchromb.2012.09.015
- [27] Gouvêa ACMS, De Araujo MCP, Schulz DF, Pacheco S, Godoy RLDO, Cabral LMC. Anthocyanins standards (cyanidin-3-O-glucoside and cyanidin-3-O-rutinoside) isolation from freeze-dried açai (*Euterpe oleraceae* Mart.) by HPLC. *Ciencia e Tecnologia de Alimentos*. 2012;**32**:43-46. DOI: 10.1590/S0101-20612012005000001
- [28] Lichtenthaler R, Rodrigues RB, Maia JGS, Papagiannopoulos M, Fabricius H, Marx F. Total oxidant scavenging capacities of *Euterpe oleracea* Mart. (Açai) fruits. *International Journal of Food Sciences and Nutrition*. 2005;**56**:53-64. DOI: 10.1080/09637480500082082

- [29] Kang J, Thakali KM, Xie C, Kondo M, Tong Y, Ou B, Jensen G, Medina MB, Schauss AG, Wu X. Bioactivities of açai (*Euterpe precatoria* Mart.) fruit pulp, superior antioxidant and anti-inflammatory properties to *Euterpe oleracea* Mart. Food Chemistry. 2012;**133**:671-677. DOI: 10.1016/j.foodchem.2012.01.048
- [30] Gordon A, Cruz APG, Cabral LMC, de Freitas SC, Taxi CMAD, Donangelo CM, de Andrade Mattietto R, Friedrich M, da Matta VM, Marx F. Chemical characterization and evaluation of antioxidant properties of Açai fruits (*Euterpe oleraceae* Mart.) during ripening. Food Chemistry. 2012;**133**:256-263. DOI: 10.1016/j.foodchem.2011.11.150
- [31] Vidigal MCTR, Minim VPR, Carvalho NB, Milagres MP, Gonçalves ACA. Effect of a health claim on consumer acceptance of exotic Brazilian fruit juices: Açai (*Euterpe oleracea* Mart.), Camu-camu (*Myrciaria dubia*), Cajá (*Spondias lutea* L.) and Umbu (*Spondias tuberosa* Arruda). Food Research International. 2011;**44**:1988-1996. DOI: 10.1016/j.foodres.2010.11.028
- [32] Hogan S, Chung H, Zhang L, Li J, Lee Y, Dai Y, Zhou K. Antiproliferative and antioxidant properties of anthocyanin-rich extract from açai. Food Chemistry. 2010;**118**:208-214. DOI: 10.1016/j.foodchem.2009.04.099
- [33] Kang J, Li Z, Wu T, Jensen GS, Schauss AG, Wu X. Anti-oxidant capacities of flavonoid compounds isolated from acai pulp (*Euterpe oleracea* Mart.). Food Chemistry. 2010;**122**:610-617. DOI: 10.1016/j.foodchem.2010.03.020
- [34] Xu Z, Wu J, Zhang Y, Hu X, Liao X, Wang Z. Extraction of anthocyanins from red cabbage using high pressure CO₂. Bioresource Technology. 2010;**101**:7151-7157. DOI: 10.1016/j.biortech.2010.04.004
- [35] Cerón IX, Higuera JC, Cardona CA. Design and analysis of antioxidant compounds from Andes berry fruits (*Rubus glaucus* Benth) using an enhanced-fluidity liquid extraction process with CO₂ and ethanol. Journal of Supercritical Fluids. 2012;**62**:96-101. DOI: 10.1016/j.supflu.2011.12.007
- [36] Santos DT, Veggi PC, Meireles MAA. Optimization and economic evaluation of pressurized liquid extraction of phenolic compounds from Jaboticaba skins. Journal of Food Engineering. 2012;**108**:444-452. DOI: 10.1016/j.jfoodeng.2011.08.022
- [37] Span R, Wagner W. A new equation of state for carbon dioxide covering the fluid region from the triple-point temperature to 1100 K at pressures up to 800 MPa. Journal of Physical and Chemical Reference Data. 1996;**25**:1509-1596. DOI: 10.1063/1.555991
- [38] Peng D-Y, Robinson DB. A new two-constant equation of state. Industrial and Engineering Chemistry Fundamentals. 1976;**15**:59-64. DOI: 10.1021/i160057a011
- [39] Soave G. Equilibrium constants from a modified Redlich-Kwong equation of state. Chemical Engineering Science. 1972;**27**:1197-1203. DOI: 10.1016/0009-2509(72)80096-4
- [40] Pfohl O, Petkov S, Brunner G. "PE" quickly makes available the newest equations of state via the internet. Industrial and Engineering Chemistry Research. 2000;**39**:4439-4440. DOI: 10.1021/ie000778t

- [41] Brunner G. Hydrothermal and Supercritical Water Processes. Amsterdam: Supercritical fluid science and technology; 2014. DOI: 10.1016/B978-0-444-59413-6.00009-1
- [42] Bertucco A, Vetter G. High Pressure Process Technology: Fundamentals and Applications. United Kingdom: Elsevier Science & Technology; 2001. DOI: 10.1016/S0926-9614(01)80016-2
- [43] Bimakr M, Rahman RA, Taip FS, Ganjloo A, Salleh LM, Selamat J, Hamid A, Zaidul ISM. Comparison of different extraction methods for the extraction of major bioactive flavonoid compounds from spearmint (*Mentha spicata* L.) leaves. Food and Bioproducts Processing. 2011;**89**:67-72. DOI: 10.1016/j.fbp.2010.03.002
- [44] Eller FJ, Cermak SC, Taylor SL. Supercritical carbon dioxide extraction of cuphea seed oil. Industrial Crops and Products. 2011;**33**:554-557. DOI: 10.1016/j.indcrop.2010.12.017
- [45] Ruttarattanamongkol K, Siebenhandl-Ehn S, Schreiner M, Petrasch AM. Pilot-scale supercritical carbon dioxide extraction, physico-chemical properties and profile characterization of *Moringa oleifera* seed oil in comparison with conventional extraction methods. Industrial Crops and Products. 2014;**58**:68-77. DOI: 10.1016/j.indcrop.2014.03.020
- [46] Ledesma-Hernandez B, Herrero M. Bioactive Compounds from Marine Foods. Chichester, UK: John Wiley & Sons Ltd; 2013. DOI: 10.1002/9781118412893
- [47] Jiao J, Fu Y-J, Zu Y-G, Luo M, Wang W, Zhang L, Li J. Enzyme-assisted microwave hydro-distillation essential oil from *Fructus forsythia*, chemical constituents, and its antimicrobial and antioxidant activities. Food Chemistry. 2012;**134**:235-243. DOI: 10.1016/j.foodchem.2012.02.114
- [48] Guan W, Li S, Yan R, Tang S, Quan C. Comparison of essential oils of clove buds extracted with supercritical carbon dioxide and other three traditional extraction methods. Food Chemistry. 2007;**101**:1558-1564. DOI: 10.1016/j.foodchem.2006.04.009
- [49] Conde-Hernández LA, Espinosa-Victoria JR, Trejo A, Guerrero-Beltrán JÁ. CO₂-supercritical extraction, hydrodistillation and steam distillation of essential oil of rosemary (*Rosmarinus officinalis*). Journal of Food Engineering. 2017;**200**:81-86. DOI: 10.1016/j.jfoodeng.2016.12.022
- [50] Shahsavarpour M, Lashkarbolooki M, Eftekhari MJ, Esmaeilzadeh F. Extraction of essential oils from *Mentha spicata* L. (Labiatae) via optimized supercritical carbon dioxide process. Journal of Supercritical Fluids. 2016;2-9. DOI: 10.1016/j.supflu.2017.02.004
- [51] Abbas A, Anwar F, Ahmad N. Variation in physico-chemical composition and biological attributes of common basil essential oils produced by hydro-distillation and supercritical fluid extraction. Journal of Essential Oil-Bearing Plants. 2017;**20**:95-109. DOI: 10.1080/0972060X.2017.1280418
- [52] Vági E, Simándi B, Suhajda Á, Héthelyi É. Essential oil composition and antimicrobial activity of *Origanum majorana* L. extracts obtained with ethyl alcohol and supercritical carbon dioxide. Food Research International. 2005;**38**:51-57. DOI: 10.1016/j.foodres.2004.07.006

- [53] Bagheri H, Bin Abdul Manap MY, Solati Z. Antioxidant activity of *Piper nigrum* L. essential oil extracted by supercritical CO₂ extraction and hydro-distillation. *Talanta*. 2014;**121**:220-228. DOI: 10.1016/j.talanta.2014.01.007
- [54] Ocaña-Fuentes A, Arranz-Gutiérrez E, Señorans FJ, Reglero G. Supercritical fluid extraction of oregano (*Origanum vulgare*) essentials oils: Anti-inflammatory properties based on cytokine response on THP-1 macrophages. *Food and Chemical Toxicology*. 2010;**48**:1568-1575. DOI: 10.1016/j.fct.2010.03.026
- [55] Pavela R, Sajfrtová M, Sovová H, Bárnét M, Karban J. The insecticidal activity of *Tanacetum parthenium* (L.) Schultz Bip. extracts obtained by supercritical fluid extraction and hydrodistillation. *Industrial Crops and Products*. 2010;**31**:449-454. DOI: 10.1016/j.indcrop.2010.01.003
- [56] Oliveira MS, da Costa WA, Pereira DS, Botelho JRS, de Alencar Menezes TO, de Aguiar Andrade EH, da Silva SHM, da Silva Sousa Filho AP, de Carvalho RN. Chemical composition and phytotoxic activity of clove (*Syzygium aromaticum*) essential oil obtained with supercritical CO₂. *Journal of Supercritical Fluids*. 2016;**118**:185-193. DOI: 10.1016/j.supflu.2016.08.010
- [57] Larkeche O, Zermane a, Meniai a-H, Crampon C, Badens E. Supercritical extraction of essential oil from *Juniperus communis* L. needles: Application of response surface methodology. *Journal of Supercritical Fluids*. 2015;**99**:8-14. DOI: 10.1016/j.supflu.2015.01.026
- [58] Khajeh M. Optimization of process variables for essential oil components from *Satureja hortensis* by supercritical fluid extraction using Box-Behnken experimental design. *Journal of Supercritical Fluids*. 2011;**55**:944-948. DOI: 10.1016/j.supflu.2010.10.017
- [59] Zermane A, Larkeche O, Meniai A-H, Crampon C, Badens E. Optimization of essential oil supercritical extraction from Algerian *Myrtus communis* L. leaves using response surface methodology. *Journal of Supercritical Fluids*. 2014;**85**:89-94. DOI: 10.1016/j.supflu.2013.11.002
- [60] Uquiche E, Cirano N, Millao S. Supercritical fluid extraction of essential oil from *Leptocarpha rivularis* using CO₂. *Industrial Crops and Products*. 2015;**77**:307-314. DOI: 10.1016/j.indcrop.2015.09.001
- [61] Chen Z, Mei X, Jin Y, Kim E-H, Yang Z, Tu Y. Optimisation of supercritical carbon dioxide extraction of essential oil of flowers of tea (*Camellia sinensis* L.) plants and its antioxidative activity. *Journal of the Science of Food and Agriculture*. 2014;**94**:316-321. DOI: 10.1002/jsfa.6260
- [62] Moreau RA, Whitaker BD, Hicks KB. Phytosterols, phytostanols, and their conjugates in foods: Structural diversity, quantitative analysis, and health-promoting uses. *Progress in Lipid Research*. 2002;**41**:457-500. DOI: 10.1016/S0163-7827(02)00006-1
- [63] Awad AB, Fink CS. Phytosterols as anticancer dietary components: Evidence and mechanism of action. *The Journal of Nutrition*. 2000;**130**:2127-2130. <http://jn.nutrition.org/content/130/9/2127.long>

- [64] Ling WH, Jones PJH. Dietary phytosterols: A review of metabolism, benefits and side effects. *Life Sciences*. 1995;**57**:195-206. DOI: 10.1016/0024-3205(95)00263-6
- [65] Ostlund RE. Phytosterols in human nutrition. *Annual Review of Nutrition*. 2002;**22**:533-549. DOI: 10.1146/annurev.nutr.22.020702.075220
- [66] Nyam KL, Tan CP, Lai OM, Long K, Man YBC. Optimization of supercritical CO₂ extraction of phytosterol-enriched oil from Kalahari melon seeds. *Food and Bioprocess Technology*. 2011;**4**:1432-1441. DOI: 10.1007/s11947-009-0253-4
- [67] Nyam KL, Tan CP, Lai OM, Long K, Che Man YB. Optimization of supercritical fluid extraction of phytosterol from roselle seeds with a central composite design model. *Food and Bioprocess Technology*. 2010;**88**:239-246. DOI: 10.1016/j.fbp.2009.11.002
- [68] Hrabovski N, Sinadinović-Fišer S, Nikolovski B, Sovilj M, Borota O. Phytosterols in pumpkin seed oil extracted by organic solvents and supercritical CO₂. *European Journal of Lipid Science and Technology*. 2012;**114**:1204-1211. DOI: 10.1002/ejlt.201200009
- [69] Uquiche E, Romero V, Ortíz J, Del Valle JM. Extraction of oil and minor lipids from cold-press rapeseed cake with supercritical CO₂. *Brazilian Journal of Chemical Engineering*. 2012;**29**:585-597. DOI: 10.1590/S0104-66322012000300016
- [70] Sajfirtová M, Ličková I, Wimmerová M, Sovová H, Wimmer Z. β -Sitosterol: Supercritical carbon dioxide extraction from sea buckthorn (*Hippophae rhamnoides* L.) seeds. *International Journal of Molecular Sciences*. 2010;**11**:1842-1850. DOI: 10.3390/ijms11041842
- [71] Botelho JRS, Medeiros NG, Rodrigues AMC, Araújo ME, Machado NT, Guimarães Santos A, Santos IR, Gomes-Leal W, Carvalho RN. Black sesame (*Sesamum indicum* L.) seeds extracts by CO₂ supercritical fluid extraction: Isotherms of global yield, kinetics data, total fatty acids, phytosterols and neuroprotective effects. *Journal of Supercritical Fluids*. 2014;**93**:49-55. DOI: 10.1016/j.supflu.2014.02.008
- [72] Wang H, Yang A, Zhang G, Ma B, Meng F, Peng M, Wang H. Enhancement of carotenoid and bacteriochlorophyll by high salinity stress in photosynthetic bacteria. *International Biodeterioration and Biodegradation*. 2017;**121**:91-96. DOI: 10.1016/j.ibiod.2017.03.028
- [73] Martins N, Ferreira ICFR. Wastes and by-products: Upcoming sources of carotenoids for biotechnological purposes and health-related applications. *Trends in Food Science and Technology*. 2017;**62**:33-48. DOI: 10.1016/j.tifs.2017.01.014
- [74] Huang JJ, Lin S, Xu W, Cheung PCK. Occurrence and biosynthesis of carotenoids in phytoplankton. *Biotechnology Advances*. 2017;**35**:597-618. DOI: 10.1016/j.biotechadv.2017.05.001
- [75] Riccioni G, D'Orazio N, Franceschelli S, Speranza L. Marine carotenoids and cardiovascular risk markers. *Marine Drugs*. 2011;**9**:1166-1175. DOI: 10.3390/md9071166
- [76] Gammone MA, Riccioni G, D'Orazio N. Carotenoids: Potential allies of cardiovascular health? *Food & Nutrition Research*. 2015;**59**:1-11. DOI: 10.3402/fnr.v59.26762

- [77] Saini RK, Keum Y-S. Carotenoid extraction methods: A review of recent developments. *Food Chemistry*. 2018;**240**:90-103. DOI: 10.1016/j.foodchem.2017.07.099
- [78] Figueira JA, Pereira JAM, Porto-Figueira P, Câmara JS. Ultrasound-assisted liquid-liquid extraction followed by ultrahigh pressure liquid chromatography for the quantification of major carotenoids in tomato. *Journal of Food Composition and Analysis*. 2017;**57**:87-93. DOI: 10.1016/j.jfca.2016.12.022
- [79] Hiranvarachat B, Devahastin S. Enhancement of microwave-assisted extraction via intermittent radiation: Extraction of carotenoids from carrot peels. *Journal of Food Engineering*. 2014;**126**:17-26. DOI: 10.1016/j.jfoodeng.2013.10.024
- [80] Goula AM, Ververi M, Adamopoulou A, Kaderides K. Green ultrasound-assisted extraction of carotenoids from pomegranate wastes using vegetable oils. *Ultrasonics Sonochemistry*. 2017;**34**:821-830. DOI: 10.1016/j.ultsonch.2016.07.022
- [81] Kwang HC, Lee HJ, Koo SY, Song DG, Lee DU, Pan CH. Optimization of pressurized liquid extraction of carotenoids and chlorophylls from *Chlorella vulgaris*. *Journal of Agricultural and Food Chemistry*. 2010;**58**:793-797. DOI: 10.1021/jf902628j
- [82] Damergi E, Schwitzguébel JP, Refardt D, Sharma S, Holliger C, Ludwig C. Extraction of carotenoids from *Chlorella vulgaris* using green solvents and syngas production from residual biomass. *Algal Research*. 2017;**25**:488-495. DOI: 10.1016/j.algal.2017.05.003
- [83] Millao S, Uquiche E. Extraction of oil and carotenoids from pelletized microalgae using supercritical carbon dioxide. *Journal of Supercritical Fluids*. 2016;**116**:223-231. DOI: 10.1016/j.supflu.2016.05.049
- [84] Egydio JA, Moraes ÂM, Rosa PTV. Supercritical fluid extraction of lycopene from tomato juice and characterization of its antioxidation activity. *Journal of Supercritical Fluids*. 2010;**54**:159-164. DOI: 10.1016/j.supflu.2010.04.009
- [85] Hsu YW, Tsai CF, Chen WK, Ho YC, Lu FJ. Determination of lutein and zeaxanthin and antioxidant capacity of supercritical carbon dioxide extract from daylily (*Hemerocallis disticha*). *Food Chemistry*. 2011;**129**:1813-1818. DOI: 10.1016/j.foodchem.2011.05.116
- [86] Chen J-R, Wu J-J, Lin J-C-T, Wang Y-C, Young C-C, Shieh C-J, Hsu S-L, Chang C-MJ. Low density supercritical fluids precipitation of 9-cis and all trans- β -carotenes enriched particulates from *Dunaliella salina*. *Journal of Chromatography. A*. 2013;**1299**:1-9. DOI: 10.1016/j.chroma.2013.05.022
- [87] Goto M, Kanda H, Wahyudiono SM. Extraction of carotenoids and lipids from algae by supercritical CO₂ and subcritical dimethyl ether. *Journal of Supercritical Fluids*. 2015;**96**:245-251. DOI: 10.1016/j.supflu.2014.10.003
- [88] Heffernan N, Smyth TJ, FitzGerald RJ, Vila-Soler A, Mendiola J, Ibáñez E, Brunton NP. Comparison of extraction methods for selected carotenoids from macroalgae and the assessment of their seasonal/spatial variation. *Innovative Food Science & Emerging Technologies*. 2016;**37**:221-228. DOI: 10.1016/j.ifset.2016.06.004

- [89] Gunstone D, Norris FA. Lipids in Foods: Chemistry, Biochemistry and Technology. Oxford: Elsevier; 1983
- [90] Stirban A, Nandrea S, Go C, Tamler R, Pop A, Negrean M, Gawlowski T. Effects of n-3 fatty acids on macro- and microvascular function in subjects with type 2 diabetes mellitus 1–3. The American Journal of Clinical Nutrition. 2010;**91**:808-813. DOI: 10.3945/ajcn.2009.28374.1
- [91] Begg DP, Sinclair AJ, a Stahl L, Premaratna SD, Hafandi A, Jois M, Weisinger RS. Hypertension induced by omega-3 polyunsaturated fatty acid deficiency is alleviated by alpha-linolenic acid regardless of dietary source. Hypertension Research. 2010;**33**:808-813. DOI: 10.1038/hr.2010.84
- [92] De CR. N-3 fatty acids in cardiovascular disease. The New England Journal of Medicine. 2011;**364**:2439-2450
- [93] Oh DY, Talukdar S, Bae EJ, Imamura T, Morinaga H, Fan W, Li P, Lu WJ, Watkins SM, Olefsky JM. GPR120 is an Omega-3 fatty acid receptor mediating potent anti-inflammatory and insulin-sensitizing effects. Cell. 2010;**142**:687-698. DOI: 10.1016/j.cell.2010.07.041
- [94] Issariyakul T, Dalai AK. Biodiesel from vegetable oils. Renewable and Sustainable Energy Reviews. 2014;**31**:446-471
- [95] Hafis SM, Ridzuan MJM, Rahayu A, Farahana RN, Nor Fatin B, Syahrullail S. Properties of palm pressed fibre for metal forming lubricant applications. Procedia Engineering. 2013;**68**:130-137
- [96] Pádua MS, Paiva LV, Labory CRG, Alves E, Stein VC. Induction and characterization of oil palm (*Elaeis guineensis* Jacq.) pro-embryogenic masses. Anais da Academia Brasileira de Ciências. 2013;**85**:1545-1556. DOI: 10.1590/0001-37652013107912
- [97] Ezeh O, Gordon MH, Niranjana K. Enhancing the recovery of tiger nut (*Cyperus esculentus*) oil by mechanical pressing: Moisture content, particle size, high pressure and enzymatic pre-treatment effects. Food Chemistry. 2016;**194**:354-361. DOI: 10.1016/j.foodchem.2015.07.151
- [98] Koubaa M, Mhemdi H, Vorobiev E. Influence of canola seed dehulling on the oil recovery by cold pressing and supercritical CO₂ extraction. Journal of Food Engineering. 2016;**182**:18-25. DOI: 10.1016/j.jfoodeng.2016.02.021
- [99] Hu B, Li C, Zhang Z, Zhao Q, Zhu Y, Su Z, Chen Y. Microwave-assisted extraction of silkworm pupal oil and evaluation of its fatty acid composition, physicochemical properties and antioxidant activities. Food Chemistry. 2017;**231**:348-355. DOI: 10.1016/j.foodchem.2017.03.152
- [100] Bernardo-Gil MG, Casquilho M, Esquível MM, Ribeiro MA. Supercritical fluid extraction of fig leaf gourd seeds oil: Fatty acids composition and extraction kinetics. Journal of Supercritical Fluids. 2009;**49**:32-36. DOI: 10.1016/j.supflu.2008.12.004

- [101] Sánchez-Camargo AP, Martínez-Correa HA, Paviani LC, Cabral FA. Supercritical CO₂ extraction of lipids and astaxanthin from Brazilian redspotted shrimp waste (*Farfantepenaeus paulensis*). *Journal of Supercritical Fluids*. 2011;**56**:164-173. DOI: 10.1016/j.supflu.2010.12.009
- [102] Tomita K, Machmudah S, Quitain AT, Sasaki M, Fukuzato R, Goto M. Extraction and solubility evaluation of functional seed oil in supercritical carbon dioxide. *Journal of Supercritical Fluids*. 2013;**79**:109-113. DOI: 10.1016/j.supflu.2013.02.011
- [103] Wang XW, Liang JR, Luo CS, Chen CP, Gao YH. Biomass, total lipid production, and fatty acid composition of the marine diatom *Chaetoceros muelleri* in response to different CO₂ levels. *Bioresource Technology*. 2014;**161**:124-130. DOI: 10.1016/j.biortech.2014.03.012
- [104] Bartolomé Ortega A, Calvo Garcia A, Szekely E, Škerget M, Knez Ž. Supercritical fluid extraction from saw palmetto berries at a pressure range between 300 bar and 450 bar. *Journal of Supercritical Fluids*. 2017;**120**:132-139. DOI: 10.1016/j.supflu.2016.11.003
- [105] De Melo MMR, Silvestre AJD, Silva CM. Supercritical fluid extraction of vegetable matrices: Applications, trends and future perspectives of a convincing green technology. *Journal of Supercritical Fluids*. 2014;**92**:115-176. DOI: 10.1016/j.supflu.2014.04.007
- [106] Vatai T, Škerget M, Knez Ž. Extraction of phenolic compounds from elder berry and different grape marc varieties using organic solvents and/or supercritical carbon dioxide. *Journal of Food Engineering*. 2009;**90**:246-254. DOI: 10.1016/j.jfoodeng.2008.06.028
- [107] Mantell C, Rodríguez M, Martínez de la Ossa E. A screening analysis of the high-pressure extraction of anthocyanins from red grape pomace with carbon dioxide and cosolvent. *Engineering in Life Sciences*. 2003;**3**:38-42. DOI: 10.1002/elsc.200390004
- [108] Ghafoor K, AL-Juhaimi FY, Choi YH. Supercritical fluid extraction of phenolic compounds and antioxidants from grape (*Vitis labrusca* B.) seeds. *Plant Foods for Human Nutrition*. 2012;**67**:407-414. DOI: 10.1007/s11130-012-0313-1
- [109] L.E. Laroze, B. Díaz-Reinoso, A. Moure, M.E. Zúñiga, H. Domínguez, Extraction of antioxidants from several berries pressing wastes using conventional and supercritical solvents, *European Food Research and Technology* 231 (2010) 669-677. doi:10.1007/s00217-010-1320-9
- [110] Seabra IJ, Braga MEM, Batista MTP, de Sousa HC. Fractioned high pressure extraction of anthocyanins from elderberry (*Sambucus nigra* L.) pomace. *Food and Bioprocess Technology*. 2010;**3**:674-683. DOI: 10.1007/s11947-008-0134-2
- [111] Blevé M, Ciurlia L, Erroi E, Lionetto G, Longo L, Rescio L, Schettino T, Vasapolo G. An innovative method for the purification of anthocyanins from grape skin extracts by using liquid and sub-critical carbon dioxide. *Separation and Purification Technology*. 2008;**64**:192-197. DOI: 10.1016/j.seppur.2008.10.012
- [112] Paula JT, Paviani LC, Foglio MA, Sousa IMO, Duarte GHB, Jorge MP, Eberlin MN, Cabral FA. Extraction of anthocyanins and luteolin from *Arrabidaea chica* by sequential extraction in fixed bed using supercritical CO₂, ethanol and water as solvents. *Journal of Supercritical Fluids*. 2014;**86**:100-107. DOI: 10.1016/j.supflu.2013.12.008

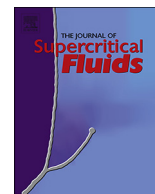
- [113] Bergeron C, Gafner S, Clausen E, Carrier DJ. Comparison of the chemical composition of extracts from *Scutellaria lateriflora* using accelerated solvent extraction and supercritical fluid extraction versus standard hot water or 70% ethanol extraction. *Journal of Agricultural and Food Chemistry*. 2005;**53**:3076-3080. DOI: 10.1021/jf048408t
- [114] Paes J, Dotta R, Barbero GF, Martínez J. Extraction of phenolic compounds and anthocyanins from blueberry (*Vaccinium myrtillus* L.) residues using supercritical CO₂ and pressurized liquids. *Journal of Supercritical Fluids*. 2014;**95**:8-16. DOI: 10.1016/j.supflu.2014.07.025

CAPÍTULO 2

2.1. Bacaba-de-leque (*Oenocarpus distichus* Mart.) Oil Extraction Using Supercritical CO₂ and Bioactive Compounds Determination in the Residual Pulp

Journal Author Rights

Please note that, as the author of this Elsevier article, you retain the right to include it in a thesis or dissertation, provided it is not published commercially. Permission is not required, but please ensure that you reference the journal as the original source. For more information on this and on your other retained rights, please visit: <https://www.elsevier.com/about/our-business/policies/copyright#Author-rights>



Bacaba-de-leque (*Oenocarpus distichus* Mart.) oil extraction using supercritical CO₂ and bioactive compounds determination in the residual pulp



Vânia Maria Borges Cunha^{a,*}, Marcilene Paiva da Silva^a, Sérgio Henrique Brabo de Sousa^a, Priscila do Nascimento Bezerra^a, Eduardo Gama Ortiz Menezes^a, Nayara Janaina Neves da Silva^a, Débora Ariane Dornelas da Silva Banna^a, Marilena Emmi Araújo^b, Raul Nunes de Carvalho Junior^{a,*}

^a LABEX (Laboratory of Supercritical Extraction), Faculty of Food Engineering, Federal University of Pará, Belém, Pará, Brazil

^b TERM@ (Laboratory of Separation Processes and Applied Thermodynamic), Faculty of Chemical Engineering, Federal University of Pará, Belém, Pará, Brazil

GRAPHICAL ABSTRACT



ARTICLE INFO

Keywords:

Oenocarpus distichus
Supercritical fluid extraction
Vegetable oil
Functional quality
Bioactive compounds

ABSTRACT

Oenocarpus distichus is a native palm from Brazilian Amazon biomes, its fruits are sources of bioactive compounds and, mainly, vegetable oil rich in unsaturated fatty acids. In this study, the supercritical CO₂ (Sc-CO₂) extraction was applied to obtain the bacaba-de-leque pulp oil, evaluating its composition and the bioactive compounds contents present in the pulp before and after the extraction. The maximum oil yields were reached at 50 °C/350 bar (45.23%) and 60 °C/270 bar (45.90%). The oleic, palmitic, and linoleic acids, as well as the predicted triglycerides OLiO, PLiO, OOO, POP, and POO were predominant in the oil composition, independent of the extraction conditions, and presented excellent functional quality. There was an increase in phenolic compounds, total anthocyanins contents, and antioxidant capacity of the bacaba-de-leque pulp extracts after the Sc-CO₂ extraction, showing possible applications for nutraceutical purposes.

1. Introduction

The palms of the *Oenocarpus* genus, from *Arecaceae* family, are native plants found in the Brazilian Amazon biomes. *O. distichus* Mart., *O.*

bacaba Mart., *O. minor* Mart., and *O. mapora* H. Karten species are some varieties of this genus that are known as bacabeiras and, like other species, are one of the most exploited by regional extractivism [1–3].

The *Oenocarpus distichus* species is popularly known as bacaba-de-

* Corresponding authors.

E-mail addresses: vaniacunha21@hotmail.com (V.M.B. Cunha), raulncj@ufpa.br (R.N.d. Carvalho Junior).

<https://doi.org/10.1016/j.supflu.2018.10.010>

Received 6 August 2018; Received in revised form 3 October 2018; Accepted 16 October 2018

Available online 19 October 2018

0896-8446/ © 2018 Elsevier B.V. All rights reserved.

leque and produces edible dark purple fruits and greenish pulp, which are collected by the local population for a drink preparation known as "bacaba wine" or transformed into fermented beverages, jellies, and ice creams. The economic importance of this species is mainly based on the palm heart exploitation and the fruits pulp oil extraction, used for edible purposes. The bacaba-de-leque pulp offers very similar products to açai (*Euterpe oleracea*) fruit in terms of flavor, having great ability to compete in the market, that can be an alternative to the use of açai, which is well known and exploited [4,5]. Despite this, there is little knowledge about this species, especially about its chemical composition. This is an important information inasmuch as it can indicate the fruit possible functional properties, encourage its consumption, and generate new alternatives of use with potential to be exploited as functional foods [6,7].

Some recent studies have shown that the fruits of species belonging to the genus *Oenocarpus* are potential sources of bioactive compounds with antioxidant capacity, such as phenolics, flavonoids, and anthocyanins determined in *Oenocarpus bacaba* [6], *Oenocarpus bataua* [8], and *Oenocarpus distichus* [9,10] fruits. The fruits of these palm trees are also a major source of high quality vegetable oils, rich in unsaturated fatty acids, which stand out for their nutritional relevance [11–14]. However, the chemical, physical, and biological properties of these oils are determined by the fatty acid type and its distribution in triglyceride (TG) molecules, which represent 95–98% of the total oil composition [15–17].

Traditionally, the vegetable oils extraction is carried out by methods with several disadvantages, especially with regard to the use of large quantities of organic solvents, where a set of refining processes is required to obtain the final product. The supercritical fluid extraction (SFE) application, using supercritical CO₂ (Sc – CO₂), can supply several of these conventional process stages, resulting from a single stage high quality oil and a residual cake completely solvent-free by simple depressurizing, and avoid thermal degradation of target compounds due to the low operating temperatures [18–20].

In the literature, some studies have applied SFE and demonstrated these advantages. Bacaba and Açai, oleaginous fruits, which belong to the *Arecaceae* family, were recently submitted to supercritical carbon dioxide extraction. Pinto et al [21] used Sc – CO₂ to extract oil from the lyophilized bacaba (*Oenocarpus bacaba*) pulp. The global yield isotherms experiments were carried out in 120, 170, and 290 bar pressures at 40 °C temperature and 190, 270, and 420 bar at 60 °C to evaluate the operating conditions that maximize the vegetable oil yield. The bacaba oil was characterized by fatty acid composition, functional quality, oxidative stability, spectroscopic profile and antioxidant activity. The results showed from their fatty acids composition and their functional quality indexes determination that bacaba oil may have cardioprotective activity due to the predominance of unsaturated fatty acids, suggesting its direct consumption as salad oil, similar to olive oil, or in the encapsulated form as a phytopharmaceutical. There was no information about the characterization of the residual defatted bacaba pulp. Batista et al [22] showed the efficiency of the SFE with Sc – CO₂ in the lyophilized açai (*Euterpe oleracea*) pulp oil extraction, rich in mono and polyunsaturated fatty acids, to obtain a residual cake concentrated in bioactive compounds (defatted pulp), where an increase in the phenolic compounds and total anthocyanins contents in the defatted acai berry pulp was observed after the Sc – CO₂ oil extraction. This shows that, unlike conventional methods, SFE can be efficient both in vegetable oils production and in the recovery of the extraction residue, been totally solvent-free.

Among the parameters that must be determined to design efficient supercritical extraction processes, the solubility in the supercritical fluid of pure compounds of interest or their mixtures is probably the most important, which should be evaluated on the basis of the effects of temperature (T), pressure (P) and density (ρ) of the solvent in order to determine the operating conditions of the extraction process [23–25].

Natural extracts such as vegetable oils are complex systems

(multicomponent mixtures) and despite the great efforts have been devoted, very little data exists in the literature concerning the phase equilibrium (both phases or solubility) measurements of complex systems such as fats and oil or any other natural extracts in supercritical CO₂, because the experimental measurements are laborious, time-consuming and expensive. For this, the uses of cubic equations of state (EOS) models are fundamental tools for the correlation of experimental and prediction of solubility data. The correlation of experimental data at high pressures using EOS is of special importance because as it provides, besides the description of the phase equilibrium, the possibility of reducing the number of experiments required to define optimal operating conditions [23,26,27].

The Soave-Redlich-Kwong [28] and Peng-Robinson [29] EOS, combined with appropriate mixing rules, such as van der Waals, are the most often used due to represent with some precision the relations between temperature, pressure, and phase equilibrium composition of multicomponent mixtures [24,25].

The approach for modeling phase equilibria using EOS of complex systems and carbon dioxide have been applied considering the multicomponent mixture represented by the key compound of different chemical functions. The interaction parameters of the mixing rules were obtained from solubility and/or vapor-liquid equilibrium data of key compounds with carbon dioxide available in the literature. For the binary systems compound *i*/compound *j*, the interaction parameters were set equal to zero because of the lack of experimental phase equilibrium data [30–33].

The objective of this work was to determine the operational conditions (T, P, ρ) of the sc – CO₂ extraction, to obtain the best oil yield of the lyophilized bacaba-de-leque pulp (LBP). The global yield isotherms experiments were carried out in 150, 220, and 350 bar pressures at 50 °C and in 190, 270, and 420 bar at 60 °C. The extracted oils were analyzed by gas chromatography to evaluate the fatty acid composition profile which was used to estimate its triglycerides probable composition. The LBP residual cake (defatted pulp) was also evaluated based on the phenolic compounds, total anthocyanins, and antioxidant activity levels after SFE. The fatty acid composition profile was also used for the bacaba-de-leque pulp oil solubility prediction in Sc – CO₂, using the Peng-Robinson (PR) cubic equation of state, for a wider pressure range between 130 and 450 bar, at the same temperatures of the global yield experiments, in order to contribute to the operating conditions definition that maximize the extraction yield.

2. Materials and methods

2.1. Pretreatment and characterization of raw material

Bacaba-de-leque (*Oenocarpus distichus* Mart) fruits used in this study were collected from a sub-sample available at the Active Germplasm Bank (AGB) of bacaba palm tree of the Brazilian Agricultural Research Corporation, Embrapa Eastern Amazon, located in Belém, Pará state, Brazil. Approximately 6 kg of fruits were selected, washed, and submitted to water at 60 °C for 15 min to facilitate the pulp extraction (traditional way of obtaining the pulp). The mechanical pulping was performed in 2:1 (fruit:water, w/v) proportion in a stainless steel vertical machine (METVISA® DG.10, Belém, Brazil) previously sanitized and the seeds were discarded.

The extracted pulp was stored in polyethylene bags (HDPE) and immediately frozen at -18 °C in a cold room. After freezing, the material was lyophilized at -55 °C for 48 h using a bench freeze dryer (Liotop, L101, São Paulo, Brazil), the samples were then vacuum packed in polypropylene bags (BOPP) and stored at 10 °C under light protection until chemical analysis and oil extraction.

For the characterization of the lyophilized bacaba-de-leque pulp (LBP) the humidity of the sample was determined by the distillation method with Jacobs immiscible solvent [34], total protein and ash content [35], total lipid content [36], and the crude fiber content were

determined by [37]. The analyses were performed in triplicate.

The true density of the particles (ρ_r) was determined with a helium pycnometer (model Ultrapyc 1200e, Quantachrome, USA) in triplicate, at the Analytical Center of the Chemistry Institute of the University of Campinas (UNICAMP). While the apparent density (ρ_a) was calculated from the ratio of the sample mass to the sample volume packed in the fixed bed extraction vessel. The porosity (ϵ) of the bed was determined from the mathematical relationship between the true and apparent densities, according to Eq. (1).

$$\epsilon = 1 - \frac{\rho_a}{\rho_r} \quad (1)$$

2.2. Supercritical fluid extraction (SFE)

Extractions of the LBP oil with supercritical carbon dioxide (Sc-CO₂) were carried out at the Supercritical Extraction Laboratory at the Federal University of Pará (LABEX/UFPA), Belém, Pará, Brazil. Using the *Spe-ed*[™] SFE of Applied Separations (model 7071, Allentown, USA) equipment, coupled to a CO₂ cylinder (99.9% purity, White Martins, Belém, Pará, Brazil), an air compressor with an internal volume of 19.71 (model CSA 7.8, Schulz S/A, Brazil), a recirculator (model F08400796, Polyscience, USA), and a CO₂ flowmeter on the system output (model M 5SLPM, Alicat Scientific system, USA). The extraction vessel capacity was 5×10^{-5} m³ (height: 0.3248 m, internal diameter: 0.0142 m).

For the global yield isotherms determination, 5 g of lyophilized pulp was used as feed mass, forming a bed of 0.066 m height and 0.0142 m diameter in the extraction vessel. The process operating temperatures were 50 °C combined with 150, 220, and 350 bar and 60 °C combined with 190, 270, and 420 bar and CO₂ mass flow rate of 5.31 g/min. The CO₂ density under these conditions was calculated using a software developed by the National Institute of Standards and Technology (NIST), which uses the Span and Wagner equation of state [38]. The extraction was performed in three periods: a 30 min static period (system stabilization time), a 180 min dynamic period (oil extraction time), and a 20 min system depressurizing period. The oil was continuously collected in glass vials used as sample collectors at ambient pressure. The extractions were performed in duplicate for each experimental condition.

The global yield (X_0) was calculated from the mathematical ratio between the mass of oil obtained (m_{oil}) and the initial mass of raw material used for extraction on a dry basis ($m_{raw\ material}$), according to Eq. (2).

$$X_0 (\%) = \frac{m_{oil}}{m_{raw\ material}} \times 100 \quad (2)$$

2.3. Oil characterization from lyophilized bacaba-de-leque pulp (LBP)

2.3.1. Fatty acids composition of LBP oil

The fatty acid profile was determined by gas chromatography (GC) of fatty acid methyl esters (FAME's). The oil was first derivatized to form the FAME's according to the method proposed by Hartman and Lago [39]. The experiment consisted basically of saponification with methanolic solution of 0.5 N potassium hydroxide followed by esterification with methanolic solution of sulfuric acid and hexane extraction. The FAME's analysis was performed in a gas chromatograph (model 6820 BPX90, Agilent, USA), equipped with a capillary column (DB23, Agilent, USA, 60 m length \times 0,25 mm internal diameter \times 0,25 μ m film thickness) and a flame ionization detector (FID). Hydrogen gas was used as a carrier gas at 1 mL/min flow. An aliquot of 1 μ L of the sample was injected with the injector at 250 °C and the detector at 280 °C. The column temperature was programmed to start at 70 °C and then increased to 250 °C at a heating rate of 5 °C/min. The qualitative fatty acids composition of the samples were determined by

comparing the peaks retention times produced after the injection with the respective fatty acid standards. The quantitative composition was obtained by the peak areas using the Agilent Cerity software and the results were expressed in percentage by mass. The experiments were performed in duplicate.

2.3.2. Functional quality of LBP oil

To evaluate the functional quality of the LBP oil, three indices of nutritional quality of the lipid fractions were determined, using the fatty acids. The ratio between hypocholesterolemic and hypercholesterolemic fatty acids (H/H) was calculated according to the formulas suggested by Santos-Silva et al. [40]:

$$H/H = \frac{C18:1\omega9 + C18:2\omega6 + C20:4\omega6 + C18:3\omega3 + C20:5\omega3 + C22:5\omega3 + C22:6\omega3}{C14:0 + C16:0} \quad (3)$$

Atherogenicity index (IA) and thrombogenicity index (IT) were calculated according to the formulas proposed by Ulbrich and Southgate [41]:

$$AI = \frac{C12:0 + 4(C14:0) + C16:0}{\sum MUFA + \sum \omega - 6 + \sum \omega - 3} \quad (4)$$

$$TI = \frac{C14:0 + C16:0 + C18:0}{0.5(\sum MUFA) + 0.5(\sum \omega - 6) + 3(\sum \omega - 3) + (\sum \omega - 3/\sum \omega - 6)} \quad (5)$$

Where: C12:0 (lauric acid); C14:0 (myristic acid); C16:0 (palmitic acid); C18:0 (stearic acid); C18:1 ω 9 (oleic acid); C18:2 ω 6 (linoleic acid); C18:3 ω 3 (linolenic acid); C20:4 ω 6 (arachidonic acid); C20:5 ω 3 (eicosapentaenoic acid); 22:5 ω 3 (docosapentaenoic acid); C22:6 ω 3 (docosahexaenoic acid), Σ MUFA (sum of the monounsaturated fatty acids concentrations); $\Sigma\omega$ -6 (sum of the polyunsaturated fatty acids ω -6 concentrations); $\Sigma\omega$ -3 (sum of the polyunsaturated fatty acids ω -3 concentrations).

2.3.3. Probable triglycerides composition of LBP oil

The difficulty in identifying the triglyceride peaks obtained in the chromatograms is due to the large number of species that may be present in a natural mixture, considering that the number of possible triglycerides with N fatty acids is N³, if all the isomers are considered. As there are not enough commercially available standards, mathematical and statistical calculations are used.

The complex triglycerides composition of the LBP was determined in this work based on random distribution theory proposed by Norris and Mattil [42], which consists of a statistical technique that uses the fatty acids molar fraction previously determined. The probable triglyceride composition profile was calculated by an Excel spreadsheet, developed by the Laboratory of Separation Processes and Applied Thermodynamic (TERM@/UFPA), which apply the knowledge of combinatorial analysis associated with an algorithm using the concept of a simple binomial tree implemented in Visual Basic for Applications in Excel (VBA) to determine the possible combinations.

2.4. Predicted solubility of LBP oil in Sc-CO₂

The solubility of LBP oil in Sc-CO₂ was determined according to the methodology described by Cunha et al [33]. The methodology assumes that the oil can be considered as a fatty acids mixture, where a cubic equation of state combined with a mixing rule is applied to describe the phase equilibrium behavior of the supercritical CO₂ + oil system over a range of temperature and pressure.

For the solubility prediction of a multicomponent mixture, using a cubic equation of state requires information about the critical temperature (T_c), critical pressure (P_c), and acentric factor (ω) of all pure components that constitute the multicomponent system, the oil

composition (experimentally determined) and the binary interaction parameters between the pure components and the CO₂. The values of the critical properties (T_c and P_c) and acentric factors (ω) of the fatty acids and the binary interaction parameters used in this study are the results of the evaluation of the physical properties predictive methods accomplished and calculated by Araújo and Meireles [43]. For the fatty acid/CO₂ binary systems, as well as the parameters for the fatty acid *i*/fatty acid *j* binary systems, equilibrium data do not exist, the binary interaction parameters were considered equal to zero, according to approach described in the literature [30,31,33].

The molar fraction of each solute of the mixture (fatty acids) in the gas phase of the LBP oil + Sc–CO₂ liquid-gas equilibrium system was calculated using the EDEFLASH program, using the Peng-Robinson (PR) cubic equation of state [29] with the van der Waals (vdW) mixing rule using two binary interaction parameters. The molar fraction values of each gas phase component of the liquid-gas equilibrium were converted to solubility (S) according to the equation below. The results were expressed in g of oil/kg of CO₂.

$$S = \frac{\sum M_i z_i}{M_{CO_2} z_{CO_2}} \quad (6)$$

Where: z_i is the component *i* molar fraction in the gas phase; *M* is the molar mass of each component.

The solubility was evaluated in the 50 and 60 °C isotherms, in the 130–450 bar pressure range, applying the fatty acid composition of the extracted oil at 50 °C/350 bar and 60 °C/420 bar.

2.5. Determination of bioactive compounds from lyophilized bacaba-de-leque pulp before and after extraction with Sc–CO₂

2.5.1. Preparation of the samples

In order to obtain the samples, the lyophilized bacaba-de-leque pulp (LBP) and the residual cake obtained after Sc–CO₂ extraction at different temperatures and pressures were solubilized in 10 mL of ethanol/water solution (70:30, v/v). The mixtures were homogenized in a light protected environment and centrifuged for 10 min at 4 °C at 3000xg (Termo Multifige Scientific, XR1, USA). After centrifugation, the supernatant was filtered on glass fiber filter paper and stored in an amber bottle protected from light at –18 °C.

2.5.2. Total phenolic compounds in LBP and defatted LBP

The total phenolic compounds determination was performed according to the colorimetric method described by Singleton & Rossi [44] and modified by Georgé et al. [45]. Aliquots of 0.5 mL from the different extracts, obtained according to item 2.5.1, were submitted to Folin-Ciocalteu reaction. For quantification, a UV–vis spectrophotometer (Thermo Scientific, Evolution 300, San Jose, USA) reading was performed at 760 nm using gallic acid as the standard, at concentrations ranging from 20 to 100 mg/L (r² = 0.99). The results of total phenolic compounds content (n = 3) were expressed in mg of gallic acid equivalents per gram of dry basis (db) sample (mg AGE/g).

2.5.3. Total anthocyanins in LBP and defatted LBP

The total anthocyanins quantification was performed according to the differential pH spectrophotometric method described by Giusti and Wrolstad [46]. Absorbance readings were performed in a spectrophotometer (Thermo Scientific, Evolution 300, San Jose, USA), at a wavelength of 510 and 700 nm. The calculations were performed according to Eqs. (7) and (8).

$$Abs = [(Abs_{510nm} - Abs_{700nm})_{pH1.0} - (Abs_{510nm} - Abs_{700nm})_{pH4.5}] \quad (7)$$

$$Total\ anthocyanins\ (mg/L) = \frac{Abs \times 10^3 \times MW \times FD}{(\epsilon \times L)} \quad (8)$$

Where: Abs is the absorbance calculated by Eq. (4); MW is the molecular weight relative to cyaniding 3-rutinoside (594 g/mol); FD is the

dilution factor given by the ratio between the volume of dilution (in liters) and the sample mass (in grams); ε is the molar absorptivity of cyanidin 3-rutinoside in buffer solution at pH 1.0 at 510 nm (28,840 L/mol/cm), and L is the cuvette optical path (1 cm). The results were expressed as mg cyaniding 3-rutinoside equivalent/g of dry basis sample (db).

2.6. Evaluation of the antioxidant capacity of LBP and defatted LBP

2.6.1. TEAC or ABTS⁺ assay

The LBP antioxidant capacity before and after extraction with Sc–CO₂ was determined by the Trolox Equivalent Antioxidant Capacity (TEAC) method according to the procedure proposed by Miller et al. [47] with adaptations. The ABTS⁺ radical was obtained from the reaction in aqueous solution of ABTS⁺ (2,2'-azino-bis (3-ethylbenzothiazoline-6-sulphonic acid) at 7 μM with potassium persulfate at 140 μM. The mixture was allowed to stand in the dark at room temperature (≈22 °C) for 12–16 hours. Once the ABTS⁺ radical was formed, the dilution was performed in ethanol: water solution (70:30 v/v) until absorbance of 0.7 ± 0.05 nm. As reference, an analytical curve was elaborated with trolox (6-hydroxy-2,5,7,8-tetramethylchroman-2-carboxylic acid) at concentrations of 0.01–0.20 mg/L (r² = 0.99) and the results calculated and expressed in μM trolox/g of dry basis sample (db).

2.6.2. DPPH' (free radical scavenging) assay

The LBP antioxidant capacity before and after Sc–CO₂ extraction was determined by the method developed by Brand-Williams et al. [48] with adaptations. Based on the elimination of the DPPH' (2,2-diphenyl-1-picrylhydrazyl) radical by the antioxidants present in the extracts An ethanol/water solution (70:30, v/v) containing 0.06 mM DPPH' was prepared. Then, after the blank adjusting with ethanol, a 100 μL aliquot of the lyophilized pulp and residual cake from Sc–CO₂ extractions were added to 3.9 mL of the solution containing 0.06 mM of DPPH'. The decrease in absorbance at 515 nm was monitored by spectrophotometry at 1 min intervals for the first 10 min and then at 5 min intervals until stabilization (60 min as determined by a preliminary study). An analytical curve was prepared with Trolox (0.01 to 0.20 mg/L) and the results (n = 3) were expressed in μmol trolox equivalent (TE) per g of dry basis sample (db).

2.7. Statistical analysis

All analyzes were performed in triplicate and the results were expressed as the mean of three independent replicates (n = 3). To verify the existence of a significant difference between SFE conditions, the results means were submitted to analysis of variance and, when significant, compared by the Tukey test at 95% probability, with the aid of the Statistica® program version 7.1 (Statsoft, Inc. Tulsa, USA).

3. Results and discussion

3.1. Characterization of the raw material

LBP presented 4.52% ± 0.02 of humidity; constituted by 1.14% ± 0.015 of ash; 44.53% ± 0.12 of lipid; 6.72% ± 0.08 of proteins; 21.58% ± 0.22 of crude fiber; and 19.9% ± 0.14 of carbohydrates. The true density was 1130 kg/m³, apparent density was 428.7 kg/m³ and the bed porosity was 0.6206. These physical characteristics of the raw material were adequate for the SFE, being considered some of the main parameters that have direct action on the mass transfer rate of the process. Generally, an increase in porosity of the solid matrix provides a faster and more efficient extraction, which is related to the distribution of the particles in the bed during the packaging of the matrix in the extraction vessel [18].

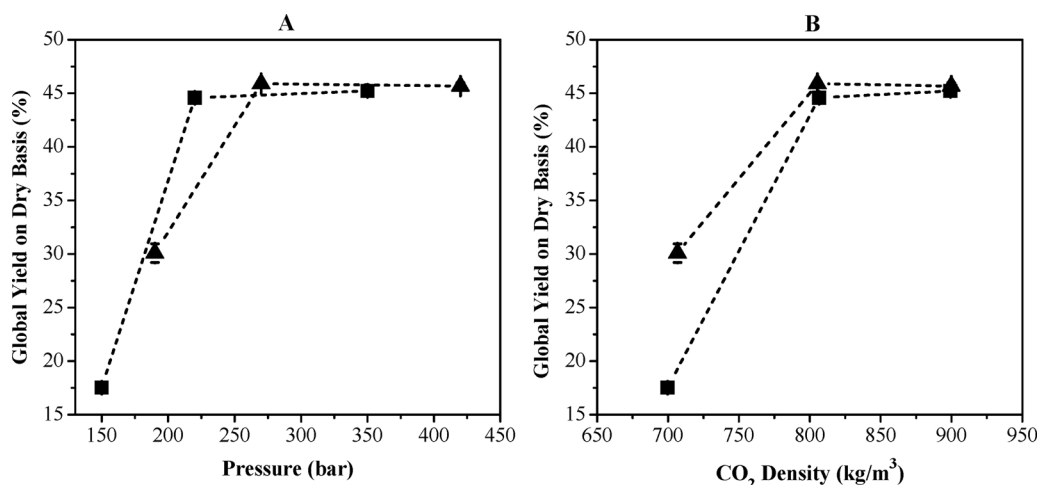


Fig. 1. Global yield isotherms obtained by SFE of lyophilized bacaba-de-leque (*O. distichus* Mart) pulp oil versus pressure (A) and CO₂ density (B), at (■) 50 °C and (▲) 60 °C.

3.2. Global yield (X_0)

The results of the global yield isotherms (dry basis) in relation to the pressure and density of CO₂ are shown in Fig. 1 (A) and (B). The standard deviation of global yields ranged from 0.147 to 0.877%. The lowest yields were $17.51\% \pm 0.18$ at 50 °C/150 bar ($\rho = 699.75 \text{ kg/m}^3$) and $30.09\% \pm 0.88$ at 60 °C/190 bar ($\rho = 706.68 \text{ kg/m}^3$); and the maximum yields were $45.23\% \pm 0.46$ at 50 °C/350 bar ($\rho = 899.23 \text{ kg/m}^3$) and $45.90\% \pm 0.15$ at 60 °C/270 bar ($\rho = 805.42 \text{ kg/m}^3$).

At the 50 °C isotherm there was an increase of approximately 2.55 times in the oil yield when the pressure was increased from 150 to 220 bar and at the pressure of 350 bar pressure, there was a small increase in yield, but without significant differences ($p < 0.05$) in relation to the result obtained at 220 bar. At the 60 °C isotherm, when the pressure was increased from 190 to 270 bar, there was also an increase in oil yield of 1.53 times and at a pressure of 420 bar the yield remained practically constant. This behavior indicates that the first increase in pressure for each isotherm is sufficient to reach the maximum amount of oil extractable from the raw material, since a further increase in pressure did not cause significant differences ($p < 0.05$) in yields obtained above 220 bar at 50 °C and 270 bar at 60 °C, as shown in Fig. 1.

The maximum yields obtained in this study were higher than those obtained by other palm fruits of the same family (*Arecaceae*), as açai (*Euterpe oleracea*) oil [22] extracted with Sc–CO₂ at 50 °C/350 bar and 60 °C/420 bar with approximately 43 and 40% yield, respectively, pataúá (*Oenocarpus bataua*) [11] and bacaba (*Oenocarpus bacaba*) oil [13] extracted by conventional method with 41.78 and 38.3% yields, respectively, but lower than the obtained by Pinto et al [21] in the bacaba (*Oenocarpus bacaba*) oil extraction (*Oenocarpus bacaba*) at 60 °C/420 bar, which achieved a 60.39% yield.

The costs and the decision on the extraction parameters at high pressures are dominated by the energy consumption, which will depend on the process operating conditions, considering the costs of refrigeration and pressurizing the system to verify if an increase in the yield would justify the use of a higher temperature and pressure [49,50]. Thus, based on the global yield and energy consumption, the ideal LBP oil extraction condition should be 50 °C/220 bar, as a further increase in the pressure in the two isotherms did not have a significant influence on the global yield.

3.3. Fatty acid composition of LBP oil

Table 1 shows the fatty acid profiles of LBP oil obtained by Sc–CO₂ extraction under different operating conditions. The standard deviations were less than 1.8% for all fatty acids determined.

The results indicate that there was no difference in the fatty acids qualitative composition detected in the LBP oil samples analyzed,

regardless of the extraction conditions. However, in quantitative terms the significant presence of some compounds was observed, such as oleic acid, which was the main fatty acid present in the oil ($\cong 66\%$), followed by palmitic ($\cong 17\%$) and linoleic acids ($\cong 12\%$). As can be seen, the oil was predominantly characterized by unsaturated fatty acids (UFA $\cong 79\%$), whose concentration was much higher than the saturated ones (SFA $\cong 20\%$) and the presence of monounsaturated fatty acids (MUFA $\cong 66\%$) was predominant in relation to polyunsaturated (PUFA $\cong 13\%$) for all operating conditions. Among the SFA, palmitic acid was the main fatty acid present in the oil, with the lowest concentration obtained at 50 °C/150 bar (17.19%) and the highest (18.81%) obtained at 60 °C/190 bar. Regarding the UFA's, the main fatty acid found was oleic acid, with approximately 66.18% concentration in almost all conditions, the exceptions were the oil extracted at 50 °C/150 bar and 60 °C/190 bar, which presented the lowest concentrations (65.38% and 64.23%, respectively), followed by linoleic acid, found in lower concentration (12.10%) at 50 °C/350 bar and higher concentration (13.35%) at 50 °C/150 bar. Other smaller compounds, such as myristic, stearic, arachidic, and behenic saturated fatty acids and the palmitoleic and linolenic unsaturated with low concentrations, are also present in LBP oil and did not present significant differences in composition for all extraction conditions.

Table 1 shows that the extracted oil has a fatty acid profile very similar to that found in olive oil evaluated by Reboredo-Rodríguez et al [51] and Caporaso et al [52], which also presented oleic acid as its main constituent, followed by palmitic acid, and linoleic acid. Reboredo-Rodríguez et al [51] evaluated two olive oil varieties and obtained an average of 70.77% of oleic acid, 13.49% of palmitic acid, and 10.34% of linoleic acid. Caporaso et al [52] evaluated 32 extra virgin olive oil samples, whose concentrations ranged from 68.1 to 76.55% for oleic acid, from 9.24 to 12.94% for palmitic acid, and from 3.83 to 9.53% for linoleic acid.

According to the literature, the oils with the highest concentration of MUFAs and lower concentration of SFAs are considered of high quality due to the MUFAs beneficial effect on serum cholesterol levels. Hence, the fatty acids composition is extremely important in determining the food properties and benefits for health, especially cardiovascular health. Substitution of SFAs by UFAs (cis-monounsaturated or cis-polyunsaturated) allows the maintenance of low-density lipoprotein (LDL) concentrations in normal blood levels. This health criterion may be used for foodstuffs whose unsaturated fatty acids account for at least 70% of the total fatty acid composition [52,53]. Therefore, considering such food characteristics, compared to olive oil, the high content of unsaturated fatty acids (more than 70% of the composition) gives the LBP oil a high nutritional value, being able to be inserted in the food in substitution of olive oil and other edible vegetable oils, mainly as omega-9 source, where a diet rich in these compounds is

Table 1Free fatty acid composition (wt.%) of lyophilized bacaba-de-leque (*O. distichus*) pulp oil obtained by supercritical fluid extraction.

Fatty acids	Symbol	Fatty acids concentration (wt%)					
		50 °C			60 °C		
		150 bar	220 bar	350 bar	190 bar	270 bar	420 bar
Miristic (C14:0)	Mi	0.18	0.16	0.16	0.29	0.16	0.15
Palmitic (C16:0)	P	17.19	17.69	17.62	18.81	17.39	17.62
Palmitoleic (C16:1 ω-7)	Pa	0.77	0.70	0.69	0.81	0.68	0.68
Stearic (C18:0)	S	2.19	2.39	2.39	2.24	2.39	2.37
Oleic (C18:1 Cis ω-9)	O	65.38	66.09	66.22	64.23	66.24	66.16
Linoleic (C18:2 Cis ω-6)	Li	13.35	12.12	12.10	12.84	12.28	12.24
Linolenic (C18:3 ω-3)	Ln	0.72	0.60	0.58	0.65	0.61	0.60
Arachidic (C20:0)	A	0.16	0.18	0.18	0.06	0.19	0.17
Behenic (C22:0)	Be	0.06	0.06	0.05	0.06	0.07	0.01
SFA ^a		19.78	20.49	20.41	21.46	20.18	20.32
UFA ^b		80.22	79.51	79.59	78.54	79.82	79.68
MUFA ^c		66.14	66.79	66.91	65.04	66.92	66.84
PUFA ^d		14.07	12.72	12.68	13.49	12.90	12.84

SFA^a = Saturated Fatty Acids; UFA^b = Unsaturated Fatty Acids; MUFA^c = Monounsaturated Fatty Acids; PUFA^d = Polyunsaturated Fatty Acids.

associated with lower risk related to heart disease [54].

3.4. Functional quality of LBP oil

The fatty acids composition allowed evaluating the functional quality of LBP oil. For this, the ratio of polyunsaturated/saturated fatty acids (PUFA/SFA) and hypocholesterolemic/hypercholesterolemic (H/H), atherogenicity index (AI) and thrombogenicity index (TI) were calculated. The results are shown in Table 2.

The ratio of polyunsaturated/saturated fatty acids (PUFA/SFA) with values less than 0.45 are deemed unsuitable for human diet due to the potential induction of increased blood cholesterol [55,56]. Therefore, in this work, a good PUFA/SFA ratio was obtained for LBP oil in all operating conditions, whose values varied from 0.62 (50 °C/220 and 350 bar) to 0.71 (50 °C/150 bar), that is, above the recommended minimum value, indicating that this oil can be considered healthy for human consumption.

The ratio index between the hypocholesterolemic and hypercholesterolemic fatty acids (H/H) showed values ranging from 4.07 (60 °C/190 bar) to 4.57(50 °C/150 bar). These values are much higher compared to those found in animal fats [57,58]. The atherogenicity index (AI) found in the oil ranged from 0.22 (50 °C/150 bar) to 0.25 (60 °C/190 bar) and the thrombogenicity index (TI) ranged from 0.47 (50 °C/150 bar) to 0.52 (60 °C/190 bar), been values below 1, which is the limit suitable for a healthy diet [59]. Pinto et al. [21], evaluating the functional quality of bacaba oil (*O. bacaba*) extracted with Sc-CO₂, obtained PUFA/SFA, H/H, AI and IT values of 0.43, 3.32, 0.30 and 0.67 respectively, but did not describe the operating condition of Sc-CO₂ extraction of the fatty acid composition profile used for calculations of the four indices.

According to the literature, low AI and TI values imply a higher amount of antiatherogenic fatty acids present in certain oils and, consequently, the greater the potential for preventing the onset of coronary diseases. The high H/H values are directly related to the benefit given

Table 2Lipid quality indices of lyophilized bacaba-de-leque (*O. distichus*) pulp oil.

Lipid quality indices	50 °C			60 °C		
	150 bar	220 bar	350 bar	190 bar	270 bar	420 bar
PUFA/SFA	0.71	0.62	0.62	0.63	0.64	0.63
H/H	4.57	4.42	4.44	4.07	4.51	4.44
AI	0.22	0.23	0.23	0.25	0.23	0.23
TI	0.47	0.49	0.49	0.52	0.48	0.49

to cholesterol metabolism and formation of high density lipoproteins (HDL), unlike the atherogenicity and thrombogenicity indexes (AI and TI), which should be reduced, making the oil suitable for human consumption [40,41,57].

3.5. Probable triglyceride composition of LBP oil

In this work, the probable triglycerides (TG) present in LBP oil were estimated for each extraction condition from the fatty acid composition. The main TG were represented by the components with the largest mass fraction ($\geq 1\%$) of the isomers set defined by the number of carbon atoms (X) and the total number of double bonds (Y) in the three fatty acid chains. Table 3 shows that the TG present in the oil are predominantly OLiO (17.14 to 18.60%), PLiO (9.13 to 10.14%), OOO (28.85 to 31.36%), POP (6.30 to 7.42%), and POO (23.96 to 25.35%), representing more than 85% of the total. These TG species were formed by a combination of oleic, palmitic, and linoleic acids. This result is in agreement with the LBP oil fatty acid composition obtained experimentally by gas chromatography (GC), in which the composition of oleic, palmitic, and linoleic acid are predominant (Table 1). Other authors used analytical methods, such as high performance liquid chromatography (HPLC), to identify the TG present in the oil of another bacaba species (*O. bacaba*) [13,60] and identified similar TG in the same order of magnitude to those determined in this study.

3.6. Predicted solubility of LBP oil in Sc-CO₂

Fig. 2 shows the LBP oil solubility behavior in Sc-CO₂ predicted with the Peng-Robinson (PR) cubic equation of state using the van der Waals (vdW) mixing rule with two binary interaction parameters in the 50 and 60 °C isotherms in a pressure range from 130 to 450 bar. The solubility values obtained ranged from 11.5 to 41.8 g oil/kg CO₂ at 50 °C and from 4.4 to 49.6 g oil/kg CO₂ at 60 °C.

The predicted solubility values in the experimental conditions of LBP oil extraction (temperatures of 50 and 60 °C and pressures from 150 to 420 bar) justified the extraction yields obtained, since the solubility was lower in operating conditions where lower yields were obtained (19.5 g oil/kg CO₂ at 50 °C/150 bar and 25.6 g oil/kg CO₂ at 60 °C/190 bar) and was higher in the conditions where the highest yields were obtained (41.8 g oil/kg CO₂ at 50 °C/350 bar, 42.6 g oil/kg CO₂ at 60 °C/270 bar, and 49.6 g oil/kg CO₂ at 60 °C/420 bar).

As can be seen in Fig. 2, an isothermal increase in pressure increased the LBP oil predicted solubility in Sc-CO₂ due to the solvent density which increased with the pressure at a constant temperature and, consequently, increased its solvation power. This effect is most evident

Table 3
Main TG estimated composition (wt.%) present in lyophilized bacaba-de-leque (*O. distichus*) pulp oil obtained by supercritical fluid extraction.

Main TG	X:Y ^a	MM ^b (g/mol)	Mass fraction (wt%)					
			T = 50 °C			T = 60 °C		
			150 bar	220 bar	350 bar	190 bar	270 bar	420 bar
OLiLi	54:5	880	3.80	3.14	3.13	3.46	3.23	3.20
PLiP	50:4	830	1.29	1.23	1.22	1.48	1.20	1.23
OLiO	54:4	882	18.60	17.14	17.16	17.31	17.44	17.29
PLiO	52:3	856	9.78	9.18	9.13	10.14	9.16	9.21
OOO	54:3	884	30.37	31.16	31.30	28.85	31.36	31.17
POP	50:1	832	6.30	6.70	6.65	7.42	6.48	6.63
POO	52:2	858	23.96	25.02	24.99	25.35	24.70	24.90
SLiO	54:3	884	1.25	1.24	1.24	1.20	1.26	1.24
SOO	54:2	886	3.05	3.38	3.39	3.01	3.39	3.35
POS	52:1	860	1.61	1.81	1.80	1.76	1.78	1.78

X = number of carbons; Y^a = number of double bonds; MM^b = molar mass.

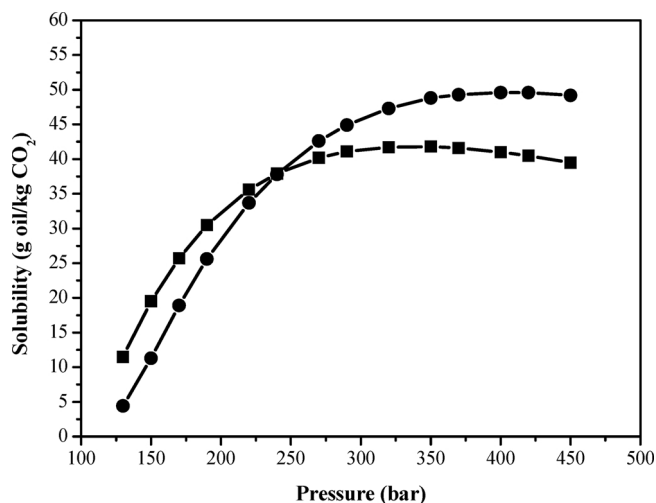


Fig. 2. Predicted solubility isotherms of lyophilized bacaba-de-leque pulp oil in Sc-CO₂, at (■) 50 °C and (●) 60 °C.

at lower pressures, where the solvent density is very sensitive to pressure changes [61].

Unlike the pressure effect, an isobaric increase in temperature at pressures below 240 bar decreased the oil predicted solubility as an effect of decreasing the Sc-CO₂ density, which caused an increase in the oil compounds vapor pressure. And at a higher pressure, mainly above 300 bar, the predicted solubility behavior changed in relation to the pressure and temperature. The crossing point of the isotherms represents the change in the temperature effect on the solubility, because in the higher pressures the oil predicted solubility increased with the temperature. In general, at low pressures, the density effect is predominant and the solubility decreases with increasing temperature, while at high pressures, the solubility increases with temperature due to the dominant vapor pressure effect. It is these two factors that lead to the cross-pressure of solubility isotherms [23,61].

A similar behavior was reported in the Zuknik et al [25] work, which measured the virgin coconut oil solubility by the dynamic extraction method at temperatures and pressures ranging from 40 to 80 °C and 207 to 345 bar, respectively. The authors described the isotherm cross-over region between 275 and 305 bar, where the coconut oil solubility in Sc-CO₂ decreased with increasing temperature at pressures below 240 bar and increased with the temperature at pressures above 310 bar. In addition, the experimental values of coconut oil solubility obtained are similar in magnitude to those found in this work, as well as the intermediate values between corn and sunflower oils, and Ucuuba (*Virola surinamensis*) and babaçu (*Attalea speciosa*) fats, measured

experimentally by Soares et al [62].

3.7. Bioactive compounds of lyophilized bacaba-de-leque pulp before and after supercritical CO₂ extraction

The results of total phenolic compounds and total monomeric anthocyanins analyzes are shown in Figs. 3 and 4, respectively.

The total LBP phenolic compounds content was 4.14 ± 0.30 mg GAE/g (db). After Sc-CO₂ extraction under different operating conditions, the contents varied from 4.30 ± 0.05 to 6.99 ± 0.05 mg GAE/g (db). As can be seen in Fig. 3, the LBP residual cake obtained after extraction showed a tendency to concentrate the phenolic compounds in comparison to lyophilized pulp. This increase was most evident at 50 °C/350 bar and 60 °C/270 and 420 bar conditions. Comparing these results with the literature, the values were higher than those found by Carvalho et al. and Sousa et al. [9,10], who evaluated several bacaba-de-leque (*O. distichus*) genotypes, whose values ranged from 2.94 to 5.89 mg GAE/g (db) and 0.82 to 3.63 mg GAE/g (db), respectively, as well as in other palm fruits from the same family (*Arecaceae*) traditionally consumed in the Amazon region, such as buriti (*Mauritia flexuosa*) (3.1 mg GAE/g db), pupunha (*Bactris gasipaes*) (0.86 mg GAE/g db), tucumã (*Astrocaryum vulgare*) (3.61 mg GAE/g db), and inajá (*Attalea maripa*) (1.10 mg GAE/g db) [7]. However, they were lower than the phenolic compounds found for bacaba (*Oenocarpus bacaba*) (16.22 mg GAE/g db) [7], açai (*Euterpe oleracea*) (32.68 mg

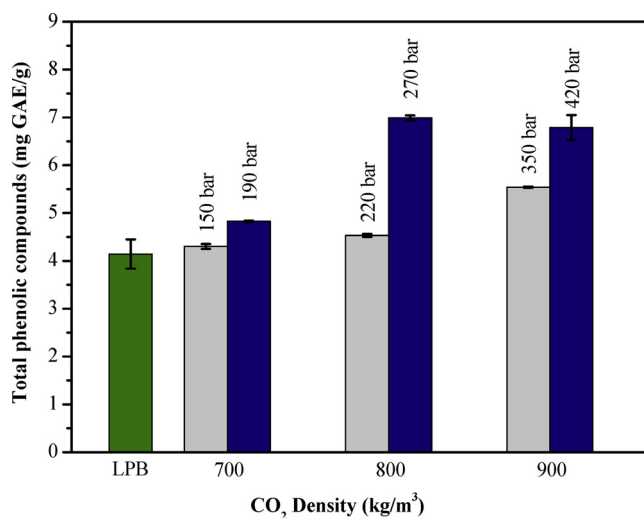


Fig. 3. Total phenolic compounds content of lyophilized bacaba-de-leque pulp (LBP) before and after supercritical CO₂ extraction at (■) 50 °C and (■) 60 °C isotherms.

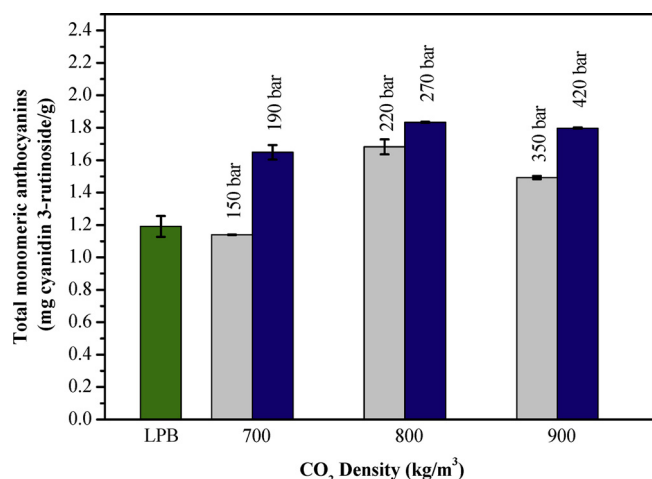


Fig. 4. Total monomeric anthocyanins content of lyophilized bacaba-de-leque pulp (LBP) before and after supercritical CO₂ extraction at (■) 50 °C and (■) 60 °C isotherms.

GAE/g db) and jussara (*Euterpe edulis*) (56.72 mg GAE /g db) [63].

The total monomeric anthocyanin levels quantified in the LBP were 1.19 ± 0.064 mg cya 3-rut/g (db) before the Sc–CO₂ extraction and, after, the contents presented variations of 1.14 ± 0.001 mg cya 3-rut/g to 1.83 ± 0.0026 mg cya 3-rut/g (db). Fig. 4 shows that there was a considerable increase in the concentration after the Sc–CO₂ extraction, and the highest content of anthocyanins was achieved in the sample obtained at 60 °C/270 bar (1.83 ± 0.0026 cya 3-rut/g db). These values were higher than those found by Sousa et al. [10] when evaluating 32 genotypes of bacaba-de-leque (*O. distichus* Mart) from different localities, which presented levels of 0.03 to 0.68 mg cya 3-rut/g (db) and those obtained by Finco et al. [6] on bacaba (*Oenocarpus bacaba*) fruit (0.61 mg cyn-3-glc/g db), but were smaller than those found in açai (*Euterpe oleracea*) (6.98 cyn-3-glc/g db) and jussara (*Euterpe edulis*) (19.59 cyn-3-glc/g db) [63].

Both the total phenolic compounds and the total monomeric anthocyanins content measured in the LBP residual cake after Sc–CO₂ extraction at 50 °C/150 bar remained approximately equal to the value obtained in the LBP before extraction. This may have occurred due to the low oil yield obtained in this condition, where the solvent temperature, pressure, and density did not guarantee the maximum extraction of the lipophilic fraction, represented by the fatty acids present in the bacaba-de-leque oil. According to Wu et al. [64], the physicochemical properties of the raw material hydrophilic and lipophilic fractions are extremely different, where the hydrophilic fraction, composed of polar compounds, for example of the phenolic compounds, and lipophilic, composed of apolar compounds such as fatty acids, must be separated to obtain the most representative analyzes results of these compounds.

3.8. In vitro antioxidant capacity of lyophilized bacaba-de-leque pulp

Table 4 shows the LBP extracts and residual cake antioxidant capacity obtained after Sc–CO₂ extraction at different temperature and pressure conditions.

The lyophilized pulp and residual cake extracts antioxidant capacity indicated that all the samples were efficient in reducing the ABTS^{•+} and DPPH[•] radicals. Before Sc–CO₂ extraction, the antioxidant capacity was 12.94 ± 0.20 (μM Trolox/g) for TEAC and 82.19 ± 1.90 (μM Trolox/g) for DPPH[•]. After extraction, there was an increase in antioxidant capacity for both methods, whose values ranged from 37.56 ± 0.99 to 238.11 ± 1.93 (μM Trolox/g) for TEAC and from 215.80 ± 17.76 to 1019.28 ± 66.77 (μM Trolox/g) for DPPH[•]. The results indicate that the samples that presented higher antioxidant

Table 4

Antioxidant capacity of lyophilized bacaba-de-leque pulp (LBP) before and after supercritical CO₂ extraction.

Amostras T (°C)/P (bar)	TEAC (μM Trolox/g)	DPPH [•] (μM Trolox/g)
LBP	12.94 ± 0.20^g	82.19 ± 1.90^g
50 °C/150 bar	37.56 ± 0.99^f	215.80 ± 17.76^f
50 °C/220 bar	49.32 ± 0.55^c	337.05 ± 17.59^c
50 °C/350 bar	66.98 ± 0.59^d	628.16 ± 38.12^c
60 °C/190 bar	131.55 ± 1.63^c	471.12 ± 28.59^d
60 °C/270 bar	177.47 ± 0.82^b	785.20 ± 47.65^b
60 °C/420 bar	238.11 ± 1.93^a	1019.28 ± 66.77^a

All data are mean ± standard deviation (n = 3 dry basis). Mean in the same column with the same letter are not statistically different at 95% of significance, by the Tukey test.

capacity were those that presented higher total phenolic compounds contents. In the literature, several authors have related phenolic compounds with antioxidant capacity, which can be attributed to the polyphenols bioactive properties, that play an important role in the free radicals absorption and neutralization [10,65].

Compared with other fruits, the antioxidant capacity of the extracts in three of the six samples obtained after Sc–CO₂ extraction (Table 4), were higher than those found in Sousa et al. [10] study in different bacaba-de-leque genotypes (*Oenocarpus distichus*), whose values ranged from 18.77 μM Trolox/g to 77.99 μM Trolox/g (db), higher than those reported for buriti (*Mauritia flexuosa*) extracts (92.8 μM Trolox/g db) [66], bacaba (*Oenocarpus bacaba*) (57.9 μM Trolox/g db) [6], and açai (*Euterpe oleracea*) (64.5 μM Trolox/g db) [63] for the TEAC method, while for DPPH[•], in 60 °C/420 bar condition, the values were close to the blueberry (*Vaccinium myrtillus*) extracts (1284 μM Trolox/g) [67] and higher than the values found for araçá (*Psidium guineense*) extracts (16.94 μM Trolox/g db), araçá-boi (*Eugenia stipitata*) (14.87 μM Trolox/g db) [68], and gojiberry (*Lycium barbarum*) (28.1 μM Trolox/g db) [69].

4. Conclusion

In this work, the effects of temperature, pressure, and solvent density on the global yield of lyophilized bacaba-de-leque pulp oil Sc–CO₂ extraction were evaluated, whose maximum yields were reached at 50 and 60 °C after the first increased pressure, presenting very similar values (44.59 to 45.9%). The fatty acid profile of the extracted oil was evaluated for all the extraction conditions, which did not influence its composition that was characterized predominantly by unsaturated fatty acids, where oleic, palmitic, and linoleic acids were predominant. These results indicated that the bacaba-de-leque oil has good functional quality, represented by good functional quality indexes calculated from the fatty acids composition. The prediction of the triglyceride profile showed that OLiO, PLiO, OOO, POP, and POO were predominant in the oil (more than 85% of the total composition) and were similar to those found in the literature determined by analytical methods.

The use of the Peng-Robinson (PR) cubic equation of state using the van der Waals (vdW) mixing rule with two parameters of binary interaction was efficient in predicting the bacaba-de-leque oil solubility in Sc–CO₂, whose predicted values justified the extraction yields obtained, where the greatest solubilities corresponded to the maximum yields reached, indicating the ideal operating conditions for the bacaba-de-leque oil extraction. The results were similar to those obtained experimentally, found in the literature for other oilseeds.

The LBP residual cake obtained after the extraction with Sc–CO₂ showed an increase in the total phenolic compounds and anthocyanins contents and, consequently, increased the extracts antioxidant capacity, which was higher in the samples that presented higher total phenolic compounds contents. This was favored by the lipophilic fraction separation from the pulp extracted by supercritical fluid, represented by

the fatty acids present predominantly in the oil.

Therefore, this study showed the efficiency of the Sc–CO₂ extraction in the production of high-quality bacaba-de-leque oil, which can offer several nutritional and functional benefits due to its high levels of monounsaturated and polyunsaturated fatty acids, besides pointing out the great potential in nutraceutical applications of the bioactive compounds concentrated in the pulp by the oil extraction.

Acknowledgements

Vânia Maria Borges Cunha thanks CAPES-Brazil for the doctoral scholarship. Process Number: 1566277/2015. The authors thank EMBRAPA for donating the Bacaba-de-leque.

References

- Henderson, *The Plams of the Amazon*, 1st ed., Oxford university press, New York (N.Y.), 1995.
- S.A. Pereira, H.P. Alves, C. da M. de Sousa, G.L. da S. Costa, Exploration on the knowledge Amazonian species - inajá (*Maximiliana maripa* Aubl.) e bacaba (*Oenocarpus bacaba* Mart.), *Geintec* 3 (2013) 110–122, <https://doi.org/10.7198/S2237-0722201300020009>.
- P. Leitman, K. Soares, A. Henderson, L. Noblick, R.C. Martins, *Areceaceae*. Lista de espécies da flora do Brasil. Jardim Botânico do Rio de Janeiro, (2015) <http://floradobrasil.jbrj.gov.br/jabot/floradobrasil/FB15727>.
- M.J. Balick, Amazonian oil palms of promise: a survey, *Econ. Bot.* 33 (1979) 11–28.
- J.P.L. Aguiar, F. das, C. do, A. Souza, Bacaba-de-leque (*Oenocarpus distichus*): a new wet tropics nutritional source, *Afr. J. Agric. Res.* 13 (2018) 803–805, <https://doi.org/10.5897/AJAR2018.13027>.
- F.D.B.A. Finco, D.R. Kammerer, R. Carle, W.-H. Tseng, S. Böser, L. Graeve, Antioxidant activity and characterization of phenolic compounds from bacaba (*Oenocarpus bacaba* Mart.) Fruit by HPLC-DAD-MSn, *J. Agric. Food Chem.* 60 (2012) 7665–7673, <https://doi.org/10.1021/jf3007689>.
- M. dos Santos, R. Mamede, M. Rufino, E. de Brito, R. Alves, Amazonian native palm fruits as sources of antioxidant bioactive compounds, *Antioxidants* 4 (2015) 591–602, <https://doi.org/10.3390/antiox4030591>.
- A. Rezaire, J.C. Robinson, D. Bereau, A. Verbaere, N. Sommerer, M.K. Khan, P. Durand, E. Prost, B. Fils-Lycaon, Amazonian palm *Oenocarpus bataua* (“patawa”): chemical and biological antioxidant activity - phytochemical composition, *Food Chem.* 149 (2014) 62–70, <https://doi.org/10.1016/j.foodchem.2013.10.077>.
- A.V. Carvalho, T.F. da Silveira, S.H.B. de Sousa, M.R. de Moraes, H.T. Godoy, Phenolic composition and antioxidant capacity of bacaba-de-leque (*Oenocarpus distichus* Mart.) genotypes, *J. Food Compos. Anal.* 54 (2016) 1–9, <https://doi.org/10.1016/j.jfca.2016.09.013>.
- S.H.B. de Sousa, R. de A. Mattietto, R.C. Chisté, A.V. Carvalho, Phenolic compounds are highly correlated to the antioxidant capacity of genotypes of *Oenocarpus distichus* Mart. fruits, *Food Res. Int.* 108 (2018) 405–412, <https://doi.org/10.1016/j.foodres.2018.03.056>.
- A.M. da C. Rodrigues, S. Darnet, L.H.M. da Silva, Fatty Acid Profiles and Tocopherol Contents of Buriti (*Mauritia flexuosa*), Patawa (*Oenocarpus bataua*), Tucuma (*Astrocaryum vulgare*), Mari (Poraqueiba *paraensis*) and Inaja (*Maximiliana maripa*) Fruits, *J. Braz. Chem. Soc.* 21 (2010) 2000–2004.
- R. Montúfar, A. Laffargue, J.C. Pintaud, S. Hamon, S. Avallone, S. Dussert, *Oenocarpus bataua* Mart. (arecaceae): rediscovering a source of high oleic vegetable oil from Amazonia, *JAOCs* 87 (2010) 167–172, <https://doi.org/10.1007/s11746-009-1490-4>.
- M.F.G. Santos, S. Marmesat, E.S. Brito, R.E. Alves, M.C. Dobarganes, Major components in oils obtained from Amazonian palm fruits, *Grasas y Aceites* 64 (2013) 531–536, <https://doi.org/10.3989/gya.048913>.
- C. Puerari, K.T. Magalhães-Guedes, R.F. Schwan, Bacaba beverage produced by umutina Brazilian amerindians: microbiological and chemical characterization, *Braz. J. Microbiol.* 46 (2015) 1207–1216, <https://doi.org/10.1590/S1517-838246420140964>.
- L.J. Pham, P.J. Pham, Biocatalyzed production of structured olive oil triacylglycerols, in: Dr. Dimitrios Boskou (Ed.), *Olive Oil - Constituents, Quality, Health Properties and Bioconversions*, 1st ed., InTech, 2012, p. 510, <https://doi.org/10.5772/13378>.
- S. Indelicato, D. Bongiorno, R. Pitonzo, V. Di Stefano, V. Calabrese, S. Indelicato, G. Avellone, Triacylglycerols in edible oils: determination, characterization, quantitation, chemometric approach and evaluation of adulterations, *J. Chromatogr. A* 1515 (2017) 1–16, <https://doi.org/10.1016/j.chroma.2017.08.002>.
- E.G. Giakoumis, Analysis of 22 vegetable oils’ physico-chemical properties and fatty acid composition on a statistical basis, and correlation with the degree of unsaturation, *Renew. Energy* 126 (2018) 403–419, <https://doi.org/10.1016/j.renene.2018.03.057>.
- C.G. Pereira, M.A.A. Meireles, Supercritical fluid extraction of bioactive compounds: fundamentals, applications and economic perspectives, *Food Bioproc. Tech.* 3 (2010) 340–372, <https://doi.org/10.1007/s11947-009-0263-2>.
- J. Martinez, A.C. de Aguiar, Extraction of triacylglycerols and fatty acids using supercritical fluids - review, *Curr. Anal. Chem.* 10 (2014) 67–77, <https://doi.org/10.2174/1573411011410010006>.
- R.P.F.F. da Silva, T.A.P. Rocha-Santos, A.C. Duarte, Supercritical fluid extraction of bioactive compounds, *TrAC - Trends Anal. Chem.* 76 (2016) 40–51, <https://doi.org/10.1016/j.trac.2015.11.013>.
- R.H.H. Pinto, C. Sena, O.V. Santos, W.A. da Costa, A.M.C. Rodrigues, R.N.C. Junior, Extraction of bacaba (*Oenocarpus bacaba*) oil with supercritical CO₂: global yield isotherms, fatty acid composition, functional quality, oxidative stability, spectroscopic profile and antioxidant activity, *Grasas y Aceites* 69 (2018) 1–8.
- C. de Cássia Rodrigues Batista, M.S. De Oliveira, M.E. Araújo, A.M.C. Rodrigues, J.R.S. Botelho, A.P. Da Silva Souza Filho, N.T. Machado, R.N. Carvalho, Supercritical CO₂ extraction of açaí (*Euterpe oleracea*) berry oil: global yield, fatty acids, allelopathic activities, and determination of phenolic and anthocyanins total compounds in the residual pulp, *J. Supercrit. Fluids* 107 (2015) 364–369, <https://doi.org/10.1016/j.supflu.2015.10.006>.
- G. Brunner, *Gas Extraction: An Introduction to Fundamentals of Supercritical Fluids and the Application to Separation Process*, 1st ed., Springer, New York, 1994, <https://doi.org/10.1007/978-3-662-07380-3>.
- E. Kiran, J.F. Brennecke, *Supercritical fluid engineering science*, ACS Symposium Series 514, 1st ed., American Chemical Society, Washington, DC, 1993.
- M.H. Zuknik, N.A. Nik Norulaini, W.S. Wan Nursuzreen Dalila, N.R. Ali, A.K.M. Omar, Solubility of virgin coconut oil in supercritical carbon dioxide, *J. Food Eng.* 168 (2016) 240–244, <https://doi.org/10.1016/j.jfoodeng.2015.08.004>.
- H. Sovová, R.P. Stateva, Supercritical fluid extraction from vegetable materials, *Rev. Chem. Eng.* 27 (2011) 79–156, <https://doi.org/10.1515/REVCE.2011.002>.
- H. Sovová, M. Sajfrová, R.P. Stateva, A novel model for multicomponent supercritical fluid extraction and its application to Ruta graveolens, *J. Supercrit. Fluids* 120 (2017) 102–112, <https://doi.org/10.1016/j.supflu.2016.10.008>.
- G. Soave, Equilibrium constants from a modified Redlich-Kwong equation of state, *Chem. Eng. Sci.* 27 (1972) 1197–1203, [https://doi.org/10.1016/0009-2509\(72\)80096-4](https://doi.org/10.1016/0009-2509(72)80096-4).
- D.Y. Peng, D.B. Robinson, A new two-constant equation of state, *Ind. Eng. Chem. Fundam.* 15 (1976) 59–64, <https://doi.org/10.1021/i160057a011>.
- M.E. Araújo, N.T. Machado, M. Angela, M. Meireles, Modeling the phase equilibrium of soybean oil deodorizer distillates + supercritical carbon dioxide using the Peng - Robinson EOS, *Ind. Eng. Chem. Res.* 40 (2001) 1239–1243, <https://doi.org/10.1021/ie0001772>.
- F. Gironi, M. Maschietti, Separation of fish oils ethyl esters by means of supercritical carbon dioxide: thermodynamic analysis and process modelling, *Chem. Eng. Sci.* 61 (2006) 5114–5126, <https://doi.org/10.1016/j.ces.2006.03.041>.
- F. Gironi, M. Maschietti, Continuous countercurrent deterpenation of lemon essential oil by means of supercritical carbon dioxide: experimental data and process modelling, *Chem. Eng. Sci.* 63 (2008) 651–661, <https://doi.org/10.1016/j.ces.2007.10.008>.
- V.M.B. Cunha, M.P. Silva, M.A.A.M. Raul, N. Carvalho Jr, N.T. Machado, M.E. Araújo, Lauric acid rich oil supercritical extraction and methodology to predict solubility, *Food Public Health* 6 (2016) 26–32, <https://doi.org/10.5923/j.fph.20160601.04>.
- M.B. Jacobs, *The Chemical Analysis of Foods and Food Products*, 1st ed., Van Nostrand Reinhold Company, Canada, 1973.
- AOAC, *Official Methods of Analysis of the Association of Official Analytical Chemists*, 20th ed., (2016) Washington.
- AOCS, *Official Methods and Recommended Practices of the AOCS*, 6th ed., (2013) Champaign.
- P.J. Van Soest, Use of detergents in the analysis of fibrous feeds. II. A rapid method for the determination of fiber and lignin, *J. AOAC Int.* 46 (1963) 829–835.
- R. Span, W. Wagner, A new equation of state for carbon dioxide covering the fluid region from the triple-point temperature to 1100 K at pressures up to 800 MPa, *J. Phys. Chem. Ref. Data* 25 (1996) 1509–1596, <https://doi.org/10.1063/1.555991>.
- L. Hartman, R.C. Lago, Rapid preparation of fatty acid methyl esters from lipids, *Lab. Pract.* 22 (1973) 475–477.
- J. Santos-Silva, R.J.B. Bessa, F. Santos-Silva, Effect of genotype, feeding system and slaughter weight on the quality of light lambs. II. Fatty acid composition of meat, *Livest. Prod. Sci.* 77 (2002) 187–194, [https://doi.org/10.1016/S0301-6226\(02\)00059-3](https://doi.org/10.1016/S0301-6226(02)00059-3).
- T.L.V. Ulbricht, D.A.T. Southgate, Coronary heart disease: seven dietary factors, *Lancet* 338 (1991) 985–992, [https://doi.org/10.1016/0140-6736\(91\)91846-M](https://doi.org/10.1016/0140-6736(91)91846-M).
- F.A. Norris, K. Mattil, A new approach to the glyceride structure of natural fats, *J. Am. Oil Chem. Soc.* 24 (1947) 274–275.
- M.E. Araújo, M.A.A. Meireles, Improving phase equilibrium calculation with the Peng – Robinson EOS for fats and oils related compounds / supercritical CO₂ systems, *Fluid Phase Equilib.* 169 (2000) 49–64.
- V.L. Singleton, J.A. Rossi, Colorimetry of total phenolics with phosphomolybdic-phosphotungstic acid reagents, *Am. J. Enol. Vitic.* 16 (1965) 144–158.
- S. Geórgé, P. Brat, P. Alter, M.J. Amiot, Rapid determination of polyphenols and vitamin C in plant-derived products, *J. Agric. Food Chem.* 53 (2005) 1370–1373, <https://doi.org/10.1021/jf048396b>.
- M.M. Giusti, R.E. Wrolstad, Characterization and measurement of anthocyanins by UV - visible spectroscopy, *Curr. Protoc. Food Anal. Chem.* (2001) 0–13, <https://doi.org/10.1002/0471142913.faf0102s00>.
- N.J. Miller, C. Rice-Evans, M.J. Davies, V. Gopinathan, A. Milner, A novel method for measuring antioxidant capacity and its application to monitoring the antioxidant status in premature neonates, *Clin. Sci.* 84 (1993) 407–412, <https://doi.org/10.1042/cs0840407>.
- W. Brand-Williams, M.E. Cuvelier, C. Berset, Use of a free radical method to evaluate antioxidant activity, *LWT - Food Sci. Technol.* 28 (1995) 25–30, [https://doi.org/10.1016/S0023-6438\(95\)80008-5](https://doi.org/10.1016/S0023-6438(95)80008-5).
- A. Bertuccio, G. Vetter, *High Pressure Process Technology: Fundamentals and*

- Applications, 1st ed., Elsevier B.V., Amsterdam, 2001.
- [50] M.A.A. Meireles, *Supercritical extraction: technical and economical issues*, *Rev. Fitos* 2 (2006) 65–72.
- [51] P. Reboredo-Rodríguez, C. González-Barreiro, B. Cancho-Grande, E. Valli, A. Bendini, T. Gallina Toschi, J. Simal-Gandara, Characterization of virgin olive oils produced with autochthonous Galician varieties, *Food Chem.* 212 (2016) 162–171, <https://doi.org/10.1016/j.foodchem.2016.05.135>.
- [52] N. Caporaso, M. Savarese, A. Paduano, G. Guidone, E. De Marco, R. Sacchi, Nutritional quality assessment of extra virgin olive oil from the Italian retail market: Do natural antioxidants satisfy EFSA health claims? *J. Food Compos. Anal.* 40 (2015) 154–162, <https://doi.org/10.1016/j.jfca.2014.12.012>.
- [53] R. Ghanbari, F. Anwar, K.M. Alkharfy, A.H. Gilani, N. Saari, Valuable nutrients and functional bioactives in different parts of olive (*Olea europaea* L.)—A review, *Int. J. Mol. Sci.* 13 (2012) 1291–1340, <https://doi.org/10.3390/ijms13033291>.
- [54] P.J.H. Jones, D.S. MacKay, V.K. Senanayake, S. Pu, D.J.A. Jenkins, P.W. Connelly, B. Lamarche, P. Couture, P.M. Kris-Etherton, S.G. West, X. Liu, J.A. Fleming, R.R. Hantgan, L.L. Rudel, High-oleic canola oil consumption enriches LDL particle cholesteryl oleate content and reduces LDL proteoglycan binding in humans, *Atherosclerosis* 238 (2015) 231–238 doi:10.1016/j.atherosclerosis.2014.12.010.
- [55] Department of Health, *Nutritional Aspects of Cardiovascular Disease*, Report on, HMSO, London, 1994.
- [56] C.M. Williams, Dietary fatty acids and human health, *Ann. Zootech.* 49 (2000) 165–180, <https://doi.org/10.1051/animres:2000116>.
- [57] P.A.V. Barros, M.B.A. Glória, F.C.F. Lopes, M.A.S. Gama, S.M. Souza, M.H.F. Mourthé, M.I. Leão, Nutritional quality and oxidative stability of butter obtained from cows fed sugar-cane supplemented with sunflower oil, *Arq. Bras. Med. Vet. Zootec.* 65 (2013) 1545–1553, <https://doi.org/10.1590/S0102-09352013000500036>.
- [58] M.H.F. Mourthé, R.B. Reis, M.A.S. Gama, P.A.V. Barros, R. Antoniassi, H.R. Bizzo, F.C.F. Lopes, Milk fatty acid profile of Holstein x Gyr cows grazing on marandugrass supplemented with increasing levels of roasted soybeans, *Arquivo Brasileiro de Medicina Veterinária e Zootecnia* 67 (2015) 1150–1158, <https://doi.org/10.1590/1678-4162-7489>.
- [59] F. Valfré, F. Caprino, G.M. Turchini, The health benefit of seafood, *Vet. Res. Commun.* 27 (2003) 507–512, <https://doi.org/10.1023/B:VERC.0000014208.47984.8c>.
- [60] N.R.A. Filho, O.L. Mendes, F.M. Lanças, Computer prediction of triacylglycerol composition of vegetable oils by HRGC, *Chromatographia* 40 (1995) 557–562, <https://doi.org/10.1007/BF02290268>.
- [61] Güçlü-Üstündağ, F. Temelli, Correlating the solubility behavior of fatty acids, mono-, di-, and triglycerides, and fatty acid esters in supercritical carbon dioxide, *Ind. Eng. Chem. Res.* 39 (2000) 4756–4766, <https://doi.org/10.1021/ie0001523>.
- [62] B.M.C. Soares, F.M.C. Gamarra, L.C. Paviani, L.A.G. Gonçalves, F.A. Cabral, Solubility of triacylglycerols in supercritical carbon dioxide, *J. Supercrit. Fluids* 43 (2007) 25–31, <https://doi.org/10.1016/j.supflu.2007.03.013>.
- [63] M. do S.M. Rufino, R.E. Alves, E.S. de Brito, J. Pérez-Jiménez, F. Saura-Calixto, J. Mancini-Filho, Bioactive compounds and antioxidant capacities of 18 non-traditional tropical fruits from Brazil, *Food Chem.* 121 (2010) 996–1002, <https://doi.org/10.1016/j.foodchem.2010.01.037>.
- [64] X. Wu, L. Gu, J. Holden, D.B. Haytowitz, S.E. Gebhardt, G. Beecher, R.L. Prior, Development of a database for total antioxidant capacity in foods: a preliminary study, *J. Food Compos. Anal.* 17 (2004) 407–422, <https://doi.org/10.1016/j.jfca.2004.03.001>.
- [65] M. Karabin, T. Hudcova, L. Jelinek, P. Dostalek, Biotransformations and biological activities of hop flavonoids, *Biotechnol. Adv.* 33 (2015) 1063–1090, <https://doi.org/10.1016/j.biotechadv.2015.02.009>.
- [66] T.L.N. Cândido, M.R. Silva, T.S. Agostini-Costa, Bioactive compounds and antioxidant capacity of buriiti (*Mauritia flexuosa* L.f.) from the Cerrado and Amazon biomes, *Food Chem.* 177 (2015) 313–319, <https://doi.org/10.1016/j.foodchem.2015.01.041>.
- [67] J. Paes, R. Dotta, G.F. Barbero, J. Martínez, Extraction of phenolic compounds and anthocyanins from blueberry (*Vaccinium myrtillus* L.) residues using supercritical CO₂ and pressurized liquids, *J. Supercrit. Fluids* 95 (2014) 8–16, <https://doi.org/10.1016/j.supflu.2014.07.025>.
- [68] M.I. Genovese, M. Da Silva Pinto, A.E. De Souza Schmidt Gonçalves, F.M. Lajolo, Bioactive compounds and antioxidant capacity of exotic fruits and commercial frozen pulps from Brazil, *Food Sci. Technol. Int.* 14 (2008) 207–214, <https://doi.org/10.1177/1082013208092151>.
- [69] A.C. Pedro, J.B.B. Maurer, S.F. Zawadzki-Baggio, S. Ávila, G.M. Maciel, C.W.I. Haminiuk, Bioactive compounds of organic goji berry (*Lycium barbarum* L.) prevents oxidative deterioration of soybean oil, *Ind. Crops Prod.* 112 (2018) 90–97, <https://doi.org/10.1016/j.indcrop.2017.10.052>.

CAPÍTULO 3

3.1. Physicochemical Properties, Thermal Behavior, and Cytotoxic Effect of bacaba-de-Leque (*Oenocarpus distichus*) Oil Extracted by Supercritical CO₂.

1 **Physicochemical properties, thermal behavior, and cytotoxic effect of bacaba-de-**
2 **leque (*Oenocarpus distichus*) oil extracted by supercritical CO₂**

3

4 Vânia Maria Borges Cunha^{a*}, Marcilene Paiva da Silva^a, Marielba de los Angeles
5 Rodriguez Salazar^a, Wanessa Almeida da Costa^a, Fernanda Wariss Figueiredo Bezerra^a,
6 Sérgio Henrique Brabo de Sousa^a, Glides Rafael Olivo Urbina^a, Marilena Emmi
7 Araújo^b, Raul Nunes de Carvalho Júnior^{a*}

8

9 ^aLABEX (Laboratory of Supercritical Extraction), Faculty of Food Engineering, Federal
10 University of Pará, Belém, Pará, Brazil.

11

12 ^bTERM@ (Laboratory of Separation Processes and Applied Thermodynamic), Faculty
13 of Chemical Engineering, Federal University of Pará, Belém, Pará, Brazil.

14

15 *Corresponding author.

16 Tel.: +55-91-984190195

17 **E-mail address:** vaniacunha21@hotmail.com (V.M.B. Cunha), raulncj@ufpa.br and
18 raulncj@gmail.com (R.N. de Carvalho Junior).

19 **Abstract**

20

21 Native palm fruits from the Amazon region represent one of the main sources of
22 vegetable oils, since they are rich in lipids and other nutrients that are indispensable for
23 human diet. The objective of this work was to evaluate the nutritional and
24 physicochemical characteristics, thermal stability, functional groups, and cytotoxic
25 effect of bacaba-de-leque oil (*Oenocarpus distichus*) extracted by supercritical CO₂ at
26 50 °C and 350 bar. The extracted oil showed 21.36 µg/g oil of total carotenoids. The
27 quality parameters evaluated presented values within the standards recommended by the
28 legislation for crude vegetable oils, and were similar to those of edible oils marketed in
29 Brazil and in other countries. The thermogravimetric profiles indicated relative thermal
30 stability at 210 °C. The spectral bands, determined by FTIR, showed that the extraction
31 method and the operating conditions applied did not alter the characteristic functional
32 group profile, and the cytotoxicity tests revealed that the extracted oil had no cytotoxic
33 effect. These results show the good quality of bacaba-de-leque oil, opening up new
34 possibilities for applications in various industrial sectors, from food formulation to
35 bioenergy production.

36

37 **Palavras chaves:** Bacaba-de-leque oil. Supercritical fluid extraction. Quality
38 parameters. Thermal stability. Cytotoxicity.

39

40 **1. Introduction**

41

42 Vegetable oils are products obtained from seeds and fruits, of great importance in
43 the national and international markets due to their applications in several areas of
44 interest, from human and animal nutrition to bioenergy generation. They are an
45 important source of lipids and other nutrients, which include essential fatty acids (ω -3
46 and ω -6), and smaller fractions of fat-soluble compounds, such as carotenoids,
47 tocopherols and phytosterols, with antioxidant properties. These compounds play a key
48 role in human nutrition because they are sources of energy stored in fatty tissues,
49 participate significantly in metabolism, control body temperature, protect body tissues,
50 act as fat-soluble vitamin carriers, and perform other important physiological functions
51 (Melo et al., 2016; Xu, Zhu, Dong, Wei, & Lei, 2015; Yang et al., 2018).

52 The properties attributed to these compounds help maintain good human health,
53 which has increased the demand for good-quality vegetable oils. This demand has also
54 led to an increase in the search for new resources to obtain such product. The fruits of
55 native palm species from the Amazon, such as bacaba-de-leque (*Oenocarpus distichus*),
56 are considered an abundant alternative source of vegetable oils, with chemical
57 composition and functional characteristics that meet the nutritional requirements, and
58 present great potential for food and non-food applications (Cunha et al., 2019; Santos,
59 Marmesat, Brito, Alves, & Dobarganes, 2013; Wang, Wang, Xiao, & Xu, 2019).

60 To ensure the good quality of vegetable oils, it is important to consider their
61 extraction method, as there is currently greater attention to the risks to human health and
62 the environment, related to the use of organic solvents in processing of foods and other
63 products. Therefore, many industrial sectors are always searching for clean separation
64 processes that enable lower environmental impact, less toxic waste, lower energy

65 consumption, more efficient use of their by-products and, mainly, that generate high
66 quality products with good nutritional and functional properties. Supercritical fluid
67 extraction (SFE) is a separation technology that stands out in this context, with great
68 potential to be applied in oils and fats processing, whose advantages over the
69 conventional methods used in the industries are widely described in the literature (Knez
70 et al., 2014; Martinez & de Aguiar, 2014; Sahena et al., 2009).

71 Vegetable oils have physical and chemical properties that can affect the sensory
72 and nutritional characteristics of foods, such as acidity, peroxide, iodine and
73 saponification values, refractive index, density, insoluble impurities, among others. The
74 determination of these parameters is fundamental to evaluate the oil quality, especially
75 in its crude state, as it can indicate what will be the next stage of processing, and which
76 treatments are needed to reach the final product. These physicochemical properties
77 affect the thermal and oxidative stability of oils, which are influenced by lipid
78 composition, mainly by the triglycerides molecular structures (Endo, 2018; Konuskan,
79 Arslan, & Oksuz, 2019).

80 In literature, there are some studies that evaluated the quality of vegetable oils
81 extracted by supercritical fluid through their thermal behavior and physicochemical
82 properties, such as free fatty acid content, peroxide and saponification values, refractive
83 index, viscosity, and density in Brazil nut oil (*Bertolletia excelsa* H.B.K) (Santos et al.,
84 2013), tucumã oil (*Astrocaryum aculeatum* Meyer and *Astrocaryum vulgare*, Mart.)
85 (Costa, Santos, Corrêa, & França, 2016), murici oil (*Byrsonima crassifolia* L.) (Santos
86 et al., 2018), babassu seed oil (*Orbignya phalerata*) (de Oliveira, Mazzali, Fukumasu,
87 Gonçalves, & Oliveira, 2019), and sapucaia oil (*Lecythis pisonis* Camb) (Santos,
88 Carvalho, Costa, & Lannes, 2019), whose thermal behavior was evaluated by
89 thermogravimetric (TG) and derivative thermogravimetric (DTG) analyses.

90 Although research on native fruits of the Amazon region has increased and
91 aroused the interest of various industrial sectors due to their high quality associated with
92 chemical composition, most of them still need additional studies to elucidate their
93 characteristics and feasibility of application in the formulation of food and non-food
94 products. An example of this is research into cytotoxic effects of vegetable oils,
95 especially those extracted from poorly known raw materials, for some of the various
96 biologically active compounds found in the oil may be toxic to the body or even present
97 mutagenic or carcinogenic activities. Thus, tests are necessary to evaluate the possible
98 cytotoxic activity of the samples (Benigni, 2005).

99 Based on these considerations, the objective of this work was to evaluate the
100 physicochemical properties (measured by quality parameters), the thermal behavior by
101 thermogravimetric and derivative thermogravimetric analysis (TG/DTG), as well as to
102 determine the functional groups from infrared spectra and the cytotoxic effect of
103 bacaba-de-leque oil (*Oenocarpus distichus*), extracted by supercritical carbon dioxide
104 (Sc-CO₂) at 50 °C and 350 bar.

105

106 **2. Materials and methods**

107

108 *2.1. Oil sample*

109

110 Bacaba-de-leque oil (*Oenocarpus distichus*) was extracted with supercritical
111 carbon dioxide (Sc-CO₂) at operating conditions of 50 °C, 350 bar, and $\rho=899,23 \text{ kg/m}^3$,
112 using the raw material and extraction unit described by Cunha et al. (2019). The
113 definition of temperature and pressure parameters applied in the experiment was based
114 on the study conducted by the same authors. Extraction occurred with CO₂ mass flow

115 rate of 5.31 g/min for 150 min, using 20 g of bacaba-de-leque. Nine extractions were
116 performed to collect the oil that was used in the subsequent analyses.

117

118 2.2. Physicochemical characterization of the extracted oil

119

120 2.2.1. Carotenoids content

121

122 Total carotenoid of bacaba-de-leque oil was determined according to the
123 methodology described by Rodriguez-Amaya and Kimura (2004). The oil sample was
124 diluted in petroleum ether (Êxodo Científica, PA-ACS, Brazil), and the absorbance
125 reading was carried out at 450 nm on a spectrophotometer (model UV-M51, BEL
126 Photonics, Italy). The analysis was performed in triplicate, and total carotenoid
127 concentration was calculated using equation 1.

128

$$129 \text{ Total carotenoid } \left(\mu \frac{g}{g} \right) = \frac{A \times V (mL) \times 10^4}{A_{1\%}^{1\text{cm}} \times m_{oil}} \quad (1)$$

130

131 Where: A is the solution absorbance at 450 nm for β -carotene; V is the total extract
132 volume; $A_{1\%}^{1\text{cm}}$ is the absorption coefficient of β -carotene in petroleum ether (2592), and
133 m_{oil} is the oil mass used.

134 The result was expressed in micrograms of carotenoids per gram of oil ($\mu\text{g/g}$ oil).

135

136 2.2.2. Acidity index

137

138 The acidity index was determined according to the official Cd 3d-63 method of
139 the American Oil Chemists' Society (AOCS, 2017). In this work, the result of this
140 analysis was expressed as a percentage of free fatty acids (%FFA) in oleic acid.

141

142 *2.2.3. Peroxide value*

143

144 The peroxide value of the oil was determined according to the official Cd 8b-90
145 methodology of the American Oil Chemists' Society (AOCS, 2017).

146

147 *2.2.4. Saponification value*

148

149 The saponification value was calculated from the standardized fatty acid
150 composition of bacaba-de-leque oil, according to the official method Cd 3a-94,
151 described by the American Oil Chemists' Society (AOCS, 2017).

152 The fatty acid composition was previously determined by gas chromatography,
153 which is published in the work of Cunha et al. (2019).

154

155 *2.2.5. Iodine value*

156

157 The iodine value was determined according to the official method Cd 1b-87 of the
158 American Oil Chemists' Society (AOCS, 2017). The oil was mixed with iodine
159 monochloride to halogenate the double bonds in the oil. Excess iodine monochloride
160 was reduced to free iodine in the presence of potassium iodide. Free iodine was
161 measured by titration with sodium thiosulfate, using a starch solution as indicator.

162

163 2.2.6. *Refractive index*

164

165 The refractive index was determined by an Abbe refractometer (Q767BO, Quimis,
166 Brazil), with reading at room temperature (25 °C), according to the official
167 methodology Cc 7-25 of the American Oil Chemists' Society (AOCS, 2017).

168

169 2.2.7. *Oil Density*

170

171 Relative density was determined according to the official methodology To 1b-64
172 of the American Oil Chemists' Society (AOCS, 2017), which, using a pycnometer,
173 applies the ratio of the weight of an unit volume of the sample at 25 °C, and the weight
174 of an unit volume of water at 25 °C.

175

176 2.2.8. *Insoluble Impurities*

177

178 The insoluble impurities in the bacaba-de-leque oil was measured according to the
179 official method Ca 3a-46 of the American Oil Chemists' Society (AOCS, 2017).

180

181 2.3. *Thermal analysis*

182

183 2.3.1. *Thermogravimetric and differential thermal analysis (TG–DTA)*

184

185 Thermal analyses were performed on a thermogravimetric analyzer, model DTG-
186 60 H (Shimadzu, Japan), with a heating rate of 10 °C/min, ranging from room

187 temperature to 600 °C. Nitrogen atmosphere (N₂) with flow rate of 50 mL/min, alumina
188 crucible, and 7 mg of sample were used.

189

190 2.4. Fourier transform infrared spectroscopy (FTIR)

191

192 FTIR spectra of bacaba-de-leque oil were recorded using a VERTEX 70v FTIR
193 spectrometer (Bruker, USA), at room temperature, at the High Pressure and Vibrational
194 Spectroscopy Laboratory (LEVAP) of the Program of Post-Graduation in Physics of the
195 Federal University of Pará (PPGF/UFGPA). The spectra were recorded in a 4 cm⁻¹
196 resolution, and optical range between 400 and 4000 cm⁻¹ with 32 scans.

197

198 2.5. Cytotoxicity assay

199

200 In order to evaluate the effects of cytotoxicity of bacaba-de-leque oil (*Oenocarpus*
201 *distichus*) on human red blood cells, hemolytic activity was performed according to
202 Sharma and Sharma (2001) and Khan et al. (2013). Hemolysis percentages were
203 calculated using the following equation:

204

$$205 \quad \% \text{ Hemolysis} = \frac{A_{492 \text{ Oil}} - A_{492 \text{ PBS}}}{A_{492 \text{ TRI}} - A_{492 \text{ PBS}}} \times 100 \quad (2)$$

206

207 Where: $A_{492 \text{ Oil}}$ is the oil absorbance at 492 nm, $A_{492 \text{ PBS}}$ is the absorbance in
208 Phosphate Buffered Saline (PBS) (negative control) at 492 nm, and $A_{492 \text{ TRI}}$ is the
209 Triton absorbance (positive control) at 492 nm.

210

211 About 2 mL of human red blood cells were washed 3 times using a centrifuge

212 prepared at 10% in phosphate buffered saline (PBS) (Sigma-Aldrich®, USA). Then, 2.5
213 mL aliquots of the red cell suspension were prepared at concentrations of 250, 500,
214 1000 and 2000 mg/L, adding 500 µL of the oil each time. The solutions were mixed and
215 originated three 1 mL aliquots each, then were stored in tubes called T0, T20, and T40,
216 which were immediately placed in a thermostated bath (Fanem Ltda, model 102/6-R,
217 Brazil), and incubated at 37 °C. Subsequently, 40 µL of 2.5% glutaraldehyde (25%,
218 Vetec®, Brazil) were added, at different times, to the three tubes to finish the reaction.
219 The solution was added immediately to tube T0, after incubation at 37 °C. After 20 min,
220 it was added to tube T20 and, after 40 min of incubation, to tube T40.

221 After addition of glutaraldehyde at the indicated times, the tubes were placed in a
222 centrifuge (Kubota, model 2100, Japan), at 2500 rpm for 15 min to allow ruptured
223 membranes and unbroken cells to settle. The supernatant was removed and transferred
224 to a 96-well plate, and the hemoglobin released into the supernatant was measured by
225 spectrophotometry at 492 nm absorbance, using a spectrophotometer (Thermoplate,
226 model TP-Reader, USA).

227 As positive and negative controls, 0.2% Triton X-100 (Sigma-Aldrich®, USA)
228 (diluted in PBS, 100% hemolysis), and PBS (0% hemolysis) were used, respectively.
229 500 µL of each control was used and added to 2.5 mL aliquots of the 10% red-cell
230 suspension.

231

232 2.6. *Statistical analysis*

233

234 All analyses were performed in triplicate, and the results were expressed as the
235 mean of three independent repetitions ($n = 3$), and their standard deviation was also
236 calculated.

237 3. Results and discussion

238

239 The yield of each extraction was, in average, $38.45 \pm 1.14\%$, affording about 7.69
240 ± 0.23 g of bacaba-de-leque oil in each extraction, and a total of 69.18 g of oil, which
241 were enough to perform all analyses described in this study.

242

243 3.1. Physicochemical properties

244

245 Table 1 shows the results of the analyses performed on bacaba-de-leque oil (*O.*
246 *distichus*) obtained with Sc-CO₂, at 50 °C/350 bar.

247

248 Table 1-Physicochemical properties of bacaba-de-leque oil.

Analysis	Values
Carotenoid content ($\mu\text{g/g}$ oil)	21.36 ± 0.38
Free Fatty Acid (% FFA) in oleic acid	7.66 ± 0.01
Peroxide value (mEq O ₂ /kg oil)	1.35 ± 0.12
Saponification value (mg KOH/g oil)	193.32 ± 0.06
Iodine Value (g I ₂ /100 g oil)	95.81 ± 0.17
Refractive index 25 °C	1.35 ± 0.001
Density (g/cm ³) a 25°C	0.91 ± 0.002
Insoluble Impurities (%)	0.045 ± 0.03

249 Data represent the mean \pm standard deviation of three replicates

250

251 Total carotenoid was 21.36 ± 0.38 $\mu\text{g/g}$ oil. Compared to other vegetable oils, this
252 value was higher than in patauá oil (*Oenocarpus bataua*) (2.38 $\mu\text{g/g}$ oil), and bacaba oil
253 (*Oenocarpus bacaba*) (13.53 $\mu\text{g/g}$ oil), determined in the work of Montúfar et al. (2010)
254 and Santos et al. (2015), who evaluated the concentration of carotenoids in oils
255 extracted by conventional methods from Brazilian Amazonian palm fruits of the same
256 family (*Arecaceae*). However, this value was lower than those found by the same

257 authors in inajá (*Attalea maripa*) (85.03 µg/g oil), peach palm (*Bactris gasipaes*)
258 (357.42 µg/g oil), and buriti oils (*Mauritia flexuosa*) (540.81 µg/oil). On the other hand,
259 it was very close to the results obtained by Bezerra et al. (2018), who extracted oil from
260 palm-pressed fibers (*Elaeis guineensis* Jacq.) by Sc-CO₂ at temperatures of 40 and 60
261 °C and pressures from 150 to 450 bar, whose values ranged from 5.32 to 26.11 µg/g oil.

262 Bacaba-de-leque oil also had a total carotenoid content similar to those found in
263 some edible vegetable oils, which are widely traded and consumed in many countries
264 around the world due to their high nutritional value, such as olive oil and chia oil.
265 Moyano et al. (2008) evaluated about 1700 samples of virgin olive oil of eight varieties
266 at different stages of maturation, and related their color to the concentration of total
267 carotenoids and other pigments, whose values ranged from 0.53 to 31.51 µg/g oil. 11
268 samples of virgin olive oil produced in different regions of Brazil and Spain studied by
269 Borges et al. (2017) showed carotenoid content between 2.42 and 9.09 µg/g oil, whereas
270 the samples of olive oil obtained by ultrasound assisted extraction on industrial scale,
271 evaluated by Taticchi et al. (2019), presented values ranging from 2.8 to 3.7 µg/g oil of
272 total carotenoids. Bodoira et al. (2017) extracted chia oil (*Salvia hispanica* L.) by
273 mechanical pressing, and determined the total carotenoid content, which was equal to
274 5.41 µg/g oil.

275 In addition to fatty acids (especially the large amount of monounsaturated fatty
276 acids (MUFAs), such as oleic acid) (Cunha et al., 2019), the presence of minor
277 compounds, such as carotenoids, may also contribute to the high functional quality of
278 bacaba-de-leque oil, which can be characterized as a food product of great nutritional
279 and medicinal values, with various biological activities. Consumption of foods
280 containing carotenoids has a major influence on human health, as some of these
281 compounds are provitamin A or can be converted to vitamin A in the body when

282 ingested, and are able to reduce the risk of disorders and diseases caused by oxidative
283 stress, due to the great antioxidant capacity of carotenoids. This property is due to the
284 physical elimination capacity of reactive oxygen species (ROS), known as singlet
285 oxygen ($^1\text{O}_2$) and free radicals (Ngamwonglumlert & Devahastin, 2019).

286 The quality of vegetable oils is also evaluated by their physicochemical
287 properties, measured by quality parameters such as those presented in Table 1: free fatty
288 acid content, peroxide, saponification and iodine values, refractive index, density, and
289 insoluble impurities. Bacaba-de-leque oil had an acidity value, expressed as a
290 percentage of free fatty acids, equal to 7.66 ± 0.01 (% FFA) in oleic acid. This value
291 was higher than the maximum limit of 2.0 (% FFA) in oleic acid (4.0 mg KOH/g oil) for
292 crude and unrefined oils, recommended by Codex Alimentarius (2015), indicating a
293 certain state of oil degradation. As reported by Cunha et al. (2019), bacaba-de-leque oil
294 is predominantly characterized by the high content of unsaturated fatty acids, especially
295 oleic and linoleic acids, which combined are part of the main triglycerides that compose
296 it. This characteristic may be attributed to the high amount of free fatty acids (FFA)
297 observed in bacaba-de-leque oil, considering that the chemical structure of unsaturated
298 fatty acids linked to triglycerides facilitates enzymatic hydrolysis, due to double bonds
299 present in carbon chains, which present low stability and, thus, favor the rupture of
300 triglycerides, and form free fatty acids. This may occur during pre-treatment of the raw
301 material and subsequent handling and storage of the extracted oil (Gharby et al., 2017;
302 Gharby et al., 2015; Gupta, 2017). Another factor to be considered is the presence of
303 water in the vegetable matrix, since the extraction solvent (Sc-CO_2) can be absorbed by
304 water, which may increase its acidity and thus favor hydrolysis reactions and sample
305 degradation. In addition, the FFA content varies according to the species and history of

306 the plant matrix from which the oil is extracted (Gupta, 2017; Turner, King, &
307 Mathiasson, 2001).

308 In literature, some studies have evaluated the FFA content of various commercial
309 and non-commercial vegetable oils, and found acidity values similar to the results
310 obtained in this work. Bezerra et al. (2018) extracted oil from palm-pressed fibers
311 (*Elaeis guineensis* Jacq.) with supercritical CO₂ at 40 °C and 300 bar, and found an FFA
312 content of 9.03 (% FFA) in oleic acid. In the work of Costa et al. (2016), the quality of
313 the oil extracted by supercritical CO₂ from two species of tucumã was studied, whose
314 values ranged from 9.59 to 10.20 (% FFA) in oleic acid for *Astrocaryum aculeatum*
315 Meyer, and from 3.21 to 3.26 (% FFA) in oleic acid for *Astrocaryum vulgare* Mart. In
316 the oil of *Moringa oleifera* seed, also extracted by supercritical CO₂, the FFA content
317 ranged from 1.89 to 3.24, and from 3.21 to 3.26 (% FFA) in oleic acid for the species
318 *Astrocaryum vulgare* Mart. In the *Moringa oleifera* seed oil, also extracted by
319 supercritical CO₂, the FFA content ranged from 1.89 to 3.24 (% FFA) in oleic acid
320 (Ruttarattanamongkol, Siebenhandl-Ehn, Schreiner, & Petrasch, 2014), and in corn oil
321 extracted by conventional methods, the FFA content was 4.22 (% FFA) in oleic acid
322 (Giakoumis, 2018). In addition, the acidity value of other oils of Amazonian species
323 extracted by conventional methods, such as bacaba (*Oenocarpus bacaba*) (2.4 % FFA in
324 oleic acid), peach palm (*Bactris gasipaes*) (2.0 % FFA in oleic acid), buriti (*Mauritia*
325 *flexuosa*) (1.5 % FFA in oleic acid), and inajá (*Maximiliana maripa*) (1.0 % FFA in
326 oleic acid) (Santos et al., 2013) had values lower than that found for bacaba-de-leque
327 oil.

328 The determination of acidity is particularly important for industrial purposes, as
329 FFAs are capable of modifying the sensory properties of the oil, and are indicative of its
330 state of preservation (Gharby et al., 2015; Santos et al., 2019). However, the isolated

331 analysis of this parameter is not sufficient to determine the vegetable oils quality due to
332 the intensity and diversity of aromas and flavors they have, so other quality parameters
333 are required for this evaluation.

334 Peroxide value (PV) is one of these required parameters. It reveals the beginning
335 of the lipid oxidation of oils when exposed to heat and oxygen, which combined with
336 the double bonds of unsaturated fatty acids, form the peroxides and hydroperoxides.
337 The evaluation of this parameter is important because peroxides are the main oxidation
338 products of triglyceride-based vegetable oils, that can negatively affect their nutritional
339 value, and form secondary oxidation products, which also affect the sensory properties
340 of oils (Gomna, N'Tsoukpoe, Le Pierrès, & Coulibaly, 2019; Reboredo-Rodríguez et
341 al., 2016; Tilahun et al., 2019). The peroxide value of bacaba-de-leque oil was equal to
342 1.35 ± 0.12 mEq O₂/kg oil. This is a considerably low number, indicating low oil
343 oxidation, as this result is way below the reference value (up to 15 mEq O₂/kg oil)
344 determined by Codex Alimentarius (2015) for virgin and cold pressed oils. In the
345 literature, the PV of various edible oils, extracted by conventional methods and with
346 good oxidative stability, were evaluated and presented values above the results found
347 for ScCO₂-extracted bacaba-de-leque oil, such as virgin olive oils evaluated by
348 Reboredo-Rodríguez et al. (2016), whose PV ranged from 9.2 to 10.4 mEq O₂/kg oil,
349 chia seed oil (4.33 mEq O₂/kg oil) (Timilsena, Vongsvivut, Adhikari, & Adhikari,
350 2017), mustard (3.66 mEq O₂/kg oil), canola (9.46 mEq O₂/kg oil), sunflower (4.19
351 mEq O₂/kg oil), and peanut (8.39 mEq O₂/kg oil) oils analyzed by Konuskan et al.
352 (2019). Other oils from Amazonian native fruits, extracted by supercritical fluids,
353 presented similar values to those found in this work, such as muruci oil (*Byrsonima*
354 *crassifolia* L.) (1.2 mEq O₂/kg oil) (Santos et al., 2018), Brazil nut oil (*Bertolletia*

355 *excelsa* H.B.K) (2.4 mEq O₂/kg oil) (Santos et al., 2013), and sapucaia oil (*Lecythis*
356 *pisonis* Camb.) (2.41 to 2.89 mEq O₂/kg oil) (Santos et al., 2019).

357 Bacaba-de-leque oil was also evaluated by the saponification value (SV), which
358 was equal to 193.32 ± 0.06 mg KOH/g oil. This result is within the range of standard
359 values for some commercial oils, such as refined virgin olive oil (184 to 196 mg KOH/g
360 oil), corn oil (187 to 195 mg KOH/g oil), soy oil (189 to 195 mg KOH/g oil), and
361 sunflower oil (188 to 194 mg KOH/g oil) (Codex Alimentarius, 2013, 2015), suggesting
362 the presence of long-chain fatty acids and few amount of impurities. SV is inversely
363 proportional to the average length of the original fatty acid chain. For example, bacaba-
364 de-leque oil, which is rich in oleic acid (C18:1) (Cunha et al., 2019), presented SV
365 lower than palm-pressed fibers oil (*Elaeis guineensis* Jacq.) (231.84 mg KOH/g oil)
366 (Bezerra et al., 2018), and coconut oil (250.07 to 260.67 mg KOH/g oil) (Marina, Che
367 Man, Nazimah, & Amin, 2009), both rich in lauric acid (C12:0), which has a smaller
368 carbon chain. Due to these differences, the determination of SV becomes a relevant tool
369 for the characterization of vegetable oils, since it is a parameter that provides
370 information about the average molecular weight of oils, so that a reduction in its value
371 would be an indication of degradation of the original long-chain fatty acids of the oil in
372 smaller molecules, due to oxidation processes and rupture of bonds (Al-Bachir, 2015;
373 dos Santos et al., 2019; Zamora & Hidalgo, 2015).

374 Iodine value (IV) was one more parameter measured to evaluate the quality of
375 bacaba-de-leque oil, which presented value of 95.81 ± 0.17 g I₂/100 g oil. This
376 parameter is characteristic of each vegetable oil, and is used to measure the degree of
377 fatty acids unsaturation that compose it, which means that the higher the IV, the greater
378 the amount of unsaturated fatty acids. This information may be useful to evaluate the
379 oxidative rancidity and chemical stability of various types of oils, depending on their

380 fatty acid profiles, and especially their polyunsaturated fatty acid content (Gomna et al.,
381 2019; Ismail & Ali, 2015). The IV of bacaba-de-leque oil is similar to the results found
382 by Costa and Jorge (2012) in native fruit oils from the Amazon region, extracted by
383 cold pressing, such as Brazil nut oil (*Bertolletia excelsa*) (103.36 g I₂/100 g oil), and
384 sapucaia oil (*Lecythis pisonis*) (100.36 g I₂/100 g oil), both also rich in unsaturated fatty
385 acids (C18:1 and C18:2). It is also within the range of standard values determined for
386 edible mustard (92 to 125 g I₂/100 g oil), peanut (86 to 107 g I₂/100 g oil), and corn oils
387 (103 to 135 g I₂/100 g oil) (Codex Alimentarius, 2015), showing that the oil evaluated
388 in this work has a suitable oxidation stability, since a smaller amount of iodine absorbed
389 by the oil could be associated with the rupture of double bonds, as a result of oxidation
390 and polymerization reactions, which would decrease the unsaturated fatty acid content
391 of the oil (Gomna et al., 2019). In addition, the degree of unsaturation, measured by IV,
392 and the average molecular weight of fatty acids, measured by SV, have an influence on
393 the kinematic viscosity of the vegetable oil (Toscano, Riva, Foppa Pedretti, & Duca,
394 2012).

395 The refractive index (RI) determined for bacaba-de-leque oil was 1.35 ± 0.001 , at
396 25 °C. Like SV and IV, this parameter is specific for each type of oil, and has a direct
397 relationship with the degree of fatty acid saturation, oxidation state, heat treatment, and
398 probable impurities present in the oil. The higher the RI, the longer the fatty acid chain
399 length and the number of conjugated double bonds, and consequently, the greater the
400 amount of polyunsaturated fatty acid concentration (Davis, Sweigart, Price, Dean, &
401 Sanders, 2013; Timilsena et al., 2017). In bacaba-de-leque oil, RI was slightly below the
402 value found for chia oil (1.48, at 40 ° C), evaluated by Timilsena et al. (2017), and for
403 sesame seed oil (1.472, at 20 °C) evaluated by Gharby et al. (2017), which are oils that

404 have concentration of polyunsaturated fatty acids higher than bacaba-de-leque oil,
405 especially linoleic (C18:2) and linolenic (C18:3) acids.

406 Density is another important property for the quality evaluation of vegetable oils,
407 since this factor is also information that is related to the oil composition in terms of fatty
408 acids. It is useful to observe possible changes in the composition and degree of
409 hydrogenation/saturation during processing, and to understand transport phenomena in
410 industrial processes, specifically for products with unknown physical properties, such as
411 the oil evaluated in this work (Noureddini, Teoh, & Davis Clements, 1992; Timilsena et
412 al., 2017). The density of the bacaba-de-leque oil was evaluated at 25 ° C, and was
413 equal to $0.91 \pm 0.002 \text{ g/cm}^3$. This result is comparable to standard values for olive oil
414 (0.91 to 0.916 g/cm^3), edible corn (0.917 to 0.925 g/cm^3), soy (0.919 to 0.925 g/cm^3),
415 and canola (0.91 to 0.92 g/cm^3) oils, established by Codex Alimentarius (2015, 2013).
416 This result is also similar to those determined for some oils extracted with supercritical
417 fluid, such as moringa seed oil (0.93 to 0.94 g/cm^3 at 25 °C) (Ruttarattanamongkol et
418 al., 2014), babassu seed oil (*Orbignya phalerata*) (0.9141 to 0.9165 g/cm^3 at 25 °C) (de
419 Oliveira et al., 2019), and Brazil nut oil (*Bertolletia excelsa*) (0.91 g/cm^3 at 25 °C)
420 (Santos et al., 2012).

421 Crude vegetable oils have a different chemical composition, which varies
422 according to the species of the vegetable matrix. Predominantly, they are composed of
423 triglycerides, but are also made up of several other substances, such as insoluble
424 impurities, which include proteins, fibers, dirt, excess moisture, among others. These
425 substances can act as contaminants in food or industrial applications, and influence on
426 sensory properties (Dayton & Galhardo, 2014). In bacaba-de-leque oil, the impurities
427 content was $0.045 \pm 0.03 \%$, which is below the standard maximum value of 0.05%

428 determined by the Codex Alimentarius (2015) for crude oils, indicating that the
429 evaluated oil is suitable for food applications.

430 It is important to highlight that the standard values of the quality parameters
431 established by Codex Alimentarius (2015) make no mention of bacaba-de-leque oil, as
432 this product is not marketed in Brazil. But the results found in this study are allowed for
433 crude vegetable oils and apply to edible oils commercialized in Brazil and other
434 countries, thus confirming the good quality of the extracted oil.

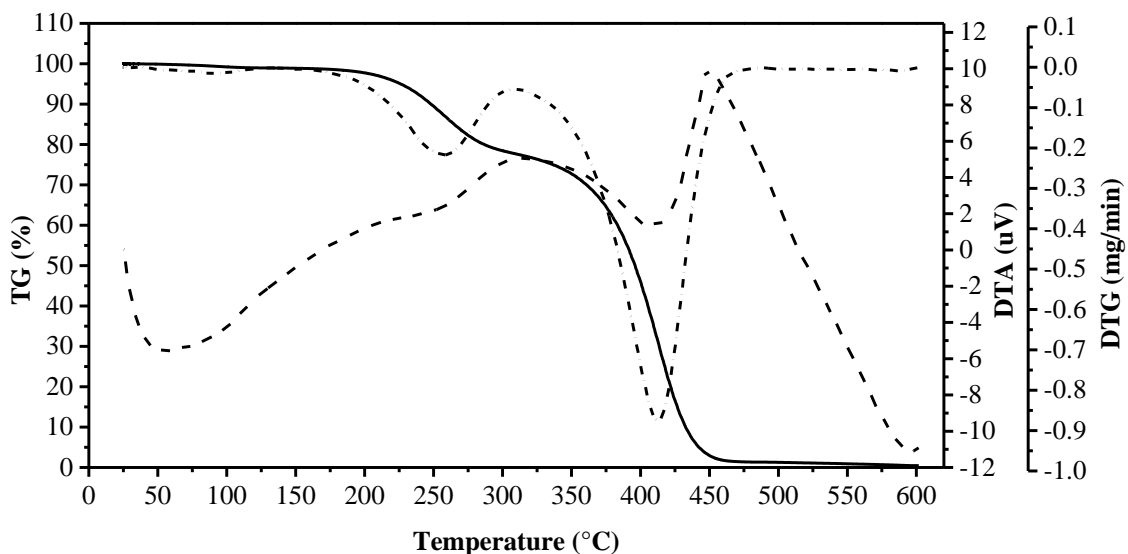
435

436 3.2 Thermal behavior

437

438 Fig.1 shows the results of differential thermal analysis (DTA), and
439 thermogravimetric (TG) and derivative thermogravimetric (DTG) analyses of Sc-CO₂-
440 extracted bacaba-de-leque oil, performed at heating rate of 10 °C/min until 600 °C,
441 under N₂ atmosphere. These analyses show the mass loss and thermal decomposition
442 profile of the oil, as a result of formation and rupture of its physicochemical bonds, at
443 elevated temperatures (Wan Nik, Ani, & Masjuki, 2005).

444



445

446

Fig. 1. Thermogravimetric behavior of bacaba-de-leque oil obtained by Sc-CO₂.

447

— TG (%) - - DTA (uV) - . . . DTG (mg/min)

448 As can be seen from the TG curve shown in Fig. 1, bacaba-de-leque oil showed
449 relative thermal stability up to temperature close to 210 °C, from which it was observed
450 the beginning of the oil mass loss, and its conclusion around 560 °C. This thermal
451 degradation process took place in three stages. The first stage occurred in the range of
452 220 to 280 °C, where about 20% of the oil mass was lost. During this temperature
453 range, the DTG curve exhibited a smaller, broad first peak towards the baseline, at 250
454 °C, indicating considerable mass loss. The second stage was observed in the
455 temperature range from 280 to 350 °C, where there was little mass loss. According to
456 Fan et al. (2014), this may happen due to the low reaction rate in this range, or because
457 there is a short induction period for oxidation reactions, with high activation energy.
458 The third stage was observed from 350 °C on, in which there was a sharp reduction in
459 the oil mass until there was no more residue. In this last interval, DTG curve exhibited a
460 second peak, with greater amplitude, at 405 °C, showing, with greater clarity, the
461 intense reduction in mass.

462 DTA curve shows this oil behavior, when subjected to temperature changes,
463 where peaks can be identified in the regions with greater sample degradation. The first
464 peak is smaller, being displayed in the region between 250 and 380 °C, where the oil
465 decomposition was smaller compared to the second peak, displayed in the region
466 between 420 and 550 °C. These events indicated the predominance of exothermic
467 reactions caused by the release of energy from the decomposition of bacaba-de-leque
468 oil. This behavior is a result of oxidative degradation reactions in lipid materials caused
469 by temperature rise, which may increase further due to the high degree of unsaturation
470 of the vegetable oil (Santos et al., 2012).

471 Bacaba-de-leque oil consists mainly of polyunsaturated, monounsaturated, and
472 saturated fatty acids, respectively (Cunha et al., 2019). Therefore, the three stages of oil

473 decomposition may be related to the degradation of these major compounds during
474 material heating, in which the first stage may correspond to the decomposition of the
475 most unstable polyunsaturated fatty acids, and the second and third, respectively, may
476 correspond to the decomposition of monounsaturated and saturated fatty acids (Syah
477 Lubis, Ariwahjoedi, & Bin Sudin, 2015).

478 Compared with the results found in the literature, the thermogravimetric behavior
479 of bacaba-de-leque oil was similar to those of other vegetable oils, also rich in mono
480 and polyunsaturated fatty acids. Syah Lubis et al. (2015) investigated the thermal
481 stability of jatropha oil by TG/DTG, under O₂ and N₂ atmospheres, showing that the oil
482 is thermally stable below 225 °C in N₂ atmosphere, and below 168 °C in O₂ atmosphere.
483 It is also completely decomposed around 550 °C. Santos et al. (2019) extracted sapucaia
484 oil (*Lecythis pisonis* Camb.) by SFE, and evaluated the thermal stability by TG/DTG.
485 The oil remained stable until around 200 °C, from which it presented intense mass loss,
486 followed by complete decomposition of the sample around 650 °C.

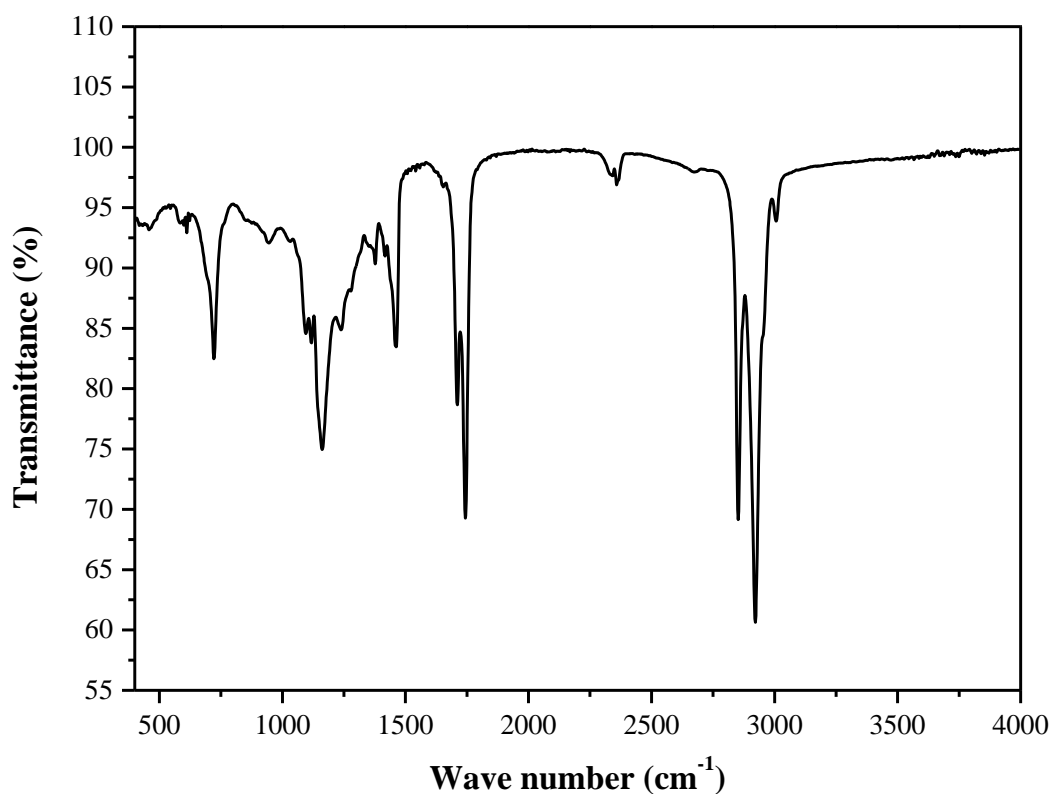
487

488 3.3. *Fourier transform infrared spectroscopy (FTIR)*

489

490 FTIR spectra of bacaba-de-leque oil were obtained and analyzed between 400 and
491 4000 cm⁻¹. This analysis provided information on the spectral bands related to the
492 groups of chemical compounds present in the oil sample, as shown in Fig. 2.

493



494
495 Fig. 2: Spectroscopic profile of bacaba-de-leque oil.
496

497 The most intense absorption bands at 2924 and 2853 cm⁻¹ are attributed to the
498 vibrations of symmetric and asymmetric axial deformation of the CH bonds from
499 methyl (CH₃), methylene (CH₂), and double bonds (= C-H) groups, belonging to the
500 groups of fatty acids in triglycerides (Teixeira, Ávila, Silveira, Ribani, & Ribani, 2017;
501 Thakore, Rathore, Jadeja, Thounaojam, & Devkar, 2014). The visible spectral bands at
502 1750 and 1746 cm⁻¹ are characteristic of stretch vibrations of the carbonyl group (C=O)
503 present in triglycerides, tocopherols, and other phenolic compounds (Teixeira et al.,
504 2017; Thakore et al., 2014; Zahir, Saeed, Hameed, & Yousuf, 2017).

505 The intermediate intensity band, which appears at 1460 cm⁻¹, is attributed to the
506 vibrations of angular deformation of C-H bonds present in methyl and methylene
507 groups. The visible spectral band with absorbance at 1160 cm⁻¹ is characteristic of the
508 axial deformation of the C-O group of ethers. The smallest spectrum observed with
509 absorption band at 721 cm⁻¹ suggest the presence of R-CH group, and angular

510 deformation of the aromatic C-H group of the aliphatic chain of fatty acids
511 (Albuquerque, Guedes, Alcantara, & Moreira, 2003; Guillén & Cabo, 2002; Teixeira et
512 al., 2017; Thakore et al., 2014; Zahir et al., 2017).

513 These spectral bands are similar to those of oils extracted from native fruits of the
514 Amazon region, such as sapucaia oil (*Lecythis pisonis* Camb.), researched by Santos et
515 al. (2019), bacaba oil (*Oenocarpus bacaba*), evaluated by Pinto et al. (2018), both
516 extracted with Sc-CO₂, and buriti oil (*Mauritia flexuosa* L.) (Albuquerque et al., 2003),
517 extracted by conventional method. They were also found in edible sunflower (Thakore
518 et al., 2014), chia, olive, and canola oils, evaluated by Timilsena et al. (2017).

519 FTIR analysis not only provides information on the different functional groups
520 present in an oil sample, but it can also be applied to study the oxidation process of
521 edible oils. This is based on spectral changes of the analyzed material as a result of the
522 appearance of spectral bands attributed to oxidation products, such as aldehydes,
523 ketones, alcohols, carboxylic acids, peroxides, and hydroperoxides (Guillén & Cabo,
524 2002; Syah Lubis et al., 2015). These products were not observed in the spectral bands
525 of bacaba-de-leque oil, leading to the belief that the extraction method used (SFE) and
526 the operating conditions applied did not cause changes in its chemical composition. This
527 analysis also confirms the fatty acid profile previously determined by Cunha et al.
528 (2019), and the nutritional and functional properties of the oil.

529

530 3.4. Cytotoxic effects

531

532 Bacaba-de-leque oil (*Oenocarpus distichus*) showed no hemolysis at its respective
533 tested concentrations. Partial hemolysis (7.77%) was observed only at one
534 concentration. Complete hemolysis was demonstrated by Triton X-100 0.2 % (v/v) as a

535 positive control, and there was no evidence for hemolysis by phosphate buffered saline
536 (PBS) as a negative control (Table 2).

537

538 Table 2. Hemolytic activity of bacaba-de-leque oil (*Oenocarpus distichus*)

Sample	Compounds concentrations (mg/L)			
	250	500	1000	2000
	Hemolysis percentage of red blood cells			
Bacaba-de-leque oil	0.77	1.87	4.36	7.77

539

540 In the results of the cytotoxic analysis based on hemolytic activity, 100%
541 hemolysis is represented by the 0.2 % Triton positive control. Thus, the data observed in
542 Table 2 are expressed as percentage of hemoglobin release compared to 100 %
543 hemolysis of the same number of cells using Triton 100-X. The mechanical stability of
544 the erythrocyte membrane is an indicator of the effect imposed by various compounds
545 on cytotoxicity determination, and depends on their physical and structural properties
546 (Sharma & Sharma, 2001). Hemolysis represents the disruption of the integrity of the
547 red blood cell (RBC) membrane causing the release of hemoglobin. Therefore,
548 hemolysis usually manifests itself by the presence of free hemoglobin in the erythrocyte
549 suspension medium, such as plasma or additive solutions. (Makroo et al., 2011;
550 Sowemimo-Coker, 2002).

551 Several studies point out that oils obtained by supercritical technology have no
552 cytotoxic effects. A study of pomegranate oil (*Punica granatum* L.), obtained by SFE at
553 47 °C and 379 bar, was tested for cytotoxic potential by cell viability tests using 3-(4,5-
554 dimethylthiazole-2-yl)-2,5-diphenyltetrazolium bromide (MTT). The oil exhibited
555 cytotoxic effect against the malignant cells HeLa, LS174, and A549; but showed no
556 cytotoxicity to normal cells, indicating the safety of oil extracted by supercritical fluid
557 (Durđević et al., 2018). Similarly, a study of nutmeg oil (*Myristica fragrans*), obtained

558 by SFE, at 40 and 50 °C, and pressures of 200 to 415 bar, was tested for its cytotoxic
559 activity by MTT assay on two types of human tumor cells. The results indicated that all
560 oils obtained under different extraction parameters were not cytotoxic (Al-Rawi et al.,
561 2011). These studies have shown that supercritical extraction is a promising technique
562 for obtaining high quality solvent-free oils and extracts without cytotoxic effects, and is
563 suitable for obtaining high value-added products from natural sources that can be
564 applied to the human diet, with no risk of contamination.

565

566 **4. Conclusion**

567

568 Nutritional, physical, and chemical properties of scCO₂-extracted bacaba-de-leque
569 oil were similar to those of good quality edible oils already established in the market. It
570 showed significant carotenoid content and good quality parameters, within acceptable
571 levels for oils and fats from vegetable sources, showing that the extraction method used
572 caused little oxidative changes in the oil, and maintained its nutritional and functional
573 characteristics.

574 Thermogravimetric (TG/DTG) and differential thermal (DTA) analyses revealed
575 the thermal decomposition profile of the oil during heating, and showed that it is
576 thermally stable at temperatures up to 210 °C, and fully decomposed at 560 °C. It goes
577 through three stages of degradation, probably attributed to the decomposition of
578 polyunsaturated, monounsaturated, and saturated fatty acids, respectively.

579 The FTIR spectra provided information on the functional groups present in the
580 bacaba-de-leque oil, which showed standard peaks attributed to the characteristic
581 compounds of edible vegetable oils, especially those found in unsaturated fatty acids.

582 There was not the occurrence of spectral bands attributed to compounds that indicate a
583 high degree of oxidation.

584 The cytotoxicity tests showed that the bacaba-de-leque oil extracted using Sc-CO₂
585 had no cytotoxic effect, indicating that the oil can be consumed without harm to human
586 health.

587 All the results obtained in this study reinforce the efficiency of supercritical
588 technology to obtain high value-added products, and open new possibilities for
589 applications of bacaba-de-leque oil in food, cosmetics, and pharmaceutical industries, as
590 well as in bioenergy production. The functional quality of the oil, attributed to its
591 composition and physicochemical properties, is indicative of a product of great
592 nutritional and medicinal value with various biological activities.

593

594 **References**

595

596 Al-Bachir, M. (2015). Quality characteristics of oil extracted from gamma irradiated
597 peanut (*Arachis hypogea* L.). *Radiation Physics and Chemistry*, *106*, 56–60.
598 <https://doi.org/10.1016/j.radphyschem.2014.06.026>

599 Al-Rawi, S. S., Ibrahim, A. H., Rahman, N. N. N. A., Nama, M. M. Ben, Majid, A. M.
600 S. A., & Kadir, M. O. A. (2011). The Effect of Supercritical Fluid Extraction
601 Parameters on the Nutmeg Oil Extraction and Its Cytotoxic and Antiangiogenic
602 Properties. *Procedia Food Science*, *1*, 1946–1952.
603 <https://doi.org/10.1016/j.profoo.2011.09.286>

604 Albuquerque, M. L. S., Guedes, I., Alcantara, P., & Moreira, S. G. C. (2003). Infrared
605 absorption spectra of Buriti (*Mauritia flexuosa* L.) oil. *Vibrational Spectroscopy*,
606 *33*(1–2), 127–131. [https://doi.org/10.1016/S0924-2031\(03\)00098-5](https://doi.org/10.1016/S0924-2031(03)00098-5)

607 AOCS. (2017). *Official Methods and Recommended Practices of the AOCS* (7th ed.).

608 Benigni, R. (2005). Structure-activity relationship studies of chemical mutagens and
609 carcinogens: Mechanistic investigations and prediction approaches. *Chemical*
610 *Reviews*, 105(5), 1767–1800. <https://doi.org/10.1021/cr030049y>

611 Bezerra, F. W. F., Costa, W. A. da, Oliveira, M. S. de, Aguiar Andrade, E. H. de, &
612 Carvalho, R. N. de. (2018). Transesterification of palm pressed-fibers (*Elaeis*
613 *guineensis* Jacq.) oil by supercritical fluid carbon dioxide with entrainer ethanol.
614 *Journal of Supercritical Fluids*, 136(November 2017), 136–143.
615 <https://doi.org/10.1016/j.supflu.2018.02.020>

616 Bodoira, R. M., Penci, M. C., Ribotta, P. D., & Martínez, M. L. (2017). Chia (*Salvia*
617 *hispanica* L.) oil stability: Study of the effect of natural antioxidants. *LWT - Food*
618 *Science and Technology*, 75, 107–113. <https://doi.org/10.1016/j.lwt.2016.08.031>

619 Borges, T. H., Pereira, J. A., Cabrera-Vique, C., Lara, L., Oliveira, A. F., & Seiquer, I.
620 (2017). Characterization of Arbequina virgin olive oils produced in different
621 regions of Brazil and Spain: Physicochemical properties, oxidative stability and
622 fatty acid profile. *Food Chemistry*, 215, 454–462.
623 <https://doi.org/10.1016/j.foodchem.2016.07.162>

624 Codex Alimentarius. (2013). Codex alimentarius, Standard for olive oils and olive
625 pomace oils. CODEX STAN 33-1981. *Codex Alimentarius*.
626 <https://doi.org/10.1017/CBO9781107415324.004>

627 Codex Alimentarius. (2015). SECTION 2. *Codex Standards for Fats and Oils from*
628 *Vegetable Sources (CODEX-STAN 210 - 1999)*. *Codex Alimentarius*.
629 <https://doi.org/10.1017/CBO9781107415324.004>

630 Costa, B. E. T., Santos, O. V. Dos, Corrêa, N. C. F., & França, L. F. De. (2016).
631 Comparative study on the quality of oil extracted from two tucumã varieties using

632 supercritical carbon dioxide. *Food Science and Technology*, 36(2), 322–328.
633 <https://doi.org/10.1590/1678-457X.0094>

634 Costa, T., & Jorge, N. (2012). Characterization and fatty acids profile of the oils from
635 Amazon nuts and walnuts: Characterization and fatty acids profile of the oilseeds.
636 *Nutrition and Food Science*, 42(4), 279–287.
637 <https://doi.org/10.1108/00346651211248647>

638 Cunha, V. M. B., Silva, M. P. da, Sousa, S. H. B. de, Bezerra, P. do N., Menezes, E. G.
639 O., Silva, N. J. N. da, ... Carvalho Junior, R. N. de. (2019). Bacaba-de-leque
640 (*Oenocarpus distichus* Mart.) oil extraction using supercritical CO₂ and bioactive
641 compounds determination in the residual pulp. *Journal of Supercritical Fluids*,
642 144(August 2018), 81–90. <https://doi.org/10.1016/j.supflu.2018.10.010>

643 Davis, J. P., Sweigart, D. S., Price, K. M., Dean, L. L., & Sanders, T. H. (2013).
644 Refractive index and density measurements of peanut oil for determining oleic and
645 linoleic acid contents. *JAOCs, Journal of the American Oil Chemists' Society*,
646 90(2), 199–206. <https://doi.org/10.1007/s11746-012-2153-4>

647 Dayton, C. L. G., & Galhardo, F. (2014). Enzymatic Degumming. In W. E. Farr & A.
648 Proctor (Eds.), *Green Vegetable Oil Processing* (1st ed.). New Jersey.
649 <https://doi.org/10.1016/c2015-0-04080-1>

650 de Oliveira, N. A., Mazzali, M. R., Fukumasu, H., Gonçalves, C. B., & Oliveira, A. L.
651 de. (2019). Composition and physical properties of babassu seed (*Orbignya*
652 *phalerata*) oil obtained by supercritical CO₂ extraction. *Journal of Supercritical*
653 *Fluids*, 150, 21–29. <https://doi.org/10.1016/j.supflu.2019.04.009>

654 dos Santos, Orquídea Vasconcelos, Agibert, S. A. C., Pavan, R., de Godoy, I. J., da
655 Costa, C. E. F., Filho, J. M., & Lannes, S. C. da S. (2019). Physicochemical,
656 chromatographic, oxidative, and thermogravimetric parameters of high-oleic

657 peanut oil (*Arachis hypogaea* L. IAC-505). *Journal of Thermal Analysis and*
658 *Calorimetry*, 0123456789. <https://doi.org/10.1007/s10973-019-08182-z>

659 Đurđević, S., Šavikin, K., Živković, J., Böhm, V., Stanojković, T., Damjanović, A., &
660 Petrović, S. (2018). Antioxidant and cytotoxic activity of fatty oil isolated by
661 supercritical fluid extraction from microwave pretreated seeds of wild growing
662 *Punica granatum* L. *Journal of Supercritical Fluids*, 133(July 2017), 225–232.
663 <https://doi.org/10.1016/j.supflu.2017.10.021>

664 Endo, Y. (2018). Analytical methods to evaluate the quality of edible fats and oils: The
665 JOCS standard methods for analysis of fats, oils and related materials (2013) and
666 advanced methods. *Journal of Oleo Science*, 67(1), 1–10.
667 <https://doi.org/10.5650/jos.ess17130>

668 Fan, C., Zan, C., Zhang, Q., Ma, D., Chu, Y., Jiang, H., ... Wei, F. (2014). The
669 oxidation of heavy oil: Thermogravimetric analysis and non-isothermal kinetics
670 using the distributed activation energy model. *Fuel Processing Technology*, 119,
671 146–150. <https://doi.org/10.1016/j.fuproc.2013.10.020>

672 Gharby, S., Harhar, H., Bouzoubaa, Z., Asdadi, A., El Yadini, A., & Charrouf, Z.
673 (2017). Chemical characterization and oxidative stability of seeds and oil of
674 sesame grown in Morocco. *Journal of the Saudi Society of Agricultural Sciences*,
675 16(2), 105–111. <https://doi.org/10.1016/j.jssas.2015.03.004>

676 Gharby, Said, Harhar, H., Guillaume, D., Roudani, A., Boulbaroud, S., Ibrahimi, M., ...
677 Charrouf, Z. (2015). Chemical investigation of *Nigella sativa* L. seed oil produced
678 in Morocco. *Journal of the Saudi Society of Agricultural Sciences*, 14(2), 172–177.
679 <https://doi.org/10.1016/j.jssas.2013.12.001>

680 Giakoumis, E. G. (2018). Analysis of 22 vegetable oils' physico-chemical properties
681 and fatty acid composition on a statistical basis, and correlation with the degree of

682 unsaturation. *Renewable Energy*, 126, 403–419.
683 <https://doi.org/10.1016/j.renene.2018.03.057>

684 Gomna, A., N'Tsoukpoe, K. E., Le Pierrès, N., & Coulibaly, Y. (2019). Review of
685 vegetable oils behaviour at high temperature for solar plants: Stability, properties
686 and current applications. *Solar Energy Materials and Solar Cells*, 200(May),
687 109956. <https://doi.org/10.1016/j.solmat.2019.109956>

688 Guillén, M. D., & Cabo, N. (2002). Fourier transform infrared spectra data versus
689 peroxide and anisidine values to determine oxidative stability of edible oils. *Food*
690 *Chemistry*, 77(4), 503–510. [https://doi.org/10.1016/S0308-8146\(01\)00371-5](https://doi.org/10.1016/S0308-8146(01)00371-5)

691 Gupta, M. K. (2017). *Practical Guide to Vegetable Oil Processing*. (N. Maragioglio,
692 Ed.) (2nd ed.). Lynnwood, TX, United States: Nikki Levy.

693 Ismail, S. A. E. A., & Ali, R. F. M. (2015). Physico-chemical properties of biodiesel
694 manufactured from waste frying oil using domestic adsorbents. *Science and*
695 *Technology of Advanced Materials*, 16(3), 1–9. [https://doi.org/10.1088/1468-](https://doi.org/10.1088/1468-6996/16/3/034602)
696 6996/16/3/034602

697 Khan, M. S. A., Ahmad, I., & Cameotra, S. S. (2013). Phenyl aldehyde and propanoids
698 exert multiple sites of action towards cell membrane and cell wall targeting
699 ergosterol in *Candida Albicans*. *AMB Express*, 3(1), 1–16.
700 <https://doi.org/10.1186/2191-0855-3-1>

701 Knez, Markočič, E., Leitgeb, M., Primožič, M., Knez Hrnčič, M., & Škerget, M. (2014).
702 Industrial applications of supercritical fluids: A review. *Energy*, 77, 235–243.
703 <https://doi.org/10.1016/j.energy.2014.07.044>

704 Konuskan, D. B., Arslan, M., & Oksuz, A. (2019). Physicochemical properties of cold
705 pressed sunflower, peanut, rapeseed, mustard and olive oils grown in the Eastern
706 Mediterranean region. *Saudi Journal of Biological Sciences*, 26(2), 340–344.

707 <https://doi.org/10.1016/j.sjbs.2018.04.005>

708 Makroo, R. N., Raina, V., Bhatia, A., Gupta, R., Majid, A., Thakur, U. K., & Rosamma,
709 N. L. (2011). Evaluation of the red cell hemolysis in packed red cells during
710 processing and storage. *Asian Journal of Transfusion Science*, 5(1), 15–17.
711 <https://doi.org/10.4103/0973-6247.75970>

712 Marina, A. M., Che Man, Y. B., Nazimah, S. A. H., & Amin, I. (2009). Chemical
713 properties of virgin coconut oil. *JAOCS, Journal of the American Oil Chemists’*
714 *Society*, 86(4), 301–307. <https://doi.org/10.1007/s11746-009-1351-1>

715 Martinez, J., & de Aguiar, A. C. (2014). Extraction of Triacylglycerols and Fatty Acids
716 Using Supercritical Fluids - Review. *Current Analytical Chemistry*, 10(1), 67–77.
717 <https://doi.org/10.2174/1573411011410010006>

718 Melo, R. R. de, Borin, G. P., Zanini, G. K., Neto, A. A. K., Fernandes, B. S., &
719 Contesini, F. J. (2016). An Overview on Vegetable Oils and Biocatalysis. In B.
720 Holt (Ed.), *Vegetable oil properties, uses and benefits* (1st ed.). New York: Nova.

721 Montúfar, R., Laffargue, A., Pintaud, J. C., Hamon, S., Avallone, S., & Dussert, S.
722 (2010). *Oenocarpus bataua* Mart. (*Arecaceae*): Rediscovering a source of high
723 oleic vegetable oil from Amazonia. *JAOCS, Journal of the American Oil Chemists’*
724 *Society*, 87(2), 167–172. <https://doi.org/10.1007/s11746-009-1490-4>

725 Moyano, M. J., Meléndez-Martínez, A. J., Alba, J., & Heredia, F. J. (2008). A
726 comprehensive study on the colour of virgin olive oils and its relationship with
727 their chlorophylls and carotenoids indexes (I): CIEXYZ non-uniform colour space.
728 *Food Research International*, 41(5), 505–512.
729 <https://doi.org/10.1016/j.foodres.2008.03.007>

730 Ngamwonglumlert, L., & Devahastin, S. (2019). Carotenoids. *Encyclopedia of Food*
731 *Chemistry*, 1, 40–52. <https://doi.org/10.1016/B978-0-08-100596-5.21608-9>

732 Nouredini, H., Teoh, B. C., & Davis Clements, L. (1992). Viscosities of vegetable oils
733 and fatty acids. *Journal of the American Oil Chemists Society*, 69(12), 1189–1191.
734 <https://doi.org/10.1007/BF02637678>

735 Pinto, R. H. H., Sena, C., Santos, O. V., Costa, W. A. da, Rodrigues, A. M. C., &
736 Junior, R. N. C. (2018). Extraction of bacaba (*Oenocarpus bacaba*) oil with
737 supercritical CO₂: Global yield isotherms, fatty acid composition, functional
738 quality, oxidative stability, spectroscopic profile and antioxidant activity. *Grasas y*
739 *Aceites*, 69(2), 1–8.

740 Reboredo-Rodríguez, P., González-Barreiro, C., Cancho-Grande, B., Valli, E., Bendini,
741 A., Gallina Toschi, T., & Simal-Gandara, J. (2016). Characterization of virgin
742 olive oils produced with autochthonous Galician varieties. *Food Chemistry*, 212,
743 162–171. <https://doi.org/10.1016/j.foodchem.2016.05.135>

744 Rodriguez-Amaya, D. B., & Kimura, M. (2004). HarvestPlus Handbook for Carotenoid
745 Analysis. *HarvestPlus Technical Monograph 2*, 2068(1), 71–77.
746 <https://doi.org/10.3141/2068-08>

747 Ruttarattanamongkol, K., Siebenhandl-Ehn, S., Schreiner, M., & Petrasch, A. M.
748 (2014). Pilot-scale supercritical carbon dioxide extraction, physico-chemical
749 properties and profile characterization of Moringa oleifera seed oil in comparison
750 with conventional extraction methods. *Industrial Crops and Products*, 58, 68–77.
751 <https://doi.org/10.1016/j.indcrop.2014.03.020>

752 Sahena, F., Zaidul, I. S. M., Jinap, S., Karim, A. A., Abbas, K. A., Norulaini, N. A. N.,
753 & Omar, A. K. M. (2009). Application of supercritical CO₂ in lipid extraction – A
754 review. *Journal of Food Engineering*, 95(2), 240–253.
755 <https://doi.org/10.1016/j.jfoodeng.2009.06.026>

756 Santos, Orquidea Vasconcelos dos, Carvalho, R. N., Costa, C. E. F. da, & Lannes, S. C.

757 da S. (2019). Chemical, chromatographic-functional, thermogravimetric-
758 differential and spectroscopic parameters of the sapucaia oil obtained by different
759 extraction methods. *Industrial Crops and Products*, 132(February), 487–496.
760 <https://doi.org/10.1016/j.indcrop.2019.02.043>

761 Santos, Orquidea Vasconcelos dos, Corrêa, N. C. F., Soares, F. A. S. M., Gioielli, L. A.,
762 Costa, C. E. F., & Lannes, S. C. S. (2012). Chemical evaluation and thermal
763 behavior of Brazil nut oil obtained by different extraction processes. *Food*
764 *Research International*, 47(2), 253–258.
765 <https://doi.org/10.1016/j.foodres.2011.06.038>

766 Santos, M. F. G., Alves, R. E., & Roca, M. (2015). Carotenoid composition in oils
767 obtained from palm fruits from the Brazilian Amazon; Composición de
768 carotenoides en aceites obtenidos a partir de frutos de palma de la Amazonia
769 Brasileña. *Grasas Y Aceites*, 66(3). <https://doi.org/10.3989/gya.1062142>

770 Santos, M. F. G., Marmesat, S., Brito, E. S., Alves, R. E., & Dobarganes, M. C. (2013).
771 Major components in oils obtained from Amazonian palm fruits. *Grasas y Aceites*,
772 64(3), 328–334. <https://doi.org/10.3989/gya.023513>

773 Santos, Orquidea Vasconcelos, Correa, N. C. F., Carvalho Junior, R., da Costa, C. E. F.,
774 Moraes, J. de F. C., & Lannes, S. C. da S. (2018). Quality parameters and
775 thermogravimetric and oxidative profile of muruci oil (*Byrsonima crassifolia* L.)
776 obtained by supercritical CO₂. *Food Science and Technology*, 38(1), 172–179.
777 <https://doi.org/10.1590/1678-457x.30616>

778 Santos, O. V., Corrêa, N. C. F., Carvalho, R. N., Costa, C. E. F., & Lannes, S. C. S.
779 (2013). Yield, nutritional quality, and thermal-oxidative stability of Brazil nut oil
780 (*Bertolletia excelsa* H.B.K) obtained by supercritical extraction. *Journal of Food*
781 *Engineering*, 117(4), 499–504. <https://doi.org/10.1016/j.jfoodeng.2013.01.013>

782 Sharma, P., & Sharma, J. D. (2001). In vitro hemolysis of human erythrocytes - By
783 plant extracts with antiplasmodial activity. *Journal of Ethnopharmacology*, 74(3),
784 239–243. [https://doi.org/10.1016/S0378-8741\(00\)00370-6](https://doi.org/10.1016/S0378-8741(00)00370-6)

785 Sowemimo-Coker, S. O. (2002). Red blood cell hemolysis during blood bank stora.
786 *Transfusion Medicine Reviews*, 16(1), 46–60. <https://doi.org/10.1053/tmrv.2002.29404>

787

788 Syah Lubis, A. M. H., Ariwahjoedi, B., & Bin Sudin, M. (2015). Investigation on
789 oxidation and thermal stability of jatropha oil. *Jurnal Teknologi*, 77(21), 79–83.
790 <https://doi.org/10.11113/jt.v77.6611>

791 Taticchi, A., Selvaggini, R., Esposito, S., Sordini, B., Veneziani, G., & Servili, M.
792 (2019). Physicochemical characterization of virgin olive oil obtained using an
793 ultrasound-assisted extraction at an industrial scale: Influence of olive maturity
794 index and malaxation time. *Food Chemistry*, 289(November 2018), 7–15.
795 <https://doi.org/10.1016/j.foodchem.2019.03.041>

796 Teixeira, G. L., Ávila, S., Silveira, J. L. M., Ribani, M., & Ribani, R. H. (2017).
797 Chemical, thermal and rheological properties and stability of sapucaia (*Lecythis*
798 *pisonis*) nut oils: A potential source of vegetable oil in industry. *Journal of*
799 *Thermal Analysis and Calorimetry*, 131(3), 2105–2121.
800 <https://doi.org/10.1007/s10973-017-6742-1>

801 Thakore, S., Rathore, P. S., Jadeja, R. N., Thounaojam, M., & Devkar, R. V. (2014).
802 Sunflower oil mediated biomimetic synthesis and cytotoxicity of monodisperse
803 hexagonal silver nanoparticles. *Materials Science and Engineering C*, 44, 209–
804 215. <https://doi.org/10.1016/j.msec.2014.08.019>

805 Tilahun, W. W., Grossi, J. A. S., Favaro, S. P., Sedyama, C. S., Goulart, S. D. M.,
806 Pimentel, L. D., & Motoike, S. Y. (2019). Increase in oil content and changes in

807 quality of macauba mesocarp oil along storage. *OCL - Oilseeds and Fats, Crops*
808 *and Lipids*, 26(2). <https://doi.org/10.1051/ocl/2019014>

809 Timilsena, Y. P., Vongsvivut, J., Adhikari, R., & Adhikari, B. (2017). Physicochemical
810 and thermal characteristics of Australian chia seed oil. *Food Chemistry*, 228, 394–
811 402. <https://doi.org/10.1016/j.foodchem.2017.02.021>

812 Toscano, G., Riva, G., Foppa Pedretti, E., & Duca, D. (2012). Vegetable oil and fat
813 viscosity forecast models based on iodine number and saponification number.
814 *Biomass and Bioenergy*, 46, 511–516.
815 <https://doi.org/10.1016/j.biombioe.2012.07.009>

816 Turner, C., King, J. W., & Mathiasson, L. (2001). Supercritical fluid extraction and
817 chromatography for fat-soluble vitamin analysis. *Journal of Chromatography A*,
818 936(1–2), 215–237. [https://doi.org/10.1016/S0021-9673\(01\)01082-2](https://doi.org/10.1016/S0021-9673(01)01082-2)

819 Wan Nik, W. B., Ani, F. N., & Masjuki, H. H. (2005). Thermal stability evaluation of
820 palm oil as energy transport media. *Energy Conversion and Management*, 46(13–
821 14), 2198–2215. <https://doi.org/10.1016/j.enconman.2004.10.008>

822 Wang, W., Wang, H. L., Xiao, X. Z., & Xu, X. Q. (2019). Chemical composition
823 analysis of seed oil from five wild almond species in China as potential edible oil
824 resource for the future. *South African Journal of Botany*, 121, 274–281.
825 <https://doi.org/10.1016/j.sajb.2018.11.009>

826 Xu, H. Y., Zhu, L. R., Dong, J. E., Wei, Q., & Lei, M. (2015). Composition of *Catalpa*
827 *ovata* seed oil and flavonoids in seed meal as well as their antioxidant activities.
828 *JAOCS, Journal of the American Oil Chemists' Society*, 92(3), 361–369.
829 <https://doi.org/10.1007/s11746-015-2595-6>

830 Yang, R., Zhang, L., Li, P., Yu, L., Mao, J., Wang, X., & Zhang, Q. (2018). A review of
831 chemical composition and nutritional properties of minor vegetable oils in China.

832 *Trends in Food Science and Technology*, 74(March 2017), 26–32.
833 <https://doi.org/10.1016/j.tifs.2018.01.013>

834 Zahir, E., Saeed, R., Hameed, M. A., & Yousuf, A. (2017). Study of physicochemical
835 properties of edible oil and evaluation of frying oil quality by Fourier Transform-
836 Infrared (FT-IR) Spectroscopy. *Arabian Journal of Chemistry*, 10, S3870–S3876.
837 <https://doi.org/10.1016/j.arabjc.2014.05.025>

838 Zamora, R., & Hidalgo, F. J. (2015). Fatty Acids. In L. M. L. Nollet & F. Toldrá (Eds.),
839 *Handbook of food analysis* (3rd ed., Vol. 53, pp. 53-2898-53–2898). New York:
840 Taylor & Francis Group. <https://doi.org/10.5860/choice.194412>

841

CAPÍTULO 4

4.1. Supercritical Extraction Kinetics of the Bacaba-de-leque (*Oenocarpus distichus*) Oil: Experimental Data, Mathematical Modeling and Scaling Up Study.

1 **Supercritical extraction kinetics of bacaba-de-leque (*Oenocarpus distichus*) oil:**

2 **Experimental Data, mathematical modeling and scale-up study**

3
4 Vânia Maria Borges Cunha^{a*}, Marcilene Paiva da Silva^a, Lucas Cantão Freitas^a,
5 Marielba de los Angeles Rodriguez Salazar^a, Fernanda Wariss Figueiredo Bezerra^a,
6 Marilena Emmi Araújo^b, Raul Nunes de Carvalho Júnior^{a*}

7
8 ^aLABEX (Extraction Laboratory), Faculty of Food Engineering, Federal University of
9 Pará, Belém, Pará, Brazil.

10
11 ^bTERM@ (Laboratory of Separation Processes and Applied Thermodynamic), Faculty
12 of Chemical Engineering, Federal University of Pará, Belém, Pará, Brazil.

13
14 *Corresponding author.

15 Tel.: +55-91-984190195

16 **E-mail address:** vaniacunha21@hotmail.com (V.M.B. Cunha), raulncj@ufpa.br and
17 raulncj@gmail.com (R.N. de Carvalho Junior).

18

19 **Abstract**

20

21 This work aimed to study of the supercritical extraction kinetics of bacaba-de-leque (*O.*
22 *distichus*) oil was carried out in two extraction vessels (V_1 and V_2) at different solvent
23 flows (Q_{CO_2}) and operational conditions. Experimental and predicted scale-up
24 procedures were evaluated, correlating operational variables in different bed geometries.
25 The behavior of the extraction kinetics was visibly affected by the operational
26 parameters. The use of the correlation between bed height and diameter (H_b/D_b) and
27 Q_{CO_2} , for the same feed mass (F), was not enough to reproduce the experimental kinetic
28 from V_1 ($5 \times 10^{-5} \text{ m}^3$) to V_2 (10^{-4} m^3). However, when expressed as a function of solvent
29 consumption, the curves converged, showing that the total amount of CO_2 consumed
30 was responsible for the process efficiency. In predicting scale-up, the increase of F and
31 Q_{CO_2} for the same H_b/D_b proved to be adequate to reproduce the kinetic behavior of the
32 experimental scale in larger scales.

33

34 **Keywords:** Supercritical fluid extraction. Modeling. Kinetic parameters. Mass transfer
35 phenomena. Scale up

36 **1. Introduction**

37

38 In recent years, the supercritical fluid extraction (SFE) process has achieved
39 significant advances due to the development of scientific research and technology,
40 which aim to insert new processes in several industrial sectors (Zabot et al., 2014a).
41 Although there is much information about obtaining products from different vegetable
42 raw materials using supercritical fluid, more studies are needed in order to provide
43 richer data regarding the influence of operational variables, bed configurations and the
44 phenomena that control the SFE , so that it is possible to scale systems beyond the
45 laboratory scale (De Melo et al., 2014). These information are still scarce, especially
46 when it comes to raw materials from the Amazon region.

47 In order to understand the influence of these parameters on the SFE, the extraction
48 kinetics is determined, which can be followed by the measurement of the extract mass
49 or accumulated yield as a function of the operation time or solvent consumption,
50 generating an overall extraction curve (OEC) (Brunner, 1994; da Silva et al., 2016;
51 Mendiola et al., 2013). The study of this curve can be done through mathematical
52 modeling of experimental data, since it is a useful tool to optimize and evaluate the
53 effect of operational variables. In addition, it can show an insight into the dominant
54 mechanisms of mass transport by measuring kinetic parameters, as this information
55 helps to describe the behavior of kinetic curves, reported in several studies (Benito-
56 Román et al., 2018; Jesus et al., 2013; Pavlić et al., 2020; Soares et al., 2016; Xiong et
57 al., 2019; Zabot et al., 2014a). The application of the optimal operational parameters in
58 the extraction experiments can significantly increase the recovery of a target compound
59 or the process yield (Herrero et al., 2010).

60 The mathematical models based mainly on the differential mass balance for fixed
61 bed are the most accurate and generally accepted, as they present the advantages of
62 using less thermodynamic parameters and a better description of the mass transfer
63 mechanisms for the SFE process (Huang et al., 2012; Taher et al., 2014; Xiong et al.,
64 2019). The model proposed by Sovová (1994) is one of the most widely used to adjust
65 supercritical extraction curves, being based on the Broken-and-Intact Cell (BIC)
66 concept, which describes the availability of the solute present in the cells of the plant
67 material to access the solvent, taking into account the characteristics of the solid matrix.

68 In this model, Sovová (1994) considers that the extraction process occurs in three
69 periods: the constant extraction rate (CER), where extraction proceeds rapidly at a
70 constant rate due to the transfer of mass by convection; the falling extraction rate (FER),
71 which is an intermediate period where extraction is controlled by the diffusion
72 mechanism combined with convection; and the diffusion-controlled (DC) period, where
73 the mass transfer occurs mainly by diffusion within the solid particles. The author
74 addresses the definition of the mass transfer coefficients for the solid and fluid phases in
75 order to describe the resistance to internal and external mass transfer.

76 Based on the BIC concept, other modifications were made in order to simplify the
77 Sovová (1994) model with less complex computation or with fewer model variables.
78 For instance, Patel et al. (2011) reformulated this three-stage model to a simpler one
79 with the extraction curve divided into only two stages, integrating the middle part of the
80 Sovová (1994) model to the stage controlled by diffusion, which can be applied to raw
81 materials with high and low vegetable oil content.

82 Mathematical modeling is also an important tool for developing scale-up
83 procedures, as well as for the design and improvement of an industrial plant through the
84 simulation of supercritical extraction curves, which can greatly reduce the number of

85 laboratory experiments (Duba and Fiori, 2015; Xiong et al., 2019). Therefore, it is
86 important to study scale-up criteria in order to establish a methodology that allows the
87 prediction of the process behavior in an expanded-scale plant, based on the previous
88 optimization of the operational variables in the laboratory, taking into account the
89 differences observed in the experiments conducted in extraction vessels of different
90 sizes (De Melo et al., 2014; Garcez et al., 2017; Prado et al., 2011).

91 The bed geometry can influence the processes of SFE, being a relevant factor
92 when establishing a scale-up criterion, since similar profiles of OECs on larger scales
93 must be achieved successfully when the studies of SFE involve different extractors on
94 different scales (De Melo et al., 2014; Zabet et al., 2014a). The ratio of height (H_b) and
95 diameter (D_b) of the bed, for example, has been used to validate some scaling up
96 procedures with the development of empirical equations based on bed configuration, as
97 reported in studies by Carvalho Jr et al. (2005), Zabet et al. (2014b), López-Padilla et al.
98 (2016) and Paula et al. (2016). However, it is important to highlight that the data
99 available in the literature suggest that there is no single scale-up criterion that can be
100 applied effectively to all SFE systems. Although the selection of the criterion is
101 adequate, the results may not be confirmed on larger scales as a consequence of
102 negligible phenomena on smaller scales that become considerable on higher scales, as
103 reviewed by Zabet et al. (2014a). The challenge is to simulate and predict the behavior
104 of the supercritical extraction curves by means of mathematical models and, thus,
105 determine the optimal parameters for scaling up.

106 Cunha et al. (2019) applied supercritical carbon dioxide ($Sc\text{-CO}_2$) for the
107 extraction of bacaba-de-leque (*Oenocarpus ditichus*) oil, which is a palm tree native to
108 the Brazilian Amazon biomes, to determine the operational conditions that provided the
109 best oil yields. Thus, in order to obtain more data to optimize this process for possible

110 commercial implementation, the purpose of this work is to study the extraction kinetics
111 of bacaba-de-leque oil obtained in different extraction vessels and solvent flow, as well
112 as to evaluate the suitability of the modified BIC model, proposed by Patel et al. (2011),
113 in order to determine and assess the kinetic parameters by adjusting the experimental
114 data and, finally, to study the scale-up process from the correlation of the operational
115 variables (solvent flow and feed mass) in different bed geometries (H_b e D_b).

116

117 **2. Materials and methods**

118

119 *2.1. Raw material*

120

121 The raw material used in this study was the freeze-dried bacaba-de-leque
122 (*Oenocarpus distichus* Mart) pulp, obtained from a sample of fruits collected in the
123 Germplasm Active Bank (GAB) of bacaba palm tree from Brazilian Agricultural
124 Research Corporation (Embrapa Eastern Amazon), located in Belém, Pará state, Brazil.
125 Pretreatment experiments, material characterization and determination of the true
126 particle density (ρ_r) were previously carried out in the study developed by Cunha et al.
127 (2019). The bulk density (ρ_b) and bed porosity (ϵ) were determined according to the
128 methodology described by the same authors, considering the mass and volume of
129 sample packaged in the fixed bed extraction vessel, applied for this work. The average
130 particle diameter (d_p) was determined according to the methodology described by
131 Botelho et al. (2014).

132

133 *2.2. Experiments of supercritical extraction kinetics*

134

135 The extraction kinetics experiments were carried out in a supercritical extraction
136 plant on a laboratory scale, *Spe-edTM SFE* from Applied Separations (model 7071,
137 Allentown, USA), equipped with an automatic control system to monitor the extraction
138 temperature and pressure, as described and represented schematically by Bezerra et al.
139 (2018). It was used carbon dioxide (CO₂, 99.9% pure, White Martins, Belém, Pará,
140 Brazil) as a supercritical solvent and two extraction vessels (V₁ and V₂), with volumes
141 equal to $5 \times 10^{-5} \text{ m}^3$ (height = 0.3248 m and internal diameter = 0.0142 m) and 10^{-4} m^3
142 (height = 0.1262 m and internal diameter = 0.0317 m), respectively.

143 The kinetic curves were obtained under the operational conditions of 50 °C/350
144 bar ($\rho_{\text{CO}_2} = 899.23 \text{ kg/m}^3$) and 60 °C/270 bar ($\rho_{\text{CO}_2} = 805.42 \text{ kg/m}^3$), selected based on
145 the results of bacaba-de-leque oil yields presented by Cunha et al. (2019). In each
146 experiment, a fixed mass of 0.01 kg from lyophilized pulp was used to feed the two
147 extraction vessels. The extractions were carried out with a mass CO₂ flow rate of
148 $1.19 \times 10^{-4} \text{ kg/s}$ in V₁ vessel and $5.34 \times 10^{-5} \text{ kg/s}$ in V₂ vessel, initially with 30 min of
149 static extraction to balance the system at the temperatures and pressures studied,
150 followed by 145 to 190 min of dynamic extraction. The oil fractions were collected in
151 glass bottles at intervals of 5, 10 and 15 min. At the end of each interval, the flask was
152 replaced by an empty one, being weighed before and after collection, in order to
153 determine the oil mass extracted at each point throughout the extraction time. All
154 experiments were performed in duplicate. The results were expressed as the average of
155 two independent repetitions and the standard deviation between them was calculated.

156 The oil yield (X_0) was calculated by dividing the accumulated oil mass (m_{oil}) at
157 each extraction interval by the mass of raw material (on a dry basis) fed into the vessels.
158 Finally, the kinetic curves were constructed relating the oil yield as a function of time
159 and the solvent mass/feed mass (S/F) ratio to observe the kinetic behavior in each

160 extraction vessel and operational condition, in addition to being used for mathematical
161 modeling.

162

163 *2.3. Mathematical modeling*

164

165 *2.3.1. Kinetic parameters*

166

167 For the calculation of the kinetic parameters and mass transfer rates, experimental
168 data on the extraction kinetics of bacaba-de-leque oil were submitted to the adjustment
169 of a three-line spline, according to the methodology described by Botelho et al. (2014).
170 The first line corresponds to the period of constant extraction rate (CER), the second
171 corresponds to the period of falling extraction rate (FER) and the third represents the
172 extraction controlled by diffusion phenomena (DC) (López-Padilla et al., 2017). From
173 the straight line of the CER period, it was estimated the values of t_{CER} (CER period
174 length), M_{CER} (mass transfer rate in the CER period), X_{CER} (CER period yield), $S/F_{(CER)}$
175 (ratio of mass of solvent to mass of feed in the CER period) and Y_{CER} (mass ratio of
176 solute in the fluid phase at the extractor outlet during the CER period), that was
177 obtained by dividing M_{CER} by the solvent flow rate (Q_{CO_2}) in the period of constant
178 extraction rate. The value of t_{FER} (FER period length) was estimated from the straight
179 line of the FER period. The quality of the adjustments was assessed by calculating the
180 R^2 coefficient (Adj. R-Square).

181

182 *2.3.2. Mass transfer model description*

183

184 The experimental kinetics data were obtained by oil yield *versus* extraction time,
185 describing the different stages of extraction (CER, FER and DC periods). The modeling
186 of these curves is linked to scale-up studies, since the parameters obtained from the
187 adjustment of experimental kinetics with the use of mathematical models from mass
188 transfer are applied to scale-up projects. (Mezzomo et al., 2009).

189 In this study, the mathematical model proposed by Patel et al. (2011) was used to
190 adjust the experimental data of the kinetics obtained in V_1 and V_2 vessels, in order to
191 define the main mass transfer mechanisms of the supercritical fluid extraction (SFE)
192 process, being also chosen to predict the kinetic curves of scale increase due to its good
193 performance in representing the experimental data and reliable physical interpretation of
194 the transfer mechanisms of mass.

195 Patel et al. (2011) reformulated the BIC (Broken-and-Intact Cell) model by
196 Sovová (1994), which describes the process of supercritical extraction in three stages
197 (CER, FER and DC), for a new simpler model, based mainly on two mass transfer
198 mechanisms: solubility and diffusion. This new model proposes that the extraction
199 curve is divided into only two sections: an initial stage of constant extraction rate
200 (CER), controlled by solubility, where the easily accessible solute available on the
201 external surface of the particles is extracted, followed by a falling extraction rate (FER)
202 stage, where the easily accessible oil is depleted and the extraction process is controlled
203 by the diffusion mechanism. The authors do not take into account the complexity of the
204 transition phase in which convection and diffusion are considered, according to the
205 model proposed by Sovová (1994). They assume that the easily accessible solute is
206 completely depleted at the extractor entrance at the end of the CER period, thus
207 incorporating the transition stage to the diffusion-controlled stage. The model suggested
208 by Patel et al. (2011) was validated under different operational conditions for modeling

209 extraction curves with supercritical CO₂ (Sc-CO₂), being applied both for raw materials
 210 with a high oil content and for those with low oil content.

211 According to the model, the extraction curve can be expressed to provide the
 212 amount of solute carried by a specific amount of solvent in the different extraction
 213 periods, being described by the following equations:

214 For $q < q_m$ or $t < t_{CER}$

215

$$216 \quad e = q \times y^* \times [1 - \exp(-Z)] \quad (3)$$

217

218 For $q \geq q_m$ or $t \geq t_{CER}$

219

$$220 \quad e = X_0 - \exp[(q - q_m) \cdot W] \times [X_0 - q_m \cdot y^* (1 - \exp(-Z))] \quad (4)$$

221

222 Where:

$$223 \quad q = \frac{m_S}{m_F} = \frac{Q_{CO_2} \cdot t}{m_F}, \quad \dot{q} = \frac{q}{t} \quad \text{and} \quad q_m = \frac{X_0 - X_k}{y^* \cdot Z} \quad (5)$$

224

$$225 \quad X_p = X_0 - X_k \quad (6)$$

226

$$227 \quad Z = \frac{k_f a_0 \rho_f}{[\dot{q}(1-\varepsilon)\rho_r]} \quad (7)$$

228

$$229 \quad W = \frac{k_s a_0}{[\dot{q}(1-\varepsilon)]} \quad (8)$$

230

231 Where e is the extraction yield in relation to the feed mass (kg oil/kg solute-free
 232 solid), m_S is the mass of consumed solvent (Sc-CO₂), m_F is the mass of feed loaded into

233 the bed and t is the extraction time. The parameters q and \dot{q} are, respectively, the
 234 specific mass and the specific mass flow rate of the solvent that flows in the course of
 235 extraction, X_p is the mass ratio of easily accessible solute, X_0 is the initial solute content
 236 in the solid matrix and X_k is the mass ratio from the solute of difficult access. The
 237 parameter y^* is the solute solubility in the solvent, q_m is the amount of CO₂ consumed in
 238 the CER period (kg of CO₂/kg solute-free solid), Z is the dimensionless mass transfer
 239 parameter in the fluid phase, W is the dimensionless mass transfer parameter in the solid
 240 phase, $k_f a_0$ is the mass transfer coefficient in the fluid phase, $k_s a_0$ is the mass transfer
 241 coefficient in the solid phase, a_0 is the surface area of the particles ($a_0 = 6 \cdot (1 - \varepsilon) \cdot$
 242 d_p^{-1}) and ρ_f is the solvent density.

243 There are two ways to represent the extraction curves, either as a function of t or
 244 as a function of q . According to Huang et al. (2012), if the kinetic curve is expressed as
 245 a function of the extraction time, the t_{CER} and t_{FER} times can be obtained by the
 246 following equations:

$$247 \quad t_{CER} = \frac{X_0 - X_k}{y^* \cdot Z \cdot \dot{q}} \quad (9)$$

248

$$249 \quad t_{FER} = t_{CER} + \frac{1}{W \cdot \dot{q}} \cdot \ln \left(\frac{X_k + (X_0 - X_k) \cdot \exp(W \cdot X_0 / y^*)}{X_0} \right) \quad (10)$$

250

251 To estimate the model parameters, the X_0 value was considered equal to the total
 252 extraction yield. The Y_{CER} values were used to estimate the solubility of the extract in
 253 the supercritical solvent, calculated as described in section 2.3.1. Z and W are adjustable
 254 parameters. The Z parameter was adjusted using equation 3, considering the linear
 255 tracking of the curve ($t < t_{CER}$) and W was adjusted using equation 4 from the second
 256 stage of the curve ($t \geq t_{CER}$). The t_{CER} and t_{FER} times were initially estimated by spline

257 adjustment, as described previously. The coefficients $k_f a_0$ and $k_s a_0$ were calculated
258 using equations 7 and 8, respectively. To assess the quality of the mathematical
259 adjustment, it was calculated the R^2 coefficient (Adj. R-Square).

260

261 2.4. Scale-up study

262

263 In this work, the scale-up procedures were carried out correlating the operational
264 variables (F and Q_{CO_2}) and the bed geometry in the extraction vessels of different scales,
265 characterized by the height (H_b) and diameter (D_b) of the bed. These variables are very
266 important for the SFE process, as they can influence both the extraction yield and the
267 composition of the extracted material (De Melo et al., 2014; Zabet et al., 2014a).

268 To make it possible to compare the kinetics behavior, the extraction temperature
269 (T) and the pressure (P) were kept constant. In addition, the average diameter and the
270 true density of the particles, as well as the bulk density and bed porosity were also
271 preserved in all extractors.

272 Initially, the kinetic behavior was evaluated from the experimental curves
273 obtained in vessels V_1 and V_2 , maintaining the same feed mass (F) and different mass
274 flow rates of solvent. For this, the characteristics of the packed bed (H_{b1} and D_{b1}) and
275 the CO_2 mass flow ($Q_{CO_2(1)}$) applied for extraction in vessel V_1 ($5 \times 10^{-5} \text{ m}^3$) were
276 considered as a reference for determining the new bed height (H_{b2}) and new CO_2 mass
277 flow ($Q_{CO_2(2)}$) applied for extraction in vessel V_2 (10^{-4} m^3), with known bed diameter
278 (D_{b2}). The calculations were performed according to equations 1 and 2.

279

$$280 \frac{H_{b2}}{H_{b1}} = \frac{F_2}{F_1} \times \left(\frac{D_{b1}}{D_{b2}} \right)^2 \quad (1)$$

281

282
$$\frac{Q_{CO_2(2)}}{Q_{CO_2(1)}} = \left(\frac{F_2}{F_1}\right)^2 \times \frac{H_{b1}}{H_{b2}} \times \left(\frac{D_{b1}}{D_{b2}}\right)^3 \quad (2)$$

283

284 Subscribers 1 and 2 refer to V_1 and V_2 , respectively. Equation 1 was obtained
285 considering the same bulk density ($\rho_b = m_F/V_{bed}$) and bed porosity ($\varepsilon = 1 - (\rho_b/\rho_r)$)
286 in V_1 and V_2 , being applied for the H_{b2} determination. Equation 2 was proposed by
287 Carvalho Jr. et al. (2005) that correlates process parameters (F and Q_{CO_2}) in different
288 bed geometries (H_b and D_b), being used to calculate $Q_{CO_2(2)}$. This correlation allows the
289 determination of a solvent flow rate necessary to maintain the same kinetic behavior
290 between two different extraction units.

291 Subsequently, the kinetic curve obtained in vessel V_2 was used as a reference
292 kinetics to predict the increase in scale of the bed for two extraction vessels with larger
293 dimensions: one with a volume equal to $2.7 \times 10^{-4} \text{ m}^3$ (V_{PS1}), described by López-Padilla
294 et al. (2017), and the other with a volume equal to 10^{-3} m^3 (V_{PS2}), described by França et
295 al. (1999). The comparison was performed by fixing the H_b/D_b ratio between V_2 , V_{PS1}
296 and V_{PS2} vessels with different feed masses and solvent flow rates. For this, the bed
297 geometry (H_b and D_b) of V_2 was considered to calculate, previously, the new bed height
298 in V_{PS1} and V_{PS2} , maintaining the same H_b/D_b of V_2 . Then, considering the parameters
299 of the reference kinetics (F and Q_{CO_2}), it was calculated new power mass by applying
300 equation 1, and the new solvent flow rate by applying equation 2, for the two vessels of
301 larger scale. With the determination of the scale expansion parameters (H_b , F and Q_{CO_2}),
302 the kinetic curves of the V_{PS1} and V_{PS2} vessels were predicted using the modified BIC
303 model equations by Sovová (1994), developed by Patel et al. (2011), described in
304 section 2.3.2.

305 This criterion was not applied experimentally in V_1 and V_2 due to the equipment
 306 limitations and the vessels geometries, in which it would not be possible to package
 307 larger feed masses, when calculated by the correlation of equation 1.

308

309 3. Results and discussion

310

311 Table 1 shows the geometric characteristics of the different extraction beds, feed
 312 mass (F), properties of the raw material and process operation for the experiments
 313 carried out on a laboratory scale.

314

315 **Table 1.** Bed characterization and operational data of kinetics experiments.

Parameters	V_1	V_2
Volume (m ³)	5×10^{-5}	10^{-4}
F (kg)	0.01	0.01
Q_{CO_2} (kg/s)	1.19×10^{-4}	5.34×10^{-5}
U (%)*	4.52	4.52
ε	0.636	0.636
ρ_b (kg/m ³)	411	411
ρ_r (kg/m ³)*	1130	1130
d_p (m)	3.43×10^{-4}	3.43×10^{-4}
H_b (m)	0.1536	0.0308
D_b (m)	0.0142	0.0317
H_b/D_b	10.82	0.97
v (m/s)	0.42	0.039

316 V_1 and V_2 =Extraction vessel; F=feed mass; Q_{CO_2} =CO₂ mass flow rate; U=moisture
 317 content; ε =bed porosity; ρ_b =bulk density; ρ_r =true particle density; d_p = particle diameter;
 318 H_b =bed height; D_b =bed diameter, H_b/D_b =bed height to bed diameter ratio; v =CO₂
 319 superficial velocity.

320 *Cunha et al. (2019)

321

322 The bacaba-de-leque pulp mass (with $\rho_r=1130$ kg/m³), fed in each vessel, was
 323 applied to preserve the same bulk density ($\rho_b=411$ kg/m³) and porosity ($\varepsilon=0.636$) in the
 324 two packed beds. The average particle diameter ($d_p=3.43 \times 10^{-4}$ m) proved to be adequate

325 for the extraction process. According to Pereira and Meireles (2010), this parameter
 326 should vary from 2.5×10^{-4} to 1.8×10^{-3} m, but it can be assessed according to each study.
 327 The CO₂ mass flow rates (Q_{CO_2}), applied to the extractions, resulted in the superficial
 328 solvent velocity (v) equal to 0.42 m/s in V_1 and 0.039 m/s in V_2 , defined as Q/A , where
 329 Q (m³/s) is the volumetric flow rate of the solvent and A (m²) is the cross-sectional area
 330 of each extractor vessel.

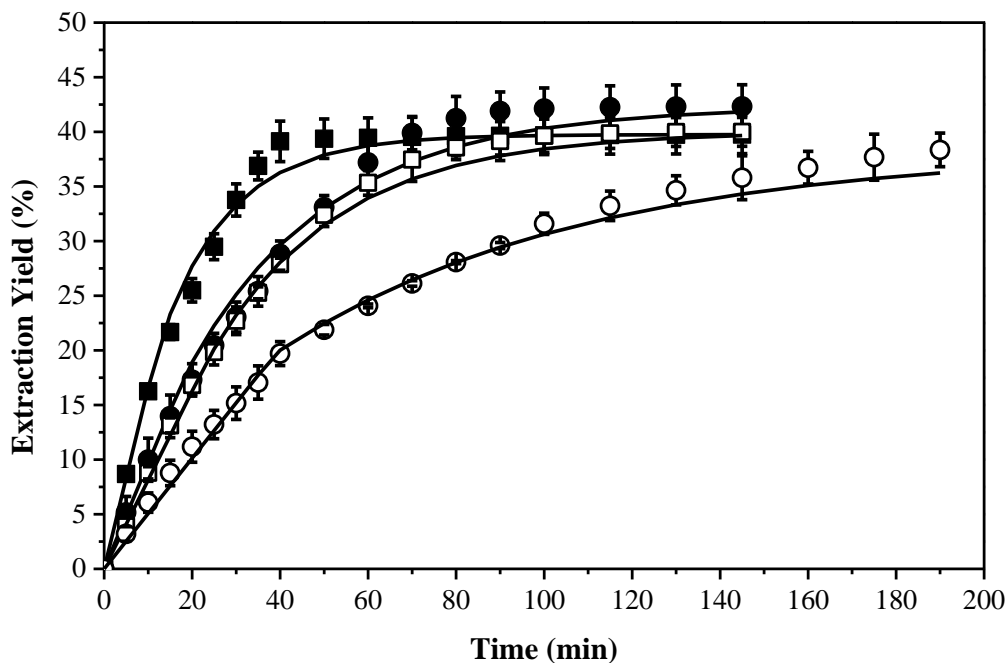
331

332 3.1. Experimental extraction kinetics and mathematical modeling

333

334 Figure 1 shows the experimental and adjusted extraction kinetics, which contain
 335 the averages and standard deviations of accumulated yields of bacaba-de-leque oil as a
 336 function of time, obtained at 50°C/350 bar and 60°C/270 bar in different bed
 337 configurations and mass flow rates of solvent.

338



339

340 **Fig. 1.** Experimental and fitted kinetic curves of bacaba-de-leque oil obtained using two
 341 extraction vessels and constant mass feed, at different temperature/pressure conditions,
 342 CO₂ mass flow rates, and bed configurations. (■) 50°C /350 bar and (●) 60°C /270 bar

343 for $V_1 = 5 \times 10^{-5} \text{ m}^3$, $Q_{CO_2(1)} = 1.19 \times 10^{-4} \text{ kg/s}$ and $H_{b1}/D_{b1} = 10.82$; (\square) $50^\circ\text{C} / 350 \text{ bar}$ and
 344 (\circ) $60^\circ\text{C} / 270 \text{ bar}$ for $V_2 = 10^{-4} \text{ m}^3$, $Q_{CO_2(2)} = 5.34 \times 10^{-5} \text{ kg/s}$ and $H_{b2}/D_{b2} = 0.97$; (—)
 345 Modified BIC model.
 346

347 Table 2 shows the final yields of the oil (X_0) and the kinetic parameters of the
 348 extraction curves for the CER period (X_{CER} , S/F_{CER} , M_{CER} , t_{CER} and Y_{CER}) and for the
 349 FER period (t_{FER}). These parameters were determined because they describe the initial
 350 stages of the supercritical extraction process (CER and FER) and the moment in the
 351 process when the diffusion mechanisms begin to control the extraction, in comparison
 352 to the convective mechanisms. In the same table, the parameters of mass transfer ($k_f a_0$
 353 e $k_s a_0$) are also presented, estimated by the modification of the BIC model proposed by
 354 Patel et al. (2011), which was able to adequately adjust and describe the experimental
 355 data of the extraction kinetics for all operational conditions and tested extraction beds.

357 **Table 2.** Extraction yield (X_0), kinetic parameters ^(a), and calculated parameters of the
 358 modified BIC model ^(b) applied to kinetic curves of bacaba-de-leque oil for V_1 and V_2

Kinetic Parameters	V_1		V_2	
	$50^\circ\text{C}/350 \text{ bar}$	$60^\circ\text{C}/270 \text{ bar}$	$50^\circ\text{C}/350 \text{ bar}$	$60^\circ\text{C}/270 \text{ bar}$
X_0 (%)	39.75	42.32	40.00	38.35
X_{CER} (%) ^a	18.49	15.97	17.99	17.41
S/F	103.54	103.58	48.53	63.07
S/F_{CER} ^a	8.58	12.87	7.37	12.49
M_{CER} (kg/s) ^a	2.57×10^{-6}	1.48×10^{-6}	1.30×10^{-6}	0.74×10^{-6}
t_{CER} (min) ^a	12	18	23	39
t_{FER} (min) ^a	38	66	64	106
Y_{CER} (kg oil/kgCO ₂) ^a	0.0215	0.0124	0.0244	0.0139
$k_f a_0$ (s ⁻¹) ^b	10.1×10^{-4}	11.8×10^{-4}	4.35×10^{-4}	5.21×10^{-4}
$k_s a_0$ (s ⁻¹) ^b	0.61×10^{-4}	0.31×10^{-4}	0.33×10^{-4}	0.14×10^{-4}
R^2	0.9997	0.9989	0.9972	0.9986

359
 360 The lowest accumulated oil yield ($38.35\% \pm 0.54$) was obtained in the extraction
 361 kinetics performed in vessel V_2 at $60^\circ\text{C}/270 \text{ bar}$ ($\rho_{CO_2} = 805.42 \text{ kg/m}^3$), with

362 $Q_{CO_2}=5.34\times 10^{-5}$ kg/s, while the highest accumulated yield (42.32%±0.98) was obtained
363 in the extraction kinetics performed in vessel V₁, in the same operational condition, but
364 with $Q_{CO_2}=1.19\times 10^{-4}$ kg/s.

365 In general, there were no considerable differences between the final yields
366 obtained in vessel V₁, as well as between those obtained in vessel V₂, in the two
367 conditions evaluated. The main difference occurred only between the yields reached at
368 60 °C/270 bar, which was approximately 3.97% higher in vessel V₁ when compared to
369 vessel V₂. This may have occurred due to the lower solvent flow rate and bed height in
370 V₂ (Table 1), which caused a slower extraction rate and shorter contact time between
371 CO₂ and the raw material along the extraction bed, an effect also observed by Lu et al.
372 (2007).

373 This behavior also influenced the total extraction time in V₂ at 60 ° C/270 bar,
374 which was longer (190 min) compared to the other extractions (145 min), being
375 necessary to exhaust more than 90% of the extractable oil from raw material and obtain
376 complete extraction curves. In vessel V₂, although the kinetics were performed with the
377 same bed configuration and the same Q_{CO_2} , the total extraction time was different for
378 each condition (Figure 1). This was probably due to the difference in density of CO₂,
379 which is higher at 50 °C/350 bar ($\rho_{CO_2}= 899.23$ kg/m³) than at 60 °C/270 bar ($\rho_{CO_2}=$
380 805.42 kg/m³), which facilitated the solubilization of the oil in Sc-CO₂, induced by the
381 increase of the solvation power. This effect provided the faster oil extraction and,
382 consequently, a shorter operational time in the condition of 50 °C/350 bar (Jokić et al.,
383 2012; Zeković et al., 2017). However, the effect of the temperature and operational
384 pressure of the process did not cause considerable differences in the values of the final
385 yields of bacaba-de-leque oil, which is in agreement with what was discussed in the
386 study conducted by Cunha et al. (2019).

387 As can be seen in Figure 1, the behavior of the extraction curves, in all
388 experiments, is typical of kinetics reported in studies that obtained oil from vegetable
389 matrices using supercritical CO₂ (Sc-CO₂) (Benito-Román et al., 2018; Botelho et al.,
390 2015; Costa et al., 2019; Jokić et al., 2012; Mezzomo et al., 2009; Özkal and Yener,
391 2016), where it is observed the presence of an initially high extraction rate, controlled
392 by solubility, which decreases as the process progresses. This was due to the
393 solubilization of the oil close to the surface of the solid particles, which has less
394 resistance to mass transfer in the early stages of extraction. As the process continues, the
395 extraction rate decreases due to the depletion of easily accessible oil, and because
396 extraction is subjected to internal diffusion limitations caused by high resistance to
397 intraparticle mass transfer (Benito-Román et al., 2018; Westerman et al., 2006).

398 The shape of the curves indicates that the extractions took place in three distinct
399 phases: a period of constant extraction rate (CER), followed by a period of falling
400 extraction rate (FER) and, lastly, a period of extraction rate controlled mainly by
401 diffusion within the solid particles (DC). The first part of the curve is always a straight
402 line, the slope of which defines a value close to the oil solubility in the Sc-CO₂ under
403 the extraction conditions evaluated (Clavier and Perrut, 2004; Huang et al., 2012;
404 Sovová, 1994).

405 Comparing the extraction kinetics obtained in vessel V₁ in the same Q_{CO_2} , but
406 under different conditions of temperature and pressure, it is observed that, initially,
407 there are great differences in the extraction process between the curves obtained at 50
408 °C/350 bar ($\rho_{CO_2} = 899.23 \text{ kg/m}^3$) and 60 °C/270 bar ($\rho_{CO_2} = 805.42 \text{ kg/m}^3$), being more
409 evident in the CER and FER periods and converging in the DC period to approximate
410 values of accumulated oil yield (X_0). These differences can be better observed by the
411 values of the mass transfer rate from the CER (M_{CER}) period (Table 2), which was

412 higher for the extraction kinetics in the condition of 50 °C/350 bar ($M_{CER}=2.57\times 10^{-6}$
413 kg/s). Such behavior caused a greater inclination of the first part of the curve (CER
414 period), in comparison to the kinetics obtained at 60 °C/270 bar, where the mass transfer
415 rate was lower ($M_{CER}=1.48\times 10^{-6}$ kg/s) and, consequently, leading to a lower slope of the
416 line in the same region. The kinetics obtained in vessel V_2 showed a tendency very
417 similar to this behavior, as can be seen in Figure 1 and in the results shown in Table 2.

418 The increase in mass transfer rates in the CER stage, in the two extraction beds at
419 50 °C/350 bar, may be attributed to the increase in the density of Sc-CO₂ in this
420 operational condition, which led to higher oil concentrations in the solvent phase (Y_{CER})
421 in shorter extraction times (t_{CER}). Consequently, it induced higher yields (X_{CER}) in the
422 CER stage, consuming less solvent (S/F_{CER}) during that same period, as shown in the
423 results presented in Table 2. Similar effects have been reported by Mezzomo et al.
424 (2009), Özkal and Yener (2016), Lu et al. (2007) and Soares et al. (2016).

425 When evaluating the influence of the variation in solvent flow (Q_{CO_2}) from V_1 to
426 V_2 in terms of extractions behavior over time, it is also noticed that the extraction rate
427 was significantly affected in the early stages of the process, including the slope and
428 duration of the CER stage. The highest flow rate applied in V_1 ($Q_{CO_2}=1.19\times 10^{-4}$ kg/s)
429 resulted in higher mass transfer rates in the CER stage ($M_{CER}=2.57\times 10^{-6}$ kg/s at 50
430 °C/350 bar and $M_{CER}=1.48\times 10^{-6}$ kg/s at 60 °C/270 bar) and, consequently, higher slopes
431 of the straight lines. On the other hand, the kinetics of vessel V_2 , where less solvent
432 flow was applied ($Q_{CO_2}=5.34\times 10^{-5}$ kg/s), mass transfer rates were lower at the same
433 stage of extraction ($M_{CER}=1.30\times 10^{-6}$ kg/s at 50 °C/350 bar and $M_{CER}=0.76\times 10^{-6}$ kg/s at
434 60 °C/270 bar), causing a slope in the first part of the curves. As a result, the duration of
435 the CER stage was shorter in vessel V_1 ($t_{CER}=12$ min at 50 °C/350 bar and $t_{CER}=18$ min
436 at 60 °C/270 bar), compared to those of the vessel V_2 ($t_{CER}=23$ min at 50 °C/350 bar and

437 $t_{CER}=39$ min at 60 °C/270 bar). These results show, in fact, that the higher solvent flow
438 rate applied in V_1 increased convection in the first phase of the extraction process. The
439 higher availability of Sc-CO₂ inside the extractor per unit of time causes a greater
440 concentration gradient between the solid and the supercritical fluid, increasing M_{CER} due
441 to reduced resistance to mass transfer as an effect of increased convection, caused by
442 the non-saturation of the solvent by the oil. In addition, this effect can be attributed to
443 the higher surface velocity of the solvent in the bed (Table 1), caused by the Q_{CO_2}
444 increase, which reduced the thickness of the film surrounding the solid particles, thus
445 improving the extraction rate (Mezzomo et al., 2009; Özkal and Yener, 2016; Zeković
446 et al., 2017).

447 Another factor to be considered about the curves behavior in the CER stage is the
448 correlation between the height and the diameter of the bed (H_B/D_B) for the same mass of
449 raw material fed in the two vessels (Table 1). In V_1 , the bed height was greater due to
450 the smaller diameter of the extractor, where the H_B/D_B ratio was equal to 10.82. Due to
451 this and the higher flow rate applied to the vessel, the solvent ran a longer path through
452 the solid matrix at a higher surface velocity (0.42 m/s). This may have caused the easily
453 accessible oil to be dragged more strongly during a shorter t_{CER} and with a higher M_{CER} .
454 In V_2 , the larger extractor diameter caused a decrease in bed height, also reducing the
455 H_B/D_B ratio (from 10.82 to 0.97). In this case, the solvent flowed a shorter path through
456 the solid matrix, with less force due to the lower surface velocity of the solvent (0.039
457 m/s), providing lower mass transfer rates and higher t_{CER} . Carvalho Jr. et al. (2005), de
458 Andrade Lima et al. (2018) and Lu et al. (2007) reported similar behaviors. However,
459 despite the differences in Q_{CO_2} and the bed geometry between V_1 e V_2 , approximate
460 values of X_{CER} , S/F_{CER} and Y_{CER} were obtained, both for the kinetics obtained at 50
461 °C/350 bar, and for those obtained at 60 °C/270 bar (Table 2). Therefore, there was no

462 significant influence on the yield, solvent consumption and oil solubility in the fluid
463 phase during the CER period, nor on the final oil yields (X_0).

464 The resistances to mass transfer were evaluated by the mass transfer coefficient
465 values in the fluid phase ($k_f a_0$) and in the solid phase ($k_s a_0$). As shown in Table 2, the
466 values of $k_f a_0$ (from $4.35 \times 10^{-4} \text{ s}^{-1}$ to $11.8 \times 10^{-4} \text{ s}^{-1}$) were higher than those of $k_s a_0$
467 (from $0.14 \times 10^{-4} \text{ s}^{-1}$ to $0.61 \times 10^{-4} \text{ s}^{-1}$) for all extraction kinetics. This behavior indicated
468 the predominant influence of the convective mechanism on the diffusive one, which was
469 already expected, since convection in the fluid phase is the main transport mechanism of
470 the SFE process. This is because the oil trapped inside the solid particles takes longer to
471 cross the interface between the solid and solvent phases than the oil that is easily
472 accessible on the surface of the particles. When this oil runs out, mass transfer is
473 delayed by diffusion into the solid phase. Therefore, this mechanism represents a lower
474 extraction rate compared to the convection mechanism (Hassim et al., 2019; Taher et
475 al., 2014; Weinhold et al., 2008). This behavior was most visible in the extractions
476 performed in V_1 , where the values of $k_f a_0$ ($10.1 \times 10^{-4} \text{ s}^{-1}$ and $11.8 \times 10^{-4} \text{ s}^{-1}$) were higher
477 than in V_2 ($4.35 \times 10^{-4} \text{ s}^{-1}$ and $5.21 \times 10^{-4} \text{ s}^{-1}$), which confirms the influence of the Q_{CO_2}
478 variation and solvent velocity, previously reported. This effect was also observed by
479 Özkal and Yener (2016) in the process of supercritical extraction of flaxseed oil.

480 All the kinetics presented in Figure 1 indicate that when the extractions enter the
481 diffusional period (DC), after t_{FER} , the accumulated oil yields increase slowly over time.
482 This shows that the extraction rate in DC is much lower compared to the first two stages
483 of extraction, that is, most of the oil is extracted during the CER and FER periods.
484 Therefore, in order to optimize the costs for the process of bacaba-de-leque extraction
485 oil by SFE, the most indicated would be to interrupt the extraction in the interval

486 between t_{CER} and t_{FER} , approximately. According to Soares et al. (2016), the costs of the
487 process are generally lower when the operating time is close to the end of t_{CER} or t_{FER} .

488

489 *3.2. Scale-up study of the SFE process of bacaba-de-leque oil*

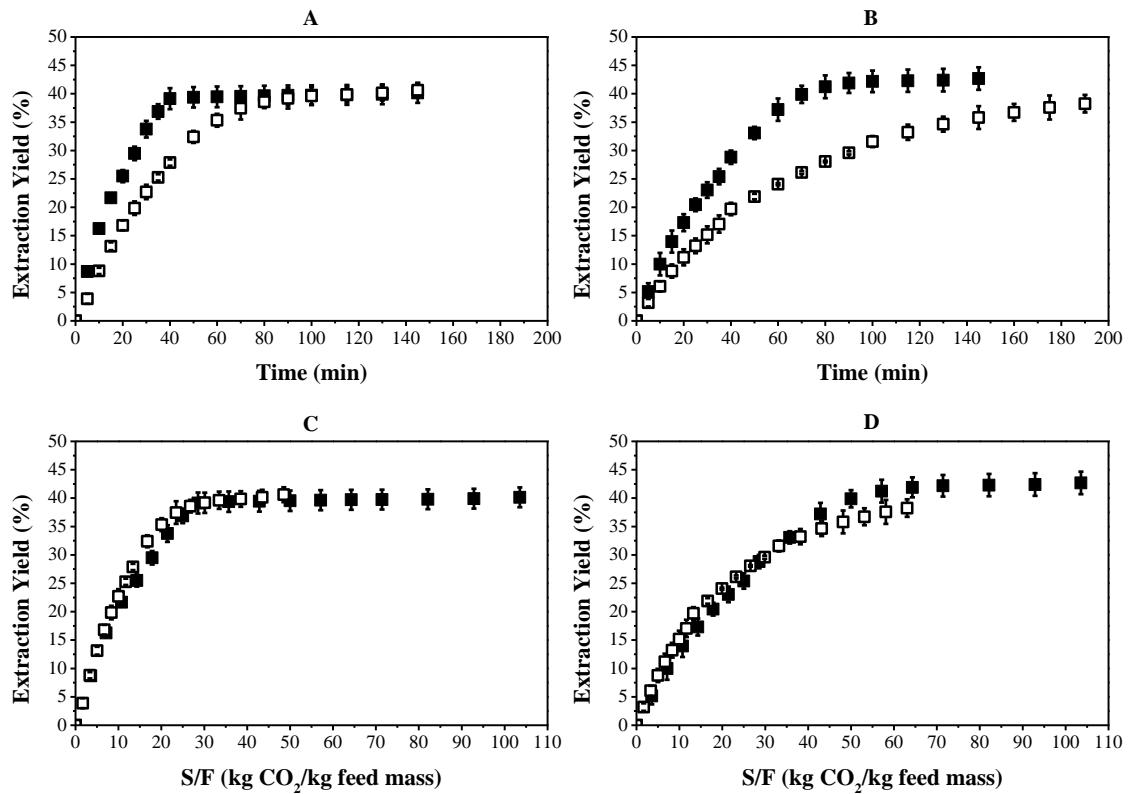
490

491 *3.2.1. Experimental scale-up of the kinetic curves*

492

493 Figure 2 compares the extraction kinetics obtained experimentally in vessels V_1
494 and V_2 , with the bacaba-de-leque accumulated oil yields as a function of the extraction
495 time and the solvent mass/feed mass ratio (S/F) at 50 °C/350 bar and 60 °C/270 bar. For
496 the scale-up study from the V_1 ($5 \times 10^{-5} \text{ m}^3$) to V_2 (10^{-4} m^3), the behavior of the kinetics
497 obtained in the two vessels was compared, applying the correlation between the bed
498 configurations (H_b/D_b) and CO_2 mass flow (Q_{CO_2}) for the same feed mass (F), as
499 proposed by Carvalho Jr. et al. (2005), having as reference kinetics the curves obtained
500 in V_1 .

501



502
 503 **Fig. 2.** Comparison of experimental extraction yields of bacaba-de-leque oil as a
 504 function of time and S/F obtained with constant mass feed, at 50°C /350 bar (**A** and **C**)
 505 and 60°C /270 bar (**B** and **D**) in (■) $V_1 = 5 \times 10^{-5} \text{ m}^3$, $Q_{CO_2(1)} = 1.19 \times 10^{-4} \text{ kg/s}$,
 506 $H_{b1}/D_{b1} = 10.82$ and (□) $V_2 = 10^{-4} \text{ m}^3$, $Q_{CO_2(2)} = 5.34 \times 10^{-5} \text{ kg/s}$, $H_{b2}/D_{b2} = 0.97$.
 507

508 When the kinetics were expressed as a function of the extraction time, it was
 509 observed that the curves were not properly reproduced from V_1 ($5 \times 10^{-5} \text{ m}^3$) to V_2 (10^{-4}
 510 m^3). The yield values were quite different during the initial periods of the extraction
 511 process, converging to approximate values in the last period in all beds and operating
 512 conditions (T, P and Q_{CO_2}), which can be better seen in Figures 2A and 2B. However,
 513 when the yields were plotted as a function of S/F (kg oil/kgCO₂), the curves converged
 514 to the same line, both at 50 °C/350 bar (Figure 2C) and at 60 °C/270 bar (Figure 2D),
 515 where no significant differences were found between the yields for S/F values
 516 evaluated. This result shows that the total amount of CO₂ consumed during the
 517 extraction was responsible for the efficiency of the process, and not the Q_{CO_2} variation,
 518 since approximate final oil yields were obtained. This also confirms that the extraction

519 process was controlled by solubility and not by external resistance to mass transfer under
520 the operational conditions evaluated in this research, corroborating that the amount of
521 oil in the extractor outlet was independent of the CO₂ flow rate. Therefore, it is possible
522 to consider that the process was in balance and the resistance to intraparticle diffusion
523 did not dominate the SFE (Rebolleda et al., 2012; Salgin et al., 2006; Sánchez-Vicente
524 et al., 2009).

525 Figures 2C and 2D show that, for $H_b/D_b=10.82$ in V_1 , the proportion of solvent
526 per mass of feed was higher ($S/F \cong 103.56$ kg CO₂/kg feed mass) than for $H_b/D_b=10.82$
527 in V_2 ($S/F=48.53$ kg CO₂/kg feed mass at 50 °C/350 bar and $S/F=63.07$ kg CO₂/kg feed
528 mass at 60 °C/270 bar). This result is an important design parameter of the SFE process,
529 because it shows the proportion of solvent consumption for a mass of raw material fed
530 in a given extraction vessel, in addition to the ideal operating time of the process,
531 obtained from the curves expressed as a function of time for the extraction of bacaba-
532 de-leque oil. According to the correlations of equations 1 and 2, the increase in bed
533 diameter from $D_{b1}=0.0142$ m to $D_{b2}=0.0317$ m provided a lower solvent flow rate and a
534 lower H_b/D_b , considering the same mass of raw material to maintain the same bulk
535 density and bed porosity. Thus, it was possible to obtain almost the same yields in both
536 vessels.

537 Although the kinetic curves of vessel V_1 were not exactly reproduced in vessel V_2
538 during the operation time (Figures 2A and 2B), the results found are quite relevant
539 because the use of the correlation between process conditions (Q_{CO_2} and F) in different
540 bed geometries (D_b e H_b) allowed to simplify the scale-up study of bacaba-de-leque oil
541 process by SFE. This was possible using only some laboratory data, kinetic calculations
542 and process parameters, which allowed us to estimate the minimum oil yield expected at
543 larger scales.

544

545 3.2.2. Predicted scale-up of the kinetic curves using the modified BIC model

546

547 Table 3 shows the information regarding the operational data and bed
548 characterization used for scale-up prediction of the process for two extraction vessels
549 with larger dimensions (V_{PS1} and V_{PS2}). In this case, the scale-up study was carried out
550 maintaining the same correlation between the bed height and diameter as that from the
551 experimental scale ($H_b/D_b=0.97$), increasing the feed mass and CO_2 flow, both
552 calculated by the correlations by Carvalho Jr. et al. (2005).

553

554 **Table 3.** Bed characterization and operational data applied to scale-up prediction.

Parameters	Experimental scale			Predicted scale-up		
	V_2	V_{PS1}	V_{PS2}			
Volume (m^3)	10^{-4}	2.7×10^{-4} *	10^{-3} **			
F (kg)	0.01	0.025	0.068			
Q_{CO_2} (kg/s)	5.34×10^{-5}	9.82×10^{-5}	19.1×10^{-5}			
E	0.636	0.636	0.636			
ρ_a (kg/m^3)	411	411	411			
H_b (m)	0.0308	0.0418	0.0584			
D_b (m)	0.0317	0.043*	0.06**			
H_b/D_b	0.97	0.97	0.97			
v (m/s)	0.039	0.038	0.038			

555 V_2 =experimental vessel scale; V_{PS} = predicted scale-up vessel; F=feed mass; Q_{CO_2} = CO_2
556 mass flow rate; ϵ =bed porosity; ρ_b =bulk density of the bed; H_b =bed height; D_b =bed
557 diameter, H_b/D_b =bed height to bed diameter ratio; v = CO_2 superficial velocity.

558 *López-Padilla et al. (2017); **França et al. (1999)

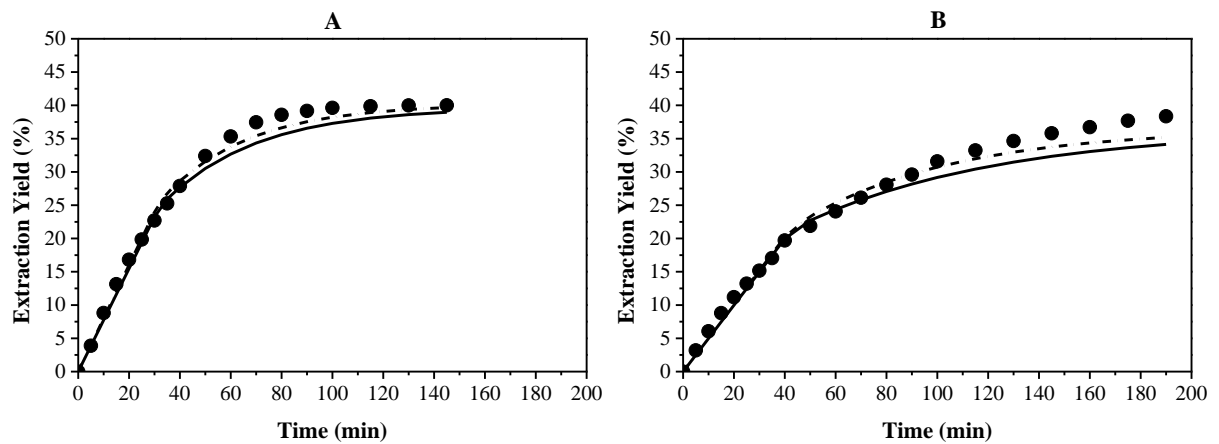
559

560 The results obtained from the calculations performed by equations 1 and 2 showed
561 that the increase in diameter (from 0.0317 m to 0.043 and 0.06 m) and bed height (from
562 0.0308 m to 0.0418 m and 0.0584 m) required an increase in the feed mass (F) and
563 solvent flow (Q_{CO_2}) in order to maintain the same H_b/D_b in all beds. Regarding the V_2

564 experimental scale, the increase in F was 2.5 times greater for V_{PS1} and 6.8 times greater
 565 for V_{PS2} , while Q_{CO_2} increased 1.84 times for V_{PS1} and 3.6 times for V_{PS2} . The solvent
 566 surface velocity remained constant.

567 Figure 3 shows a comparison between the behavior of the reference kinetics,
 568 performed experimentally in vessel V_2 , and the behavior of the two kinetics on larger
 569 scales, predicted by the modified BIC model equations proposed by Patel et al. (2011),
 570 under the same operation conditions (50 °C/350 bar and 60 °C/270 bar). The kinetic
 571 curves were generated by the accumulated mass yield of oil (experimental and
 572 calculated) as a function of the extraction time.

573



574 **Fig. 3.** Predicted kinetic curves of bacaba-de-leque oil with different feed mass and
 575 constant H_b/D_b (0.97), at 50°C /350 bar (A) and 60°C /270 bar (B). (●) Experimental
 576 laboratory scale ($V_2=10^{-4} \text{ m}^3$, $F=0.01 \text{ kg}$, $Q_{CO_2(2)} = 5.34 \times 10^{-5} \text{ kg/s}$); (- - -
 577) $V_{PS1}=2.7 \times 10^{-4} \text{ m}^3$; $F= 0.025 \text{ kg}$ and $Q_{CO_2} = 9.82 \times 10^{-5} \text{ kg/s}$; (—) $V_{PS2}=10^{-3} \text{ m}^3$;
 578 $F=0.068 \text{ kg}$ and $Q_{CO_2} = 19.1 \times 10^{-5} \text{ kg/s}$.
 579
 580

581 Table 4 compares the values of the total oil mass (m_{oil}) and final yield (X_0)
 582 achieved in the experimental and predicted scales, as well as the values of the kinetic
 583 parameters of the extraction curves.

584

585 **Table 4.** Estimated parameters using the modified BIC model, applied to scale-up prediction of the kinetic curves of bacaba-de-leque oil.

Kinetic Parameters	Experimental scale		Predicted scale-up			
	V ₂		V _{PS1}		V _{PS2}	
	50 °C/ 350 bar	60 °C/ 270 bar	50 °C/ 350 bar	60 °C/ 270 bar	50 °C/ 350 bar	60 °C/ 270 bar
m _{oil} (kg)	0.0038	0.0037	0.0099	0.0091	0.0269	0.0246
X ₀ (% , d.b)	40.00	38.35	39.68	35.19	38.96	34.14
X _(CER) (% , d.b)	23.81	18.22	25.05	21.68	25.07	21.58
S/F	48.53	63.07	34.22	44.84	24.51	32.12
S/F _(CER)	10.57	12.49	7.55	10.15	5.41	7.27
M _{CER} (kg/s)	1.30×10 ⁻⁶	0.74×10 ⁻⁶	3.26×10 ⁻⁶	2.10×10 ⁻⁶	8.85×10 ⁻⁶	5.70×10 ⁻⁶
t _{CER} (min)	23	39	32	43	32	43
t _{FER} (min)	64	106	66	106	66	106
Y _{CER} (kg oil/kgCO ₂)	0.0225	0.0146	0.0332	0.0214	0.0463	0.0298
k _f a ₀ (s ⁻¹)	4.35×10 ⁻⁴	5.21×10 ⁻⁴	1.25×10 ⁻⁴	1.27×10 ⁻⁴	0.32×10 ⁻⁴	0.33×10 ⁻⁴
k _s a ₀ (s ⁻¹)	0.33×10 ⁻⁴	0.14×10 ⁻⁴	0.12×10 ⁻⁴	0.051×10 ⁻⁴	0.045×10 ⁻⁴	0.019×10 ⁻⁴
R ²	0.9972	0.9986	0.9973	0.9964	0.9962	0.9965

586

587

588 As can be seen, the behavior of the experimental kinetics (V_2) was reproduced in
589 the predicted extraction curves on a larger scale (V_{PS1} and V_{PS2}). Such behavior
590 indicates that the correlations of the process parameters in different bed geometries
591 (Carvalho Jr. et al., 2005) proved to be adequate when the geometric factor H_b/D_b was
592 kept constant, demonstrating a good agreement between the smallest and largest scale
593 data. The similar shapes of the curves also suggest that the application of the modified
594 BIC model (Patel et al., 2011) was successful in predicting the scale-up process of
595 bacaba-de-leque oil extraction.

596 The data presented in Table 4 show that the oil mass calculated for V_{PS1} and V_{PS2} ,
597 in both operational conditions, increased with the increase of F and Q_{CO_2} . In comparison
598 to the experimental kinetic curve of V_2 , the total oil mass calculated for V_{PS1} was 2.6
599 times greater at 50 ° C/350 bar and 2.5 times greater at 60 ° C/270 bar. For V_{PS2} , it was
600 7.1 times greater at 50 ° C/350 bar and 6.8 times greater at 60 ° C/270 bar.

601 The calculated final yields (from 34.14% to 39.68%) presented values close to
602 those reached experimentally (from 38.35% to 40.0%), with a difference of 1.04% and
603 4.21% between the lowest calculated X_0 (V_{PS2}) and the experimental X_0 (V_2) at 50 °
604 C/350 bar and 60 ° C/270 bar, respectively. During the first 45 min of extraction, the
605 accumulated yields showed quite similar values in the two operational conditions,
606 followed by a slight deviation up to 130 min to 50 ° C/350 bar (Fig. 3A) and until the
607 end of the extraction to 60 ° C/270 bar (Fig. 3B), where the deviation was slightly
608 greater. This behavior was also observed by Taher et al. (2014) when studying the scale-
609 up extraction of lipids from microalgae by SFE, keeping H_b/D_b constant.

610 As the feed mass and CO_2 flow increased in the predicted scales, the mass transfer
611 rate (M_{CER}) also increased, since the height and diameter of the bed were also increased,
612 maintaining the same H_b/D_b to obtain yields similar to the experimental ones. Similarly,

613 the yields of the CER period (X_{CER}) showed a brief increase. Consequently, the amount
614 of oil solubilized in the solvent (Y_{CER}) was also higher, with less solvent consumption
615 (S/F and S/F_{CER}) as the scale was increased.

616 Furthermore, it was observed that the parameter $k_f a_0$ decreased when F and Q_{CO_2}
617 increased, which resulted in a higher t_{CER} , while t_{FER} remained constant. Fernández-
618 Ponce et al. (2016) reports that, in general, the opposite behavior is observed in SFE
619 processes, where the resistance to mass transfer around solid particles is reduced due to
620 the increase in convection at higher solvent flow rates, as a consequence, the t_{CER}
621 decreases. However, the authors point out that it is important to consider that the flow
622 rate affects the local driving force for mass transfer, especially for the easily accessible
623 solute. In addition, higher Q_{CO_2} can lead to a shorter contact time between the solid and
624 the solvent, which in turn leads to a higher t_{CER} . Despite the reduction of $k_f a_0$, its
625 values were still higher than those of the parameter $k_s a_0$, which also decreased with the
626 increase of F and Q_{CO_2} , indicating that the SFE process is mainly controlled by the
627 mechanism of mass transfer by convection.

628

629 **4. Conclusion**

630

631 The kinetics study of bacaba-de-leque (*O. distichus*) oil extraction indicated that
632 the variation of Q_{CO_2} and the bed geometry, in the two operational conditions (50
633 °C/350 bar and 60 °C/270 bar), did not cause considerable differences in the final oil
634 yields, since approximate values were obtained. However, the extraction behavior over
635 time was visibly affected, mainly during the CER and FER periods of the kinetic
636 curves, being better observed by the values of the mass transfer rate of the CER period.
637 The application of the modified BIC model proved to be adequate to adjust and describe

638 the experimental data of the extraction kinetics for all the operational conditions and
639 extraction beds tested. The values from the mass transfer parameters ($k_f a_0$ and $k_s a_0$),
640 estimated by the model, showed that the oil extraction had a predominant influence
641 from the mass transfer mechanism by convection when compared to diffusion.

642 In the scale-up study, the use of the correlation between the bed configuration (H_b
643 and D_b) and Q_{CO_2} , for the same feed mass, was not enough to reproduce the
644 experimental kinetic curves from V_1 ($5 \times 10^{-5} \text{ m}^3$) to V_2 (10^{-4} m^3), expressed as a function
645 of the extraction time. However, when expressing as a function of S/F, the curves
646 converged to the same line, showing that the total amount of CO_2 consumed during the
647 extraction was responsible for the process efficiency. For the scale-up prediction, using
648 the modified BIC model, the reproduction of the kinetics behavior of the experimental
649 scale (V_2) for the larger predicted scales (V_{PS1} and V_{PS2}) showed that the application of
650 the correlations of the process parameters in different bed geometries was adequate
651 when H_b/D_b was kept constant, varying the feed mass and Q_{CO_2} .

652 The results evaluated in this study provide information that allows the
653 improvement and technical feasibility of bacaba-de-leque oil extraction for possible
654 application on a commercial scale. For future researches, an economic study of the
655 process is essential in order to encourage companies to implement industrial SFE plants,
656 emphasizing the use of green technologies.

657

658 **Conflict of interest**

659

660 The authors declare that there is no conflict of interest regarding the publication of this
661 paper

662

663 **Acknowledgments**

664

665 Vânia Maria Borges Cunha thanks CAPES-Brazil for the doctoral scholarship. Process
666 Number: 1566277/2015.

667

668 **Funding**

669

670 Funding: This work was supported by the CAPES-Brazil (Process Number:
671 1566277/2015).

672

673 **References**

674

675 Benito-Román, O., Rodríguez-Perrino, M., Sanz, M.T., Melgosa, R., Beltrán, S., 2018.

676 Supercritical carbon dioxide extraction of quinoa oil: Study of the influence of
677 process parameters on the extraction yield and oil quality. *Journal of Supercritical*
678 *Fluids* 139, 62–71. <https://doi.org/10.1016/j.supflu.2018.05.009>

679 Bezerra, F.W.F., Costa, W.A. da, Oliveira, M.S. de, Aguiar Andrade, E.H. de, Carvalho,

680 R.N. de, 2018. Transesterification of palm pressed-fibers (*Elaeis guineensis* Jacq.)

681 oil by supercritical fluid carbon dioxide with entrainer ethanol. *Journal of*
682 *Supercritical Fluids* 136, 136–143. <https://doi.org/10.1016/j.supflu.2018.02.020>

683 Botelho, J.R.S., Medeiros, N.G., Rodrigues, A.M.C., Araújo, M.E., Machado, N.T.,

684 Guimarães Santos, A., Santos, I.R., Gomes-Leal, W., Carvalho, R.N., 2014. Black
685 sesame (*Sesamum indicum* L.) seeds extracts by CO₂ supercritical fluid extraction:

686 Isotherms of global yield, kinetics data, total fatty acids, phytosterols and
687 neuroprotective effects. *Journal of Supercritical Fluids* 93, 49–55.

688 <https://doi.org/10.1016/j.supflu.2014.02.008>

689 Botelho, J.R.S., Santos, A.G., Araújo, M.E., Braga, M.E.M., Gomes-Leal, W., Carvalho
690 Junior, R.N., Meireles, M.A.A., Oliveira, M.S., 2015. Copaíba (*Copaifera* sp.) leaf
691 extracts obtained by CO₂ supercritical fluid extraction: Isotherms of global yield,
692 kinetics data, antioxidant activity and neuroprotective effects. *Journal of*
693 *Supercritical Fluids* 98, 167–171. <https://doi.org/10.1016/j.supflu.2014.12.006>

694 Brunner, G., 1994. *Gas Extraction: An Introduction to Fundamentals of Supercritical*
695 *Fluids and the Application to Separation Process*, 1st ed. Springer, New York.
696 [https://doi.org/DOI 10.1007/978-3-662-07380-3](https://doi.org/DOI%2010.1007/978-3-662-07380-3)

697 Carvalho, R.N., Moura, L.S., Rosa, P.T.V., Meireles, M.A.A., 2005. Supercritical fluid
698 extraction from rosemary (*Rosmarinus officinalis*): Kinetic data, extract's global
699 yield, composition, and antioxidant activity. *Journal of Supercritical Fluids* 35,
700 197–204. <https://doi.org/10.1016/j.supflu.2005.01.009>

701 Clavier, J.-Y., Perrut, M., 2004. Scale-Up Issues for Supercritical Fluid Processing in
702 Compliance with GMP, in: York, P., Kompella, U.B., Shekunov, B.Y. (Eds.),
703 *Supercritical Fluid Technology for Drug Product Development*. Marcel Dekker,
704 Inc., New York, pp. 615–650. <https://doi.org/10.1201/9780203021378.ch14>

705 Costa, W.A. da, Bezerra, F.W.F., Oliveira, M.S. de, Andrade, E.H. de A., Santos,
706 A.P.M. dos, Cunha, V.M.B., Santos, D.C.S. dos, Banna, D.A.D. da S., Teixeira, E.,
707 Carvalho Junior, R.N. de, 2019. Supercritical CO₂ extraction and
708 transesterification of the residual oil from industrial palm kernel cake with
709 supercritical methanol. *Journal of Supercritical Fluids* 147, 179–187.
710 <https://doi.org/10.1016/j.supflu.2018.10.012>

711 Cunha, V.M.B., Silva, M.P. da, Sousa, S.H.B. de, Bezerra, P. do N., Menezes, E.G.O.,
712 Silva, N.J.N. da, Banna, D.A.D. da S., Araújo, M.E., Carvalho Junior, R.N. de,

713 2019. Bacaba-de-leque (*Oenocarpus distichus* Mart.) oil extraction using
714 supercritical CO₂ and bioactive compounds determination in the residual pulp.
715 *Journal of Supercritical Fluids* 144, 81–90.
716 <https://doi.org/10.1016/j.supflu.2018.10.010>

717 da Silva, R.P.F.F., Rocha-Santos, T.A.P., Duarte, A.C., 2016. Supercritical fluid
718 extraction of bioactive compounds. *TrAC - Trends in Analytical Chemistry* 76, 40–
719 51. <https://doi.org/10.1016/j.trac.2015.11.013>

720 de Andrade Lima, M., Charalampopoulos, D., Chatzifragkou, A., 2018. Optimisation
721 and modelling of supercritical CO₂ extraction process of carotenoids from carrot
722 peels. *Journal of Supercritical Fluids* 133, 94–102.
723 <https://doi.org/10.1016/j.supflu.2017.09.028>

724 De França, L.F., Reber, G., Meireles, M.A.A., Machado, N.T., Brunner, G., 1999.
725 Supercritical extraction of carotenoids and lipids from buriti (*Mauritia flexuosa*), a
726 fruit from the Amazon region. *Journal of Supercritical Fluids* 14, 247–256.
727 [https://doi.org/10.1016/s0896-8446\(98\)00122-3](https://doi.org/10.1016/s0896-8446(98)00122-3)

728 De Melo, M.M.R., Silvestre, A.J.D., Silva, C.M., 2014. Supercritical fluid extraction of
729 vegetable matrices: Applications, trends and future perspectives of a convincing
730 green technology. *Journal of Supercritical Fluids* 92, 115–176.
731 <https://doi.org/10.1016/j.supflu.2014.04.007>

732 Duba, K.S., Fiori, L., 2015. Supercritical CO₂ extraction of grape seed oil: Effect of
733 process parameters on the extraction kinetics. *The Journal of Supercritical Fluids*
734 98, 33–43. <https://doi.org/10.1016/j.supflu.2014.12.021>

735 Fernández-Ponce, M.T., Parjikolaei, B.R., Lari, H.N., Casas, L., Mantell, C., Martínez
736 de la Ossa, E.J., 2016. Pilot-plant scale extraction of phenolic compounds from
737 mango leaves using different green techniques: Kinetic and scale up study.

738 Chemical Engineering Journal 299, 420–430.
739 <https://doi.org/10.1016/j.cej.2016.04.046>

740 Garcez, J.J., Barros, F., Lucas, A.M., Xavier, V.B., Fianco, A.L., Cassel, E., Vargas,
741 R.M.F., 2017. Evaluation and mathematical modeling of processing variables for a
742 supercritical fluid extraction of aromatic compounds from *Anethum graveolens*.
743 *Industrial Crops and Products* 95, 733–741.
744 <https://doi.org/10.1016/j.indcrop.2016.11.042>

745 Hassim, N., Markom, M., Rosli, M.I., Harun, S., 2019. Scale-up criteria and economic
746 analysis for supercritical fluid extraction of *Phyllanthus niruri*. *Chemical*
747 *Engineering and Processing - Process Intensification* 139, 14–22.
748 <https://doi.org/10.1016/j.cep.2019.03.011>

749 Herrero, M., Mendiola, J.A., Cifuentes, A., Ibáñez, E., 2010. Supercritical fluid
750 extraction: Recent advances and applications. *Journal of Chromatography A* 1217,
751 2495–2511. <https://doi.org/10.1016/j.chroma.2009.12.019>

752 Huang, Z., Shi, X. han, Jiang, W. juan, 2012. Theoretical models for supercritical fluid
753 extraction. *Journal of Chromatography A* 1250, 2–26.
754 <https://doi.org/10.1016/j.chroma.2012.04.032>

755 Jesus, S.P., Calheiros, M.N., Hense, H., Meireles, M.A.A., 2013. A Simplified Model to
756 Describe the Kinetic Behavior of Supercritical Fluid Extraction from a Rice Bran
757 Oil Byproduct. *Food and Public Health* 3, 215–222.
758 <https://doi.org/10.5923/j.fph.20130304.05>

759 Jokić, S., Nagy, B., Zeković, Z., Vidović, S., Bilić, M., Velić, D., Simándi, B., 2012.
760 Effects of supercritical CO₂ extraction parameters on soybean oil yield. *Food and*
761 *Bioproducts Processing* 90, 693–699. <https://doi.org/10.1016/j.fbp.2012.03.003>

762 López-Padilla, A., Ruiz-Rodriguez, A., Flórez, C.E.R., Barrios, D.M.R., Reglero, G.,

763 Fornari, T., 2016. Vaccinium meridionale Swartz supercritical CO₂ extraction:
764 Effect of process conditions and scaling up. *Materials* 9.
765 <https://doi.org/10.3390/ma9070519>

766 López-Padilla, A., Ruiz-Rodriguez, A., Reglero, G., Fornari, T., 2017. Supercritical
767 carbon dioxide extraction of *Calendula officinalis*: Kinetic modeling and scaling
768 up study. *Journal of Supercritical Fluids* 130, 292–300.
769 <https://doi.org/10.1016/j.supflu.2017.03.033>

770 Lu, T., Gaspar, F., Marriott, R., Mellor, S., Watkinson, C., Al-Duri, B., Seville, J.,
771 Santos, R., 2007. Extraction of borage seed oil by compressed CO₂: Effect of
772 extraction parameters and modelling. *Journal of Supercritical Fluids* 41, 68–73.
773 <https://doi.org/10.1016/j.supflu.2006.10.002>

774 Mendiola, J.A., Herrero, M., Castro-Puyana, M., Ibañez, E., 2013. Supercritical Fluid
775 Extraction, in: Mauricio A. Rostagno, Juliana M. Prado (Eds.), *Natural Product
776 Extraction Principles and Applications*. RSC Publishing, Cambridge, UK, p. 499.
777 <https://doi.org/10.1016/B978-0-12-387730-7.00021-8>

778 Mezzomo, N., Martínez, J., Ferreira, S.R.S., 2009. Supercritical fluid extraction of
779 peach (*Prunus persica*) almond oil: Kinetics, mathematical modeling and scale-up.
780 *Journal of Supercritical Fluids* 51, 10–16.
781 <https://doi.org/10.1016/j.supflu.2009.07.008>

782 Özkal, S.G., Yener, M.E., 2016. Supercritical carbon dioxide extraction of flaxseed oil:
783 Effect of extraction parameters and mass transfer modeling. *Journal of
784 Supercritical Fluids* 112, 76–80. <https://doi.org/10.1016/j.supflu.2016.02.013>

785 Patel, R.N., Bandyopadhyay, S., Ganesh, A., 2011. A simple model for super critical
786 fluid extraction of bio oils from biomass. *Energy Conversion and Management* 52,
787 652–657. <https://doi.org/10.1016/j.enconman.2010.07.043>

788 Paula, J.T., Aguiar, A.C., Sousa, I.M.O., Magalhães, P.M., Foglio, M.A., Cabral, F.A.,
789 2016. Scale-up study of supercritical fluid extraction process for *Baccharis*
790 *dracunculifolia*. *Journal of Supercritical Fluids* 107, 219–225.
791 <https://doi.org/10.1016/j.supflu.2015.09.013>

792 Pavlić, B., Pezo, L., Marić, B., Tukuljac, L.P., Zeković, Z., Solarov, M.B., Teslić, N.,
793 2020. Supercritical fluid extraction of raspberry seed oil: Experiments and
794 modelling. *Journal of Supercritical Fluids* 157.
795 <https://doi.org/10.1016/j.supflu.2019.104687>

796 Pereira, C.G., Meireles, M.A.A., 2010. Supercritical fluid extraction of bioactive
797 compounds: Fundamentals, applications and economic perspectives. *Food and*
798 *Bioprocess Technology* 3, 340–372. <https://doi.org/10.1007/s11947-009-0263-2>

799 Prado, J.M., Prado, G.H.C., Meireles, M.A.A., 2011. Scale-up study of supercritical
800 fluid extraction process for clove and sugarcane residue. *Journal of Supercritical*
801 *Fluids* 56, 231–237. <https://doi.org/10.1016/j.supflu.2010.10.036>

802 Rebolleda, S., Rubio, N., Beltrán, S., Sanz, M.T., González-Sanjosé, M.L., 2012.
803 Supercritical fluid extraction of corn germ oil: Study of the influence of process
804 parameters on the extraction yield and oil quality. *Journal of Supercritical Fluids*
805 72, 270–277. <https://doi.org/10.1016/j.supflu.2012.10.001>

806 Salgin, U., Döker, O., Çalimli, A., 2006. Extraction of sunflower oil with supercritical
807 CO₂: Experiments and modeling. *Journal of Supercritical Fluids* 38, 326–331.
808 <https://doi.org/10.1016/j.supflu.2005.11.015>

809 Sánchez-Vicente, Y., Cabañas, A., Renuncio, J.A.R., Pando, C., 2009. Supercritical
810 fluid extraction of peach (*Prunus persica*) seed oil using carbon dioxide and
811 ethanol. *Journal of Supercritical Fluids* 49, 167–173.
812 <https://doi.org/10.1016/j.supflu.2009.01.001>

813 Soares, J.F., Zobot, G.L., Tres, M. V., Lunelli, F.C., Rodrigues, V.M., Friedrich, M.T.,
814 Pazinato, C.A., Bilibio, D., Mazutti, M.A., Carniel, N., Priamo, W.L., 2016.
815 Supercritical CO₂ extraction of black poplar (*Populus nigra* L.) extract:
816 Experimental data and fitting of kinetic parameters. *Journal of Supercritical Fluids*
817 117, 270–278. <https://doi.org/10.1016/j.supflu.2016.07.005>

818 Sovová, H., 1994. Rate of the vegetable oil extraction with supercritical CO₂—I.
819 Modelling of extraction curves. *Chemical Engineering Science* 49, 409–414.
820 [https://doi.org/10.1016/0009-2509\(94\)87012-8](https://doi.org/10.1016/0009-2509(94)87012-8)

821 Taher, H., Al-Zuhair, S., Al-Marzouqi, A.H., Haik, Y., Farid, M., 2014. Mass transfer
822 modeling of *Scenedesmus* sp. lipids extracted by supercritical CO₂. *Biomass and*
823 *Bioenergy* 70, 530–541. <https://doi.org/10.1016/j.biombioe.2014.08.019>

824 Weinhold, T. de S., Bresciani, L.F.V., Tridapalli, C.W., Yunes, R.A., Hense, H.,
825 Ferreira, S.R.S., 2008. *Polygala cyparissias* oleoresin: Comparing CO₂ and
826 classical organic solvent extractions. *Chemical Engineering and Processing:*
827 *Process Intensification* 47, 109–117. <https://doi.org/10.1016/j.cep.2007.08.007>

828 Westerman, D., Santos, R.C.D., Bosley, J.A., Rogers, J.S., Al-Duri, B., 2006. Extraction
829 of Amaranth seed oil by supercritical carbon dioxide. *Journal of Supercritical*
830 *Fluids* 37, 38–52. <https://doi.org/10.1016/j.supflu.2005.06.012>

831 Xiong, K., Chen, Y., Shen, S., 2019. Experimental optimization and mathematical
832 modeling of supercritical carbon dioxide extraction of essential oil from
833 *Pogostemon cablin*. *Chinese Journal of Chemical Engineering* 27, 2407–2417.
834 <https://doi.org/10.1016/j.cjche.2019.03.004>

835 Zobot, G.L., Moraes, M.N., Meireles, M.A.A., 2014a. Influence of the bed geometry on
836 the kinetics of rosemary compounds extraction with supercritical CO₂. *Journal of*
837 *Supercritical Fluids* 94, 234–244. <https://doi.org/10.1016/j.supflu.2014.07.020>

838 Zabot, G.L., Moraes, M.N., Petenate, A.J., Meireles, M.A.A., 2014b. Influence of the
839 bed geometry on the kinetics of the extraction of clove bud oil with supercritical
840 CO₂. Journal of Supercritical Fluids 93, 56–66.
841 <https://doi.org/10.1016/j.supflu.2013.10.001>

842 Zeković, Z., Bera, O., Đurović, S., Pavlić, B., 2017. Supercritical fluid extraction of
843 coriander seeds: Kinetics modelling and ANN optimization. Journal of
844 Supercritical Fluids 125, 88–95. <https://doi.org/10.1016/j.supflu.2017.02.006>

845

CONCLUSÃO GERAL

Conforme foi relatado no capítulo 3, o rendimento máximo de óleo foi alcançado a 60 °C e 270 bar, apresentando um valor igual a 45,9 %. Nesse estudo, foi visto que o uso da tecnologia supercrítica possibilitou a obtenção de dois produtos, de alta qualidade, a partir da extração do óleo da polpa liofilizada de bacaba-de-leque. O primeiro foi uma torta residual (desengordurada) concentrada em compostos fenólicos e antocianinas totais com atividade antioxidante, mostrando possíveis aplicações para fins nutracêuticos. Essa concentração foi observada após a extração via Sc-CO₂, que possibilitou a separação da fração lipofílica da polpa. O outro produto foi o óleo extraído, o qual foi caracterizado, predominantemente, pelo alto teor de ácidos graxos insaturados, especialmente, os ácidos oleico e linoleico, que combinados fazem parte dos principais triglicerídeos de cadeia longa presentes no óleo. Essas características conferiram ao produto boa qualidade funcional, representada pelos bons índices de qualidade funcional determinados.

No capítulo 4, foi mostrado que as propriedades nutricionais e físico-químicas do óleo de bacaba-de-leque são semelhantes às de óleos comestíveis comercializados no Brasil e em outros países e que não apresenta efeito citotóxico ao ser extraído com o uso do Sc-CO₂, indicando que ele poderia ser consumido sem danos à saúde humana. Foi determinado um significativo teor de carotenoides totais e parâmetros de qualidade dentro dos níveis aceitáveis para óleos e gorduras de fontes vegetais. Também foi visto que o óleo é termicamente estável até 210 °C. Esses resultados mostram que o óleo de bacaba-de-leque pode ser utilizado para diversas finalidades, como ser inserido na alimentação em substituição ao azeite e outros óleos vegetais comestíveis, principalmente como fonte de ômega-9, na síntese de alimentos funcionais, em cosméticos e fitoterápicos.

Os resultados obtidos do estudo das cinéticas de extração e dos procedimentos de ampliação de escala, relatados no capítulo 5, mostraram que a correlação entre a vazão de solvente (Q_{CO_2}) e massa de alimentação (F) em diferentes geometrias do leito, representadas pelo diâmetro (D_b) e altura do leito (H_b), permitem aumentar a escala do processo de extração do óleo de bacaba-de-leque por fluido supercrítico, usando alguns dados de laboratório e cálculos de parâmetros cinéticos e de processo, além de estimar o rendimento mínimo esperado em escalas maiores.

TRABALHOS DESENVOLVIDOS DURANTE O PERÍODO DO DOUTORADO.

Trabalhos publicados em anais de congresso

- ALMEIDA, M. M.; PIRES, F. C. S.; SILVA, A. P. S. E.; SOUSA, S. H. B.; SILVA, M.; **CUNHA, V.M.B.**; SALAZAR, M. L. A. R.; BEZERRA, P. N.; CARVALHO JUNIOR, R. N. Supercritical fluid extraction from *Byrsonima crassifolia* leaves: experimental data, global yield, total phenolic compounds, antioxidant activity, and linear correlation. In: **Ibero American Conference on Supercritical Fluids, 2019**, Campinas. V Ibero American Conference on Supercritical Fluids, 2019.
- SALAZAR, M. L. A. R.; URBINA, G. R. O.; **CUNHA, V.M.B.**; BEZERRA, F. W. F.; BEZERRA, P. N.; DIAS, M. N. C; SANTOS, I. R. C; GOMES-LEAL, W; MARQUES DA SILVA, S. H.; CARVALHO JUNIOR, R. N. Evaluation of *Cissus sicyoides* L. supercritical extract in the cytotoxic effect in human red blood cells and as anti-inflammatory in spinal cord injury of adult rats. In: **Ibero American Conference on Supercritical Fluids, 2019**, Campinas. V Ibero American Conference on Supercritical Fluids, 2019.
- URBINA, G. R. O.; SALAZAR, M. L. A. R.; **CUNHA, V. M. B.**; BEZERRA, F. W. F.; PIRES, F. C. S.; SILVA, A. P. S. E.; BEZERRA, P. N.; SILVA, M. P.; CARVALHO JUNIOR, R. N. Evaluation of chemical composition and antioxidant activity of *Mansoa standleyi* (Steयरम) A. H. Gentry (Bignoniaceae) oil obtained by supercritical extraction. In: **Ibero American Conference on Supercritical Fluids, 2019**, Campinas. V Ibero American Conference on Supercritical Fluids, 2019.
- SILVA, M. P.; SOUSA, S. H. B.; **CUNHA, V. M. B.**; SALAZAR, M. A. R.; CARVALHO JUNIOR, R. N.; ARAÚJO, M. E. Avaliação da estrutura morfológica, química elementar, parâmetros de cor e composição em minerais da polpa de açaí (*Euterpe oleracea* Mart.) de três diferentes localidades da região amazônica. In: **XXXVI Congresso Brasileiro de Ciência e Tecnologia de Alimentos (CBCTA)**, 2018, Belém.
- **CUNHA, V. M. B.**; SILVA, M. P.; SOUSA, S. H. B.; SALAZAR, M. A. R.; ARAÚJO, M. E.; CARVALHO Jr, R. N. Caracterização físico-química da polpa liofilizada de bacaba-de-leque (*Oenocarpus distichus*) e influência dos parâmetros de extração

- supercrítica na separação de frações hidrofílicas e lipofílicas. In. **XXXVI Congresso Brasileiro de Ciência e Tecnologia de Alimentos** (CBCTA), 2018, Belém.
- URBINA, G. R. O.; SALAZAR, M. A. R.; SILVA, A. P. S.; CUNHA, V. M. B.; SILVA, M. P.; CARVALHO JUNIOR, R. N. Determinação da composição química do óleo essencial das folhas de cipó-de-alho (*Mansoa standleyi*) obtido por hidrodestilação. In. **XXXVI Congresso Brasileiro de Ciência e Tecnologia de Alimentos** (CBCTA), 2018, Belém.
 - SILVA, M. P.; LOPES, J. V. M.; CUNHA, V. M. B.; MACHADO, N. T.; CARVALHO JUNIOR, R. N.; ARAÚJO, M. E. Modelagem com os tempos característicos da cinética de extração do óleo de palmiste com CO₂ supercrítico. In. **XXXVI Congresso Brasileiro de Ciência e Tecnologia de Alimentos** (CBCTA), 2018, Belém.
 - CUNHA, V. M. B.; SILVA, M. P.; MENEZES, E. G. O.; MACHADO, N. T.; CARVALHO JUNIOR, R. N.; ARAUJO, M. E. Simulação da extração supercrítica de extratos naturais: cálculo da densidade da mistura dióxido de carbono+cossolvente. In. **XXXVI Congresso Brasileiro de Ciência e Tecnologia de Alimentos** (CBCTA), 2018, Belém.
 - SALAZAR, M. A. R.; URBINA, G. R. O.; SILVA, A. P. S.; CUNHA, V. M. B.; SILVA, M. P.; CARVALHO JUNIOR, R. N. Obtenção de fração enriquecida em flavonoides do extrato etanólico do *cissus sicyoides* L. a partir de extração em fase sólida e identificação por cromatografia líquida de alta eficiência. In. **XXXVI Congresso Brasileiro de Ciência e Tecnologia de Alimentos** (CBCTA), 2018, Belém.
 - CUNHA, V. M. B.; SILVA, W. A.; CARVALHO Jr, R. N.; MACHADO, N. T.; ARAUJO, M. E. Simulação do fracionamento em coluna em contracorrente de solução aquosa de β -caroteno com CO₂ supercrítico no Aspen Hysys. In: **15º Encontro de Profissionais da Química da Amazônia** (EPQA), 2017, Belém. (Premiado em 1º lugar como o melhor trabalho apresentado na forma de pôster).
 - CUNHA, V. M. B.; SILVA, M. P.; COSTA, E. C.; CARVALHO Jr, R. N.; MACHADO, N. T.; ARAUJO, M. E. Extração supercrítica: simulação do sistema solvente+cossolvente com o Aspen Hysys. In: **15º Encontro de Profissionais da Química da Amazônia** (EPQA), 2017, Belém.

- SOUZA, R. S.; SILVA, M. P.; CUNHA, V. M. B.; CARVALHO Jr, R. N.; MACHADO, N. T.; ARAÚJO, M. E. Tecnologia supercrítica aplicada a obtenção de extratos de açaí (*Euterpe oleracea*) e priprioca (*Cyperus articulatus*): parâmetros cinéticos. In: **15º Encontro de Profissionais da Química da Amazônia (EPQA)**, 2017, Belém.
- COSTA, E. C.; CUNHA, V. M. B.; LOPES, J. V. M.; MACHADO, N. T.; ARAÚJO, M. E. Simulações com o Aspen Hysys empregando diferentes equações de estado e regras de mistura: aplicações para o gás natural. In: **15º Encontro de Profissionais da Química da Amazônia (EPQA)**, 2017, Belém.
- SALAZAR, M. L. A. R.; URBINA, G. R. O.; CUNHA, V. M. B.; BEZERRA, V.; CARVALHO JUNIOR, R. N. Identificação e Quantificação de Compostos Fenólicos dos Extratos Etanólico e Hexânico de *Cissus sicyoides* L. In: **XX Encontro Nacional e VI Congresso Latino Americano de Analistas de Alimentos-ENAAL**, 2017, Belém. Anais do XX Encontro Nacional e VI Congresso Latino Americano de Analistas de Alimentos-ENAAL, 2017.
- SILVA, W, A.; CUNHA, V. M. B.; LOPES, J. M., SILVA, M. P.; MACHADO, N. T.; ARAUJO, M. E. Modelagem Termodinâmica de Sistemas Multicomponentes de Constituintes de Óleos Vegetais em Dióxido de Carbono Supercrítico. In: **XXI Congresso Brasileiro de Engenharia Química (COBEQ)**, 2016, Fortaleza.
- CUNHA, V. M. B.; MOREIRA, R. F.; RODRIGUES, J. E.; CARVALHO Jr, R. N.; MACHADO, N. T.; ARAUJO, M. E. Determinação da solubilidade do óleo de andiroba em dióxido de carbono supercrítico empregando o método dinâmico. In: **14º Encontro de Profissionais da Química da Amazônia (EPQA)**, 2015, Belém. (**Premiado como 3º colocado da seção técnica COMUNICAÇÃO ORAL do evento**).
- CORDEIRO, R. M.; OLIVEIRA, M. S.; CUNHA, V. M. B.; PINTO, R. H. H.; SILVA, N. J. N.; COSTA, W. A.; BEZERRA, V. M. S.; BOTELHO, J. R. S.; CARVALHO JUNIOR, R. N. Determinação de carotenoides totais em óleos de muruci (*Byrsonima crassifolia* L. Rich) obtidos por diferentes métodos de extração: CO₂ supercrítico e solvente orgânico líquido. In: **XIX Encontro Nacional e V Congresso Latino Americano de Analistas de Alimentos (ENAAL)**, 2015, Natal - RS.

Artigos publicados em periódicos.

- SALAZAR, M. A. R.; URBINA, G. R. O.; **CUNHA, V. M. B.**; BEZERRA, F. W. F.; DIAS, M. N. C.; SANTOS, I. R.; TEIXEIRA, B. J. B.; COSTA, W. A.; GOMES-LEAL, W.; SILVA E SOUZA, J. N.; SILVA, S. H. M.; CARVALHO JUNIOR, R. N. Cytotoxic effect of cipó-pucá (*Cissus sicyoides* L.) supercritical extract on human red blood cells and as anti-inflammatory in spinal cord injury in adult rats. **Journal of Supercritical Fluids**, v. 169, p. 105105, 2021.
- SILVA, M. P.; **CUNHA, V. M. B.**; SOUSA, S. H. B.; MENEZES, E. G. O.; BEZERRA, P. DO N.; FARIAS NETO, J T.; FILHO, G. N. R.; ARAÚJO, M. E.; CARVALHO JR., R. N. Supercritical CO₂ extraction of lyophilized Açaí (*Euterpe oleracea* Mart.) pulp oil from three municipalities in the state of Pará, Brazil. **Journal of CO₂ Utilization**, v. 31, p. 226-234, 2019.
- COSTA, W. A.; BEZERRA, F. W. F.; OLIVEIRA, M. S.; SILVA, M. P.; **CUNHA, V. M. B.**; ANDRADE, E. H. A.; CARVALHO JÚNIOR, R. N. Appliance of a high pressure semi-batch reactor: supercritical transesterification of soybean oil using methanol. **Food Science and Technology**, v. xxx, p. 1, 2019.
- **CUNHA, V. M. B.**; SILVA, M. P.; SOUSA, S. H. B.; BEZERRA, P. N.; MENEZES, E. G. O.; SILVA, N. J. N.; BANNA, D. A. D. S.; ARAÚJO, M. E.; CARVALHO JUNIOR, R. N. Bacaba-de-leque (*Oenocarpus distichus* Mart.) oil extraction using supercritical CO₂ and bioactive compounds determination in the residual pulp. **Journal of Supercritical Fluids**, v. 144, p. 81-90, 2019.
- COSTA, E. C.; FERREIRA, C. C.; SANTOS, A. L. B.; VARGENS, H. S.; MENEZES, E. G. O.; **CUNHA, V. M. B.**; SILVA, M. P.; MÂNCIO, A. A.; MACHADO, N. T.; ARAÚJO, M. E. Process simulation of organic liquid products fractionation in countercurrent multistage columns using CO₂ as solvent with Aspen-Hysys. **The Journal of Supercritical Fluids** 140 (2018) 101–115, <https://doi.org/10.1016/j.supflu.2018.06.004>
- SALAZAR, M. A. R.; COSTA, J. V., URBINA, G. R. O.; **CUNHA, V. M. B.**; SILVA, M. P.; BEZERRA, P. N.; PINHEIRO, W. B. S.; GOMES-LEAL, W.; LOPES, A. S.; CARVALHO JUNIOR, R. N. Chemical composition, antioxidant activity, neuroprotective and anti-inflammatory effects of cipó-pucá (*Cissus sicyoides* L.) extracts obtained from

supercritical extraction. **The Journal of Supercritical Fluids** 138 (2018) 36–45, <https://doi.org/10.1016/j.supflu.2018.03.022>.

- COSTA, W. A.; BEZERRA, F. W. F.; OLIVEIRA, M. S.; ANDRADE, E. H. A.; SANTOS, A. P. M.; CUNHA, V. M. B.; SANTOS, D. C. S.; BANNA, D. A. D. S.; CARVALHO JUNIOR, R. N. Supercritical CO₂ Extraction and Transesterification of the Residual Oil from Industrial Palm Kernel Cake with Supercritical Methanol. **Journal of Supercritical Fluids**, v. xx, p. xxx, 2018.
- CUNHA, V. M. B.; SILVA, M. P., CARVALHO JR, R. N.; MEIRELES, M. A. A.; MACHADO, N. T.; ARAÚJO, M. E. Lauric Acid Rich Oil Supercritical Extraction and Methodology to Predict Solubility. **Food and Public Health** 2016, 6(1): 26-32, DOI: 10.5923/j.fph.20160601.04

Capítulos de livro publicados.

- BEZERRA, F. W. F.; BEZERRA, P. N.; CUNHA, V. M. B.; SALAZAR, M. A. R.; BARBOSA, J. R.; SILVA, M. P.; OLIVEIRA, M. S.; COSTA, W. A.; PINTO, R. H. H.; CRUZ, J. N.; CARVALHO JUNIOR, R. N. Supercritical Green Solvent for Amazonian Natural Resources. *Nanotechnology in the Life Sciences*. 1ed.: **Springer International Publishing**, 2020, v., p. 15-31.
- SALAZAR, M. A. R.; URBINA, G. R. O.; BEZERRA, P. N.; CUNHA, V. M. B.; SILVA, M. P.; PIRES, F. C. S.; SILVA, A. P. S.; SOUSA, S. H. B.; CARVALHO JR, R. N. Antioxidant and Biological Activity of *Cissus sicyoides* and *Rosmarinus officinalis* Extracts. In: **Antioxidants**. 1ed.: Intech Open, 2019, v. v., p. 1-20.
- BEZERRA, F. W. F.; OLIVEIRA, M. S.; BEZERRA, P. N.; CUNHA, V. M. B.; SILVA, M. P.; COSTA, W. A.; PINTO, R. H. H.; CORDEIRO, R. M.; CRUZ, J. N.; CHAVES NETO, A. M. J.; CARVALHO JUNIOR, R. N. Extraction of bioactive compounds. In: Abdullah M. Asiri Dr. Inamuddin Arun Isloor. (Org.). **Green Sustainable Processes for Chemical and Environmental Engineering and Science - Supercritical Carbon Dioxide as Green Solvent**. 1ed. Amsterdã: Elsevier, 2019, v. 1, p. 140-162.
- OLIVEIRA, M. S.; SILVA, S. G.; CRUZ, J. N.; MENEZES, E. G. O.; COSTA, W. A.; BEZERRA, F. W. F.; CUNHA, V. M. B.; CORDEIRO, R. M.; CHAVES NETO, A. M. J.;

ANDRADE, E. H. A.; CARVALHO JUNIOR, R. N. Supercritical CO₂ Application in Essential Oil Extraction. In: Inamuddin, Rizwana Mobin and Abdullah M. Asiri. (Org.). **Supercritical CO₂ Application in Essential Oil Extraction**. 2ed. Millersville, USA: Materials Research Forum LLC, 2019, v. 2, p. 1-28.

- **CUNHA, V. M. B.**; SILVA, M. P.; COSTA, W. A.; OLIVEIRA, M. S.; BEZERRA, F. W. F.; MELO, A. C.; PINTO, R. H. H.; MACHADO, N. T.; ARAÚJO, M. E. CARVALHO JUNIOR, R. N. Carbon Dioxide Use in High-Pressure Extraction Processes. In: **Carbon Dioxide Chemistry, Capture and Oil Recovery**. (2018). InTech.
- OLIVEIRA, M. S.; ALMEIDA, M. M.; SALAZAR, M. A. R.; PIRES, F. C. S.; BEZERRA, F. W. F.; **CUNHA, V. M. B.**; CORDEIRO, R. M.; URBINA, G. R. O.; SILVA, M. P.; SOUZA, A. P. S.; PINTO, R. H. H.; CARVALHO JUNIOR, R. N. Potential of Medicinal Use of Essential Oils from Aromatic Plants. In: **Potential of Essential Oils**. 1ed.: InTech, 2018, v., p. 2-19.
- COSTA, W. A.; OLIVEIRA, M. S.; SILVA, M. P.; **CUNHA, V. M. B.**; PINTO, R. H. H.; BEZERRA, F. W. F.; CARVALHO JUNIOR, R. N. Açai (*Euterpe oleracea*) and Bacaba (*Oenocarpus bacaba*) as Functional Food. In: **Superfood and Functional Food-An Overview of Their Processing and Utilization**. (2017). InTech.